RECLAMATION

Managing Water in the West

Evapotranspiration Water Use Analysis of Saltcedar and Other Vegetation in the Mojave River Floodplain, 2007 and 2010

Mojave Water Agency Water Supply Management Study
Phase 1 Report

U.S. Department of the Interior
Bureau of Reclamation
Southern California Area Office

Mojave Water Agency
Apple Valley, California

Utah State University
Logan, Utah

August 2011

Mission Statements

The mission of the Department of the Interior is to protect and provide access to our Nation's natural and cultural heritage and honor our trust responsibilities to Indian Tribes and our commitments to island communities.

The mission of the Bureau of Reclamation is to manage, develop, and protect water and related resources in an environmentally and economically sound manner in the interest of the American public.

Mojave Water Agency will carry out its water management mission by observing the core values of Fiscal Responsibility, Community, Innovation, Public Safety, Conservation, Service, Dependability, Integrity, Leadership and Foresight.

The mission of Utah State University is to be one of the nation's premier student-centered land-grant and space-grant universities by fostering the principle that academics come first, by cultivating diversity of thought and culture, and by serving the public through learning, discovery, and engagement.

Evapotranspiration Water Use Analysis of Saltcedar and Other Vegetation in the Mojave River Floodplain, 2007 and 2010

Mojave Water Agency Water Supply Management Study, Phase 1 Report

Prepared by

Department of Civil and Environmental Engineering
Utah State University
Logan, UT 84322-4110

Dr. Christopher M. U. Neale, Professor
Saleh Taghvaeian, Hatim Geli, and Saravanan Sivarajan, Ph.D. graduate students
Ashish Masih, M.S. Post-graduate researcher
Remote Sensing Services Laboratory

Dr. Robert Pack, Associate Professor
Lidar Assisted Stereo Scopic Imaging Service Center

Bureau of Reclamation
Amy Witherall, Water Resources Planner
Southern California Area Office

Scott O'Meara, Botanist
Technical Services Center

Ron Simms, Geographic Information Group Manager
Mike Baker, Remote Sensing Scientist
Jeff Milliken, Remote Sensing Scientist
Lower Colorado Regional Office

Contents

Page

Glossary

Airborne Lidar: A technique that uses a scanning laser and precise positioning navigation system to scan the surface and measure the returned energy from each intercepted point in 3-D space.

Area of Interest (AOI): A polygon defining an area within which analysis is conducted.

Albedo: The total reflectance of a surface in the shortwave (solar) part of the spectrum.

Arundo: Common name for *Arundo donax*, a tall, perennial invasive grass found in damp soils, primarily along margins of streams and rivers. Also commonly known as “giant cane” or “Carrizo.”

Canopy acres: Areas covered by vegetative canopies, in acres, typically delineated by polygons encompassing the outer perimeters of individual vegetation canopies. Synonymous with MDRCD “weed acres”.

Canopy Texture: the spatial pattern of variability in reflectivity and the digital number homogeneity. Examples of smooth canopy textures are a pasture or sandy river bottom. Examples of a rough canopy texture are a forest canopy or an urban setting.

CIMIS: The California Irrigation Management Information System, a network of automated weather stations that provide reference evapotranspiration estimates.

Continuously Operating Reference Station (CORS): A network of continuously operating GPS reference stations operated by the National Oceanographic and Atmospheric Association that provide Global Navigation Satellite System data consisting of carrier phase and code range measurements in support of three dimensional positioning, meteorology, space weather, and geophysical applications throughout the United States, its territories, and a few foreign countries.

Crop coefficient: The ratio between actual evapotranspiration of a crop and reference evapotranspiration.

Cut-Stump: Method for control of woody species in which the plants are mechanically cut near ground-level followed by application of herbicides to cut surfaces shortly thereafter.

Desert Scrub: Vegetation classification for areas with xeric plant growth, primarily shrubs. Plants are generally sparse but may be dense is some areas and can be seasonally variable.

eCognition: Image processing software used to classify the airborne multispectral imagery into surface vegetation classes.

Digital Elevation Model (DEM): Digital raster cells representing elevation of a terrain surface.

Energy balance equation: Equation that describes the balance between net radiation and soil, sensible and latent heat fluxes.

Evapotranspiration (ET): The combined effect of evaporation from the soil surface and transpiration from the plant canopy.

ETai: Instantaneous actual evapotranspiration obtained by dividing the instantaneous latent heat flux from the remote sensing energy balance by the latent heat of vaporization of water.

ETo: Reference evapotranspiration for a grass reference crop.

ETrf: Evapotranspiration fraction, obtained by dividing the actual evapotranspiration of a vegetation type by the reference evapotranspiration from a reference surface (such as grass). It is similar to a crop coefficient, used for irrigated crops.

Feature Class Layers (FC): GIS layers of collections of geographic features with the same geometry type, the same attribute fields, and the same spatial reference. Grouping homogeneous GIS feature types in this way provides the ability to process them as a single unit.

Federal Geographic Data Center metadata standards (FGDC): Standards facilitate the development, sharing, and use of geospatial data.

Foliar Herbicide Management: Application of herbicides to the canopy (foliage) of the plant or tree.

Geodatabase (GDb): A database designed to store, query, and manipulate geographic information and spatial data. The GDb is a file extension used by ESRI.

Georeferencing: The process of defining the position of geographical objects relative to a standard reference grid.

Global Positioning System (GPS): A space-based global navigation satellite system (GNSS) that provides location and time information in all weather, anywhere on or near the Earth, where there is an unobstructed line of sight to four or more GPS satellites. It is maintained by the United States government and is freely accessible by anyone with a GPS receiver.

Geographic Information System (GIS): An information system that integrates, stores, edits, analyzes, shares, and displays geographic information.

Heat Flux: The rate of heat energy transfer through a given surface.

Inertial Measurement Unit (IMU): A device that keeps track of the aircraft position and orientation required to position the lidar shots and returns as well as the multispectral and color imagery in 3D space.

Infrared/Red band ratios: A vegetation index sensitive to growing vegetation obtained by dividing the surface reflectance in the near-infrared band with the red band reflectance.

Landsat Thematic Mapper: A satellite remote sensing instrument which is emulated by the USU airborne multispectral system.

Latent Heat Flux (LE): The amount of heat flux used in the evapotranspiration process.

Lidar: Laser system mounted on an aircraft that transmits pulses of light at high frequency, receiving the reflected returns from different surfaces and mapping the position and altitude of each return.

Low NDVI Vegetation: Class of vegetation that encompasses a mixture of species with low NDVI values; includes senescent and dead vegetation.

Macro: A text file containing a sequence of commands that can be executed as one command. Macros can be built to perform frequently used, as well as complex operations.

MDRCD: Mojave Desert Resource Conservation District

Mechanical Control: Management of plants by physical means, such as mowing, extraction, grinding, root raking, and hand removal.

Mesophytes: Terrestrial plants requiring moderate amounts of water. They typically cannot tolerate extremely dry or wet conditions.

Mesquite: Common name for leguminous plants of the genus *Prosopis*. Species typical in the Southwest U.S. include honey mesquite (*P. glandulosa*) and screwbean mesquite (*P. pubescens*).

MODTRAN (Moderate Resolution Transmittance): An atmospheric transmission model that is used to correct remotely sensed imagery and remove atmospheric effects that scatter and absorb radiation.

Multispectral: A remote sensing system that measures reflected light from the surface in specific bandwidths.

MWA: Mojave Water Agency

Net Radiation (Rn): The resulting amount of energy at the surface available to do work (evaporate water, heat the soil and heat the air).

Normalized Difference Vegetation Index (NDVI): A numeric ratio using the Near Infrared and Red portions of the electromagnetic spectrum, used to estimate vegetation properties and other land cover properties. High positive values generally indicate presence of live green vegetation.

Orthorectification: Process of geo-referencing images and projecting them onto the terrain.

Ortho-image mosaics: Large blocks of orthorectified images.

Phreatophyte: A type of vegetation that has a deep tap root that allows it to use water from deep groundwater systems.

Radiometric: Refers to radiation.

Radiosonde: A weather balloon that is launched to measure a profile of temperature and humidity in the atmosphere.

Reclamation: U.S. Department of the Interior, Bureau of Reclamation.

Reflectance: The property of a surface that describes its ability to reflect solar radiation at certain wavelengths.

Remote Sensing: A technique for obtaining information from a surface without coming into physical contact with it, using sensors and imagers that are sensing the electromagnetic radiation coming from the surface at specific wavelengths.

Saltcedar: Common name for several invasive plant species within the genus *Tamarix* that can grow several meters high and in dense cover. Extensive root system can utilize deep groundwater.

SEBAL (Surface Energy Balance for Land): An evapotranspiration modeling approach for estimating the surface energy balance components using remotely sensed information. This ET model was tested on Block 1 data, but the Two-Source model was chosen for this Study.

Sensible Heat Flux (H): The amount of heat flux into the air.

Soil Heat Flux (G): The amount of heat flux into the ground.

Soil-Vegetation Atmosphere Transfer (SVAT) model: A model that describes the transfer of water from the soil matrix, through the vegetation and to the atmosphere.

Surface Energy Flux: Soil heat flux, sensible heat flux and latent heat flux resulting from the partitioning of net radiation.

System Noise: Noise in the electronics of the lidar system that can be confused with data.

Spectral Brightness: Reflected radiation from a surface in a particular spectral band or portion of the electromagnetic spectrum.

Thermal Infrared: A portion of the electromagnetic spectrum emitted from a surface and related to its physical temperature and surface emissivity properties.

Two-Source model: An evapotranspiration modeling approach for estimating the surface energy balance of a surface by solving for soil and canopy components separately. This ET model was selected for use in the Study.

USU: Utah State University.

UTM: Universal Transverse Mercator map projection.

Executive Summary

The Mojave Water Agency Water Supply Management Study, Phase 1 Report (Study) was developed to provide technical information on vegetation water usage in the Mojave River floodplain, with emphasis on saltcedar. Study analyses included 2007 and 2010 classification of native and non-native vegetation, vegetation evapotranspiration (ET) modeling[1], lidar elevation map development, groundwater mapping, and water evapotranspiration cost calculations. Results are presented as a whole and by Mojave Water Agency (MWA) subarea boundaries: Alto, Alto Transition, Centro, and Baja.

Data Collection

ET analysis utilized airborne lidar, multispectral and thermal infrared data collected on June 29 and June 30, 2010 under clear sky conditions along 94 miles (45,811 acres) of the Mojave River. The multispectral imagery was orthorectified using the lidar data, calibrated to a reflectance standard and stitched together to form ortho-image mosaics. The thermal infrared imagery was rectified to the multispectral mosaics. Both the multispectral imagery and thermal infrared imagery were calibrated using the Moderate Resolution Transmittance atmospheric transmission model (MODTRAN). The imagery layers were used to develop species composition Geographic Information System layers, which were inputted into the ET modeling process. Helicopter videography was captured on June 16 and 17, 2010 of the Mojave River within the Study area, and used as ground-truthing.

Data Classification

Vegetation was classified within the Area of Interest (AOI) polygon for 2007 and 2010 (see Section 3.1 figures). The 2010 classification was completed using calibrated 3-band multispectral image ortho-image mosaics acquired by Utah State University. The 2007 classification was completed using 3-band, orthorectified multispectral imagery provided by MWA. Both image sets were acquired during the summer of each respective year. ERDAS Imagine software was used to pre-process the imagery. This preprocessing was completed so both image sets had the same pixel resolution of 1 meter, were in the same Universal Transverse Mercator geographic projection, and were both digital integer (non-floating point) images. Imagery was imported into Definiens eCognition, object-based hierarchical classification software, to classify vegetation and surface types.

ET Model Selection

Two models were evaluated for calculating ET in the Study area: the Surface Energy Balance Algorithm for Land (SEBAL) model and the Two-Source model. Both models performed well in initial testing on a portion of the Mojave River, resulting in comparable saltcedar ET estimates to those measured at the Cibola National Wildlife Refuge in the Lower Colorado River region under similar climatic conditions. Estimates for alfalfa and grass ET were also comparable to independent estimates based on crop reference ET. The incorporation of lidar-derived canopy heights in both models led to nearly identical results. Therefore, it was decided that the Two-Source model, described

[1] Technical terms are defined in the Glossary.

in Section 2.4, would be used for ET estimations over the entire river as it requires less subjective operator input than the SEBAL model and is well suited for sparsely vegetated ecosystems.

The main concept behind formulation of the Two-Source model is that it separates the surface into soil and canopy components and applies the energy balance equation to each component independently in order to estimate the different energy fluxes. Then, at a level above the ground surface called air-canopy interface, the energy fluxes of each component are added to represent the total surface energy fluxes.

<u>Saltcedar Change Detection Results</u>

Delineation of saltcedar acreages from 2007 and 2010 aerial imagery indicated a net reduction of 328 canopy acres over the entire basin (Table 1). It should be noted that vegetation coverage is presented as “canopy acres”, which is the area covered by vegetation. Areas of bare ground are not included in these coverages. Canopy acres are synonymous with “weed acres” used by Mojave Desert Resource Conservation District (MDRCD).

Table 1. Saltcedar canopy acres, 2007-2010

	--------Saltcedar Canopy acres--------			
Subarea	**2007**	**2010**	**Δ**	**%Δ**
Alto	84.3	2.5	-81.9	-97.1%
Alto Transition	201.0	77.9	-123.1	-61.3%
Centro	732.9	634.1	-98.8	-13.5%
Baja	383.1	358.7	-24.4	-6.4%
MOJAVE BASIN TOTAL ACRES	**1,401**	**1,073**	**-328**	**-23.4%**

Δ=change

The greatest reduction in saltcedar presence occurred in the Alto subarea, with the least reduction found in the Baja subarea. This corresponds to MDRCD removal efforts which began in Alto, and proceeded downstream. At the time of imagery capture in June 2010, MDRCD Phase 4 efforts in most of Centro and all of Baja had not occurred, which explains the lower percent reduction in those subareas.

<u>ET Results</u>

The ET statistics were summarized by canopy closure class and vegetation type for the four groundwater subareas within the MWA service area. Saltcedar ET within the AOI was reduced by 797 acre-feet between 2007 and 2010.

Cottonwood/willow resulted in the highest ET rates followed by saltcedar, arundo, mesophytes, low Normalized Difference Vegetation Index vegetation, mesquite and desert scrub. Results show that while cottonwood/willow transpires more water than saltcedar, the latter is a major water user due to the areal extent of its invasion and high density at several locations along the Mojave River. Due to the large area that desert scrub occupies, a resulting large volume of water use from ET was estimated, though it is likely that most of the water transpired by these plants is from precipitation and not groundwater due to their shallow root systems. These results also show that potential saltcedar replacement vegetation such as mesquite and desert scrub do not use as much water because they do not reach the same density levels.

The ET rates of most species were higher in the Alto subarea due to the presence of surface water in the river system, decreasing with distance downstream. The lowest ET values for the different species were found in the Baja subarea where the water table was the deepest and the presence of saltcedar and other tree species was greatly reduced.

Groundwater

The lidar data was used to develop an accurate surface digital elevation model which was used along with groundwater well data and measured depth to groundwater to estimate the groundwater levels throughout the Mojave River area. Groundwater analysis showed that in the Alto and Alto Transition areas, the water levels generally rose between 2008 and 2010, while they decreased in the Centro and Baja subareas.

ET Water Costs

The value of reducing ET of Mojave River vegetation was calculated based on estimated amounts of water lost through ET and current water costs. Acre-feet of water lost through ET across the entire Mojave Basin by vegetation class for 2007 and 2010 are presented in Figure 1.

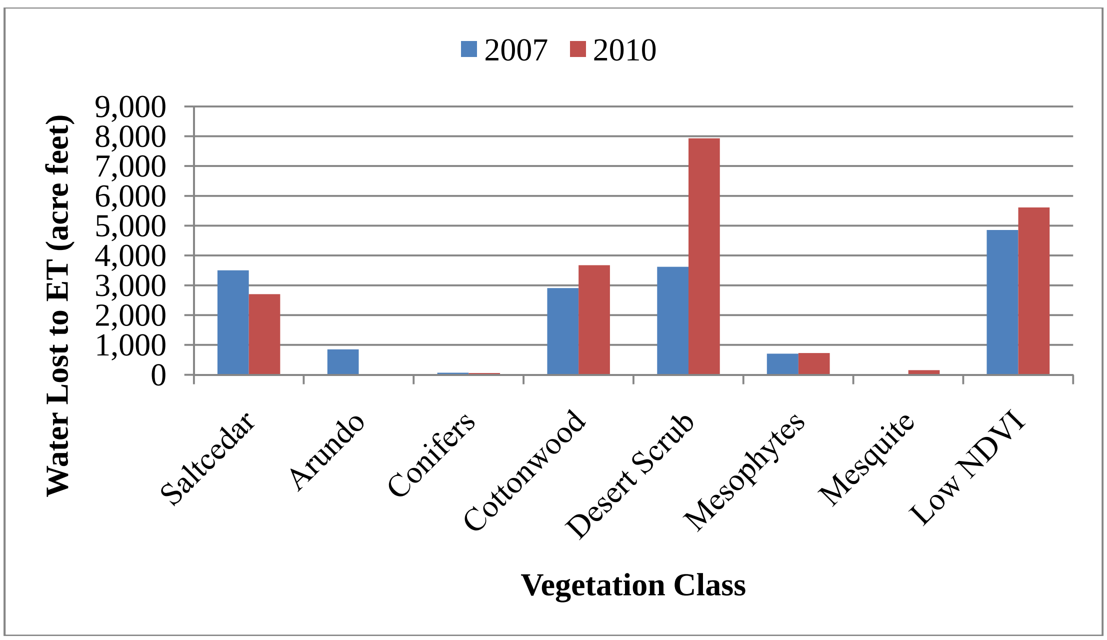

Figure 1. Water lost to ET by vegetation class in the Mojave River Basin, 2007 and 2010.

Saltcedar ET was 3,501 and 2,704 acre feet in 2007 and 2010, respectively, a water use reduction of 797 acre-feet over three years. Using the 2011 cost of $10,221 per acre foot, this translates to costs of $35.8 million in 2007 and $27.6 million in 2010, a reduction of

$8.1 million. These numbers do not include ET reductions from MDRCD's Phase 4 project in the Centro and Baja subareas which occurred after imagery capture.

Reductions in ET cannot be directly measured as additional water available for use within the system. This is due to, among other factors, uncertainties in geomorphologic and hydraulic relationships with ground/surface water interactions within the system, the time delay in the response of groundwater to changes in ET, and measurement variability. Cost savings associated with such water reductions should be interpreted only as general guidelines and not absolute dollar values that could be used in a cost-benefit analysis.

1.0 Introduction

1.1 Study Purpose

The Mojave Basin is located in a dry region of California with low annual precipitation levels of 2 to 8 inches. The population is rapidly increasing throughout the region, and the Mojave Water Agency (MWA) must find the most cost effective methods to supply additional water or reduce water use. One such method currently in use is the removal of non-native vegetation. This study was developed to analyze the amounts of water "saved" as a result of the saltcedar removal effort between 2007 and 2010, and to provide further data and analysis on vegetation along the Mojave River riparian corridor. Study analyses included classification of native and non-native vegetation in the Mojave River floodplain, vegetation evapotranspiration modeling, lidar elevation map development, groundwater mapping, and cost calculations of water transpired.

1.2 Riparian Water Use and Evapotranspiration in the West

Although a vast amount of information is available on water use by riparian species, many concepts are still poorly understood, disputed, and/or controversial. This is largely a reflection of the complex and dynamic water resource systems common to the West. There are few universal rules that can be applied to any given riparian water-use scenario. However, site-specific studies such as this one yield valuable water use information for a specific system.

Evapotranspiration (ET) is the term commonly used for describing riparian vegetation water consumption, and is defined here as the amount of water that transpires through a plant's leaves plus the amount that evaporates from the soil in which the plant is growing.

ET rates will vary considerably depending on:

- Time of day or year (Davenport et al. 1982, Gay and Hartman 1982, Gay 1985, Williams and Anderson 1977, Busch and Smith 1995, Gay and Sammis 1977, Anderson 1982, Cleverly et al. 2002).
- Plant size and age (Schaeffer et al. 2000).
- Depth to groundwater (Blaney 1933, Gatewood et al. 1950, van Hylckama 1974, Gries et al. 2003, Horton et al. 2001).
- Soil moisture availability (Davenport et al. 1982).
- Stand density (Davenport et al. 1982, Sala et al. 1996).
- Leaf area (evaporative surface area, LAI) (Sala et al. 1996, Culler et al 1976, Horton et al. 1959, Davenport et al. 1982).

- Weather and climatic conditions (humidity, temperature, wind speed, aspect and exposure, elevation, length of growing season, etc.) (Busch and Smith 1992, Cleverly et al. 2002, Davenport et al. 1982, Anderson 1982, McNaughton and Jarvis 1991).
- Water and soil salinity (van Hylckama 1970, van Hylckama 1974).

The focus of much research on riparian vegetation water consumption has been on invasive species, primarily of the genus *Tamarix* designated as "saltcedar" (Figure 2.) This genus includes a total of 54 species, ten of which have been introduced in the United States. Four of these species have become invasive in the West: *T. ramosissima*, *T. chinensis, T. canariensis,* and *T. parviflora* (Baum 1967, Gaskin and Schaal 2002, Gaskin and Schaal 2003). For this report, the term "saltcedar" will refer only to these four invasive species and their hybrids. It is differentiated from athel (*Tamarix aphylla,* Figure 2), which is a less aggressive species (although it is becoming invasive in some areas) commonly used as an ornamental, shade tree, or windbreak in northern Mexico and some parts of the southwestern U.S. (Di Tomaso 1998, Gaskin and Shafroth 2005).

Figure 2. Saltcedar (left) and athel (right).

Saltcedar is a native of Eurasia and Africa, introduced intentionally into the United States in the early 1800s. Recent estimates place saltcedar distribution as high as 2 million acres with the potential to invade much greater areas (Robinson 1965, Morisette et al. 2006). It currently infests both lowland (perennial floodplain) and upland (episodic floodplain) terraces along river channels as well as shorelines of reservoirs in all 17 Western States and into southern Canada and northern Mexico. It has very few natural competitors in North America and continues to spread in many areas.

It should be noted that saltcedar often exist as a member of a complex of plant species that contribute to riparian water use, both native and invasive. Common examples of other invasive species are Russian olive (*Elaeagnus angustifolia*), arundo (*Arundo donax*), and Siberian elm (*Ulmus pumila*). Focus of control efforts on a single species may only allow others to become more prolific, negating reductions in water use. Best management approaches will address whole-systems and integrate strategies for suppression/prevention, re-vegetation, maintenance, and monitoring.

Dense stands of saltcedar are generally considered heavy water consumers. Studies estimating the actual water use rates of saltcedar have been inconsistent due to system complexities, measurement imprecision, and methodology discrepancies (e.g. van Hylckama 1974, Nagler et al. 2003, Devitt et al. 1998). Newer methods relying on energy balance measurements and remote sensing models have been more consistent and are generally considered a more accurate measure of evapotranspiration (Westenburg et al, 2006; Coonrod et al, 2001). These studies have shown that the ET of saltcedar is variable and depends on stand density and water table depth. The exact amount of water a stand of saltcedar will use will vary with location, environment, weather, plant size, and other factors such as depth to the groundwater, water quality, and salinity. Therefore, site and time-specific measurements are necessary to produce an accurate estimate of water usage.

Water use by vegetation that will replace saltcedar after removal must also be taken into account when estimating net water savings. Native phreatophytes such as cottonwoods and willows common to the western riparian zones often have water use rates similar or greater than saltcedar. However, the deep root system of saltcedar are capable of reaching the water table at much greater depths (Davenport et al. 1982, Hagemeyer and Waisel 1990, Busch and Smith 1995, Wilkinson 1972, Anderson 1982, Nagler et al. 2003, Glenn et al. 1998, Vandersande et al. 2001, Devitt et al. 1997a&b, Cleverly et al. 1997, Blackburn et al. 1982, Smith et al. 1998, Horton et al. 2001 leaf, Gries et al. 2003, Stromberg 1993). This enables it to spread out over much wider portions of a floodplain and tap greater water supplies. Replacement vegetation along the upper dry terraces of floodplains is often sparse and/or xeric species which transpire much less water than riparian species, including saltcedar.

The net savings of water from saltcedar control is often referred to as “water salvage.” Currently we lack a universal agreement on what specifically constitutes water salvage. However, it is generally agreed that water used by saltcedar is a non-beneficial use of a scarce resource. The relationship between saltcedar removal and a gained availability of water involves complex systems and is not fully understood. Return of surface water to desiccated areas after saltcedar has been cleared has been documented in several cases. However, a direct cause-effect relationship has never been confirmed (Neill 1983, Duncan 1997, Rowlands 1990). Because of this complexity, caution should be used when discussing increased water availability as a reliable benefit of saltcedar removal. Although salvage can be difficult to quantify, non-beneficial water losses to the atmosphere from evapotranspiration are reduced when saltcedar is removed/replaced which will ultimately benefit water users in the arid West.

1.3 Summary of Procedures

Multispectral and thermal infrared imagery and lidar data were collected along the Mojave River on June 29 and June 30, 2010 with the Utah State University (USU) airborne multispectral system and the LASSI Lidar system. The multispectral imagery was rectified using the lidar data and a direct geo-referencing technique to form ortho-mosaics covering the different blocks of multispectral imagery and lidar. The image mosaics were classified into different vegetation and surface types by the Bureau of Reclamation Boulder Canyon Operations Office staff in Boulder City, Nevada using eCognition software. The thermal imagery was rectified to the multispectral ortho-mosaics and calibrated and adjusted for surface emissivity.

Two remote sensing energy balance models were initially applied to the multispectral and thermal infrared imagery acquired in 2010, namely the Two-Source model (Norman et al, 1995) and the SEBAL model (Bastiaanssen et al, 1998). The models estimate the net radiation, soil heat flux, sensible heat flux and obtain latent heat fluxes as a residual from the energy balance equation. The latent heat fluxes derived from the imagery are instantaneous values of ET for the average time of the block over flight. They were used to estimate the reference ET fraction (crop coefficient) by dividing the values by the reference ET estimated from weather data obtained at a local weather station. The fraction is assumed to be constant throughout the daytime hours and allows for extrapolating the ET values over time. Because the imagery was acquired in early summer at full leaf-out of most of the desert species, the ET fraction was assumed to be constant throughout the peak period of evapotranspiration. A crop coefficient curve was generated for each vegetation type assuming green-up and senescence phases on each side of the peak ET period. The crop coefficient was multiplied by the reference ET obtained from a local weather station to obtain seasonal values of ET for the different vegetation types. For the 2007 season, the average values of the crop coefficient for each vegetation type in each groundwater subarea derived with the 2010 data was applied to the 2007 vegetation classification along with the 2007 reference ET values, to obtain the actual seasonal ET and water use for that year.

The Mojave River is divided into four smaller “subareas” (Figure 3). These areas follow a mix of watershed, groundwater basin and geopolitical boundaries for management purposes An area of interest (AOI) polygon was digitized to include the floodplain and the riparian vegetation. This AOI excluded urban areas and upland areas that were removed and at significantly higher elevations than the floodplain, and which are not in future treatment zone areas.

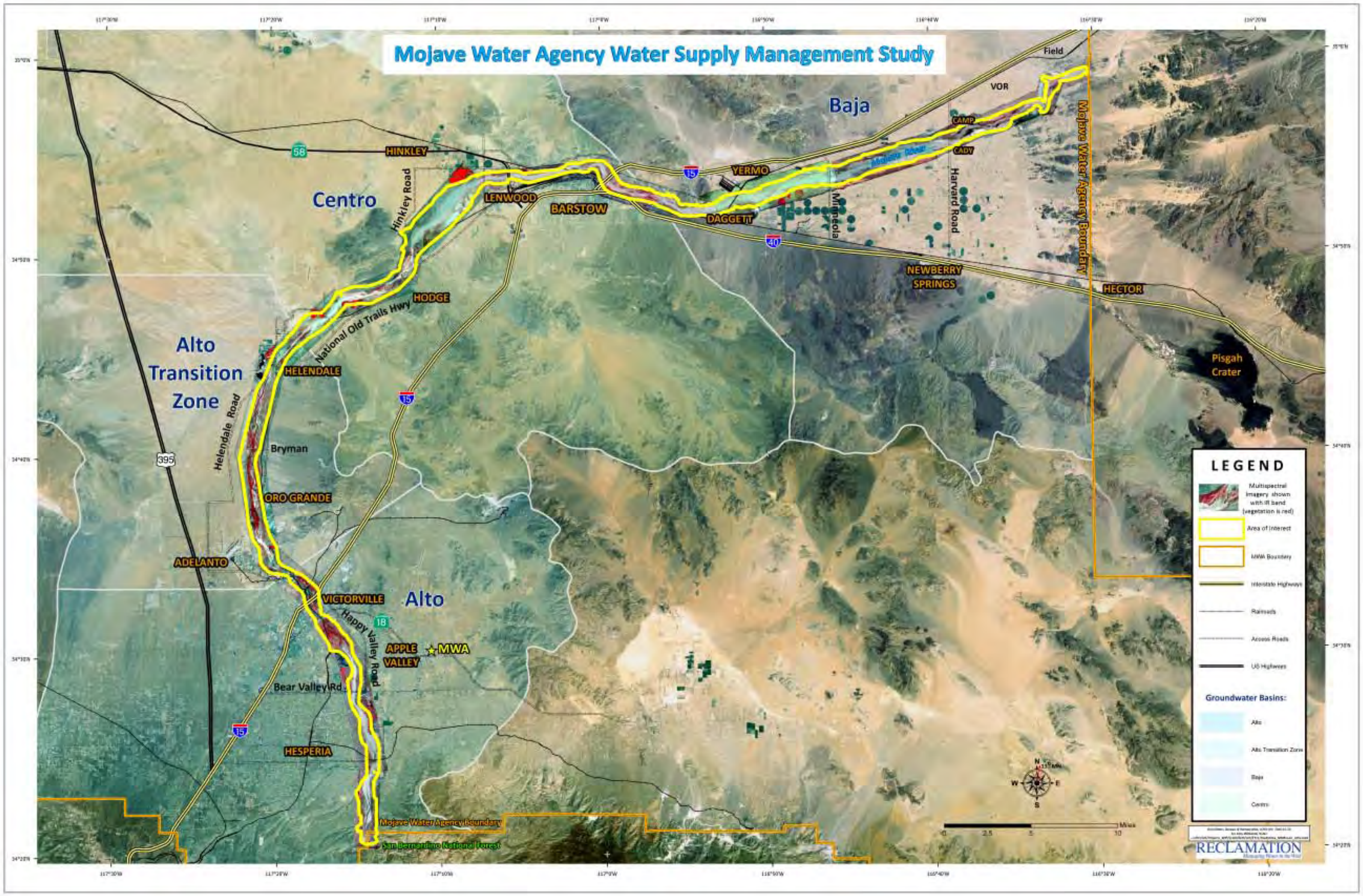

Figure 3. Mojave River study area showing multispectral imagery, area of interest polygon, and the four groundwater management subareas.

Total seasonal ET was estimated for saltcedar and other vegetation types within the AOI by canopy closure categories. Results were summarized for the four groundwater management subareas within the MWA boundaries: Alto, Alto Transition, Centro and Baja.

Cost analysis of water transpired by vegetation was performed based on the estimated ET values and costs of acquiring water per MWA protocols in 2011. Summaries of the values of water used by vegetation are presented by subarea, vegetation class, and canopy closure class for saltcedar.

Regrowth potential of saltcedar is addressed both from anecdotal information from management activities by Mojave Desert Resource Conservation District (MDRCD) from 2008 to 2010, as well as a general review of existing literature.

1.4 Subarea Delineation

Along the aquifer within the Mojave River Study area, subarea boundaries generally coexist with established fault zones or other geologic features which act as natural groundwater basin divides between subareas (Figure 4).

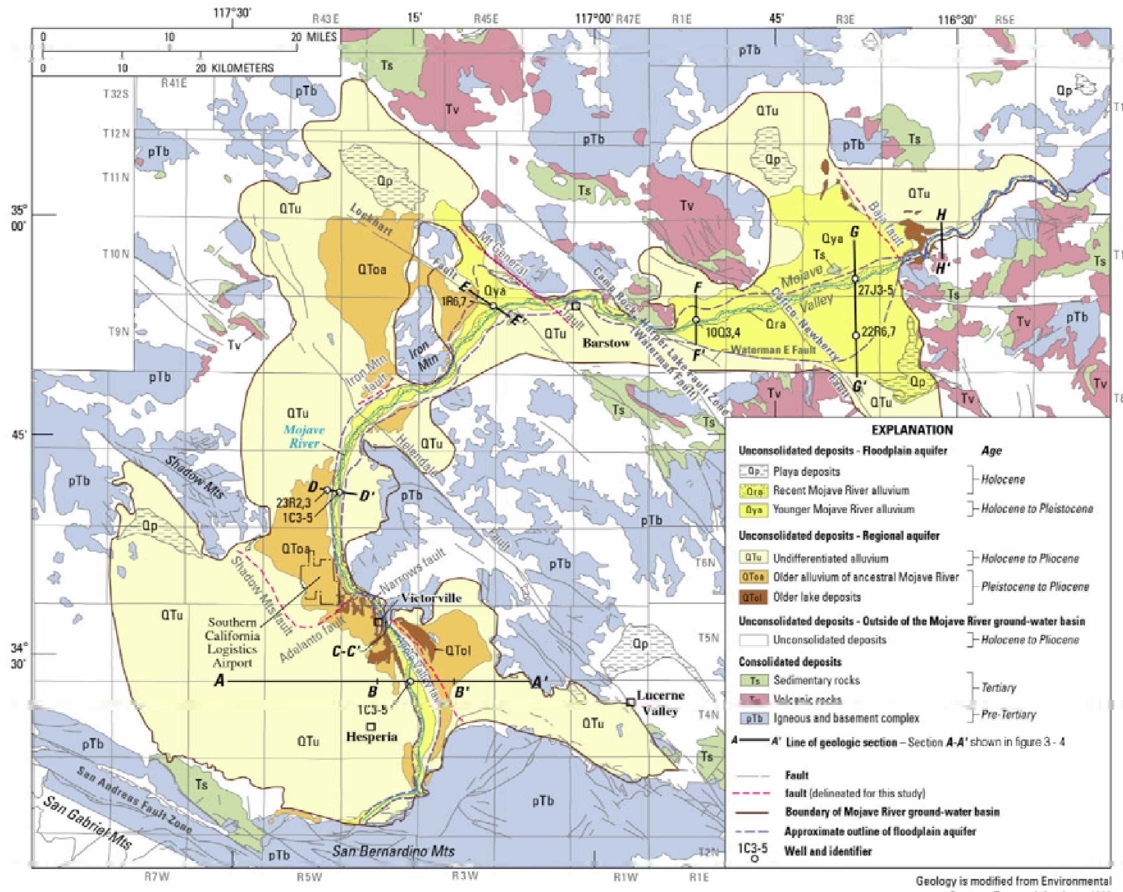

Figure 4. Geologic map of the Mojave River.

Divisions along the Floodplain Aquifer of the Mojave River between subareas are as follows:

Alto to Alto Transition Zone Subareas: A geologic outcropping of non-permeable bedrock referred to as the "Narrows" defines the boundary between the Alto and Alto Transition Zone subareas. This bedrock outcrop constrains the Mojave River to a narrow canyon and the bedrock forces high groundwater to the surface which results in a perennial discharge to the Mojave River.

Alto Transition Zone to Centro Subareas: The boundary between the Alto Transition Zone and the Centro subareas is the approximate location of the Helendale Fault Zone. The Helendale Fault acts as a local horizontal impediment to groundwater flow.

Centro to Baja Subareas: The boundary between the Centro and Baja subareas is the Camp Rock Harper Lake Fault Zone otherwise known as the Waterman Fault. The Waterman fault acts a local horizontal impediment to groundwater flow.

2.0 Methodology

2.1 Data Acquisition

2.1.1 Multispectral and Thermal Infrared Imagery and Lidar Data Acquisition

Multispectral, thermal and lidar imagery acquisition occurred on June 29, 2010 (between 13:30 and 16:30) and on June 30, 2010 (between 11:15 and 16:00). The flight lines were flown in blocks covering the natural orientation of Mojave River reaches. Figure 5 shows the layout of the flight line blocks flown on June 29, 2010, which cover the Baja subarea and a portion of the Centro subarea. These 8 blocks of flight lines were flown from east to west.

Figure 5. Blocks of flight lines flown on June 29, 2010

Figure 6 shows the blocks flown on June 30, 2011 which were flown from south to north and consisted of blocks 9 through 19.

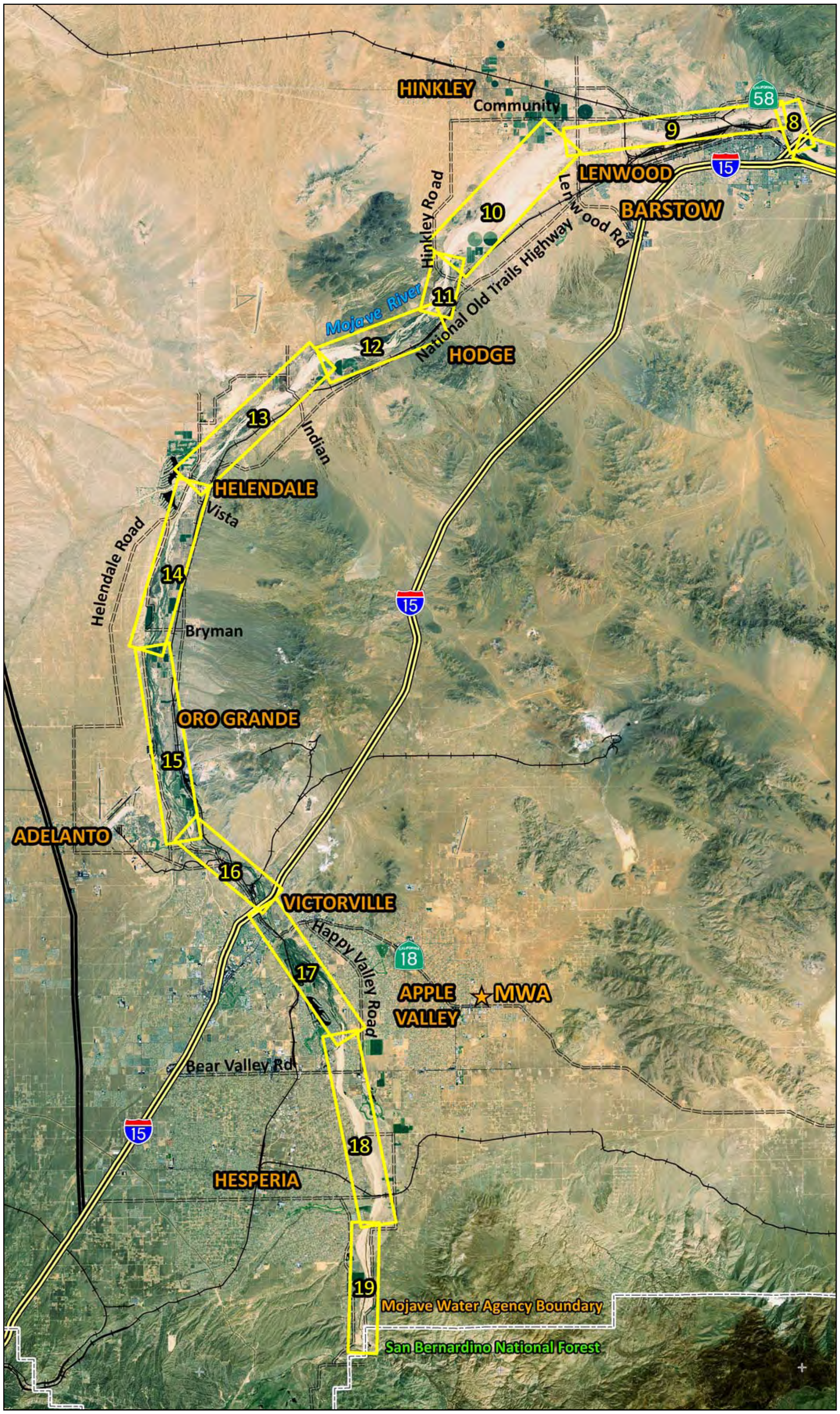

Figure 6. Flight line blocks 9 to 19 flown on June 30, 2010.

2.1.1.1 Multispectral Image Acquisition

The multispectral portion of the airborne system consisted of three Kodak Megaplus 4.2i digital cameras with interference filters forming spectral bands in the green (0.545-0.555 μm), red (0.665-0.675 μm) and near infrared (NIR) (0.790-0.810 μm) wavelengths (Cai and Neale, 1999; Neale and Crowther, 1994). The cameras were mounted alongside the lidar through a porthole in a Cessna TP206 aircraft dedicated to remote sensing missions. The cameras were controlled through special software using Epix boards in a desktop computer mounted in the equipment rack. The system's digital cameras were calibrated against a radiance standard.

A standard reflectance panel with known bi-directional properties was set up in a central location to the study area. An Exotech 4-band radiometer was mounted looking down onto the panel from nadir, measuring incoming irradiance at one-minute intervals. This information is typically used to calculate the reflectance of the pixels in the spectral imagery. However, due to a problem gathering this data during the flight campaign, the shortwave imagery was calibrated using the MODTRAN atmospheric transmission model (Berk et al., 1989) along with the system calibration information to obtain at-surface reflectance values. The MODTRAN model accounts for atmospheric scattering and absorption between the aircraft and the surface, producing accurate surface reflectance values.

The shortwave images were acquired at a nominal pixel resolution of 0.35 meters (m) with an overlap of 80% along the parallel flight lines which covered the Mojave River corridor with the lidar system. The 700 m swath width overlapped laterally at least 30% with the adjacent flight lines.

2.1.1.2 Lidar Data Acquisition

The lidar portion of the airborne system (LASSI Lidar system) consisted of a full-waveform Riegl Q560 lidar transceiver and a Novatel SPAN LN-200 GPS/IMU Navigation System. The lidar was flown at 1000 m above ground level (agl) at a pulse rate of 70,000 shots per second. Given an average flight speed of 180 kilometer per hour and a scan rate of 85 Hertz, this yielded an average shot density of 2.9 shots per square meter. The laser system has beam divergence of less than 0.5 milliradians and therefore resulted in a footprint size of less 0.5 m at 1000 m agl. Given a 50% side-lap specification, an average shot spacing of about two shots per square meter was achieved. The waveform for each shot was digitized at a rate of 500 MHz which yielded a range resolution of 0.3 m. Though not independently verified through field ground truthing, with an examination of the post-processing statistics for the navigation and lidar systems, an absolute vertical and horizontal accuracy of 8 cm and 15 cm respectively was achieved.

2.1.1.3 Thermal Infrared Image Acquisition

The airborne system included a FLIR SC640 thermal infrared camera which acquired thermal images in the 8 – 12 μm range. This instrument was mounted through a porthole aligned with the multispectral system cameras. The thermal infrared imagery was extracted from the digital video files generated during the flight at an 80% overlap. These individual images were rectified to the multispectral ortho-mosaic.

2.1.2 Groundwater Depth Acquisition

The U.S. Geological Survey (USGS) has conducted water well and associated groundwater (GW) studies for the area in and around the Mojave River every two years over the last two decades. These data are available for the Mojave River subareas through the National Water Information System (NWIS) at http://ca.water.usgs.gov/mojave/.

In June 2010, USU flew lidar and multispectral imagery over the Mojave River study area. The lidar mission provided high-accuracy ground surface topology by using the Bare Earth returns, and subtracting-out any canopy returns. The lidar data were interpolated into 1-foot contours by USU, and provided to Reclamation’s GIS Group (LCRO-GIS).

USGS groundwater elevation measurements were taken in Spring 2008, and again in the Spring of 2010. Using USU’s high-accuracy lidar surface elevations, LCRO-GIS subtracted the USGS depth to groundwater measurements at each well site within the study area to determine accurate groundwater elevation values for the years 2008 and 2010. Groundwater elevations fluctuate due to seasonal changes, but the principal GW elevations and lidar were captured by both USGS and USU at similar times of year. The temporal changes in GW elevations were compared between the years 2008 and 2010.

2.2 Data Processing

2.2.1 Multispectral Image Processing and Mosaics

The individual spectral band images were geometrically corrected for radial distortions and also radiometrically adjusted for lens vignetting effects and registered into 3-band images. These images were ortho-rectified using the lidar data. This was done using the geometric calibration parameters of the cameras and the lidar terrain parameters along with the positioning information from the lidar Novatel navigation system and local ground GPS base station. The ground station is at the Barstow-Daggett Airport and nearby Continuously Operating Reference Station Global Positioning System (GPS) base station data were used to triangulate and obtain a precise position for the local station.

The rectified images were mosaicked into larger image strips along the flight lines and stitched together to form a mosaic covering each block of imagery and lidar flown. The mosaic was calibrated in terms of reflectance and cut into tiles covering sections of the floodplain. The mosaics for Blocks 1 and 2 (See Figure 5) within the Baja subarea are shown in Figures 7 and 8. A detail of the Block 1 imagery is shown in Figure 9.

Figure 7. Calibrated multispectral orthomosaic of Block 1 in the Baja Subarea.

Figure 8. Calibrated multispectral orthomosaic of Block 2 in the Baja Subarea.

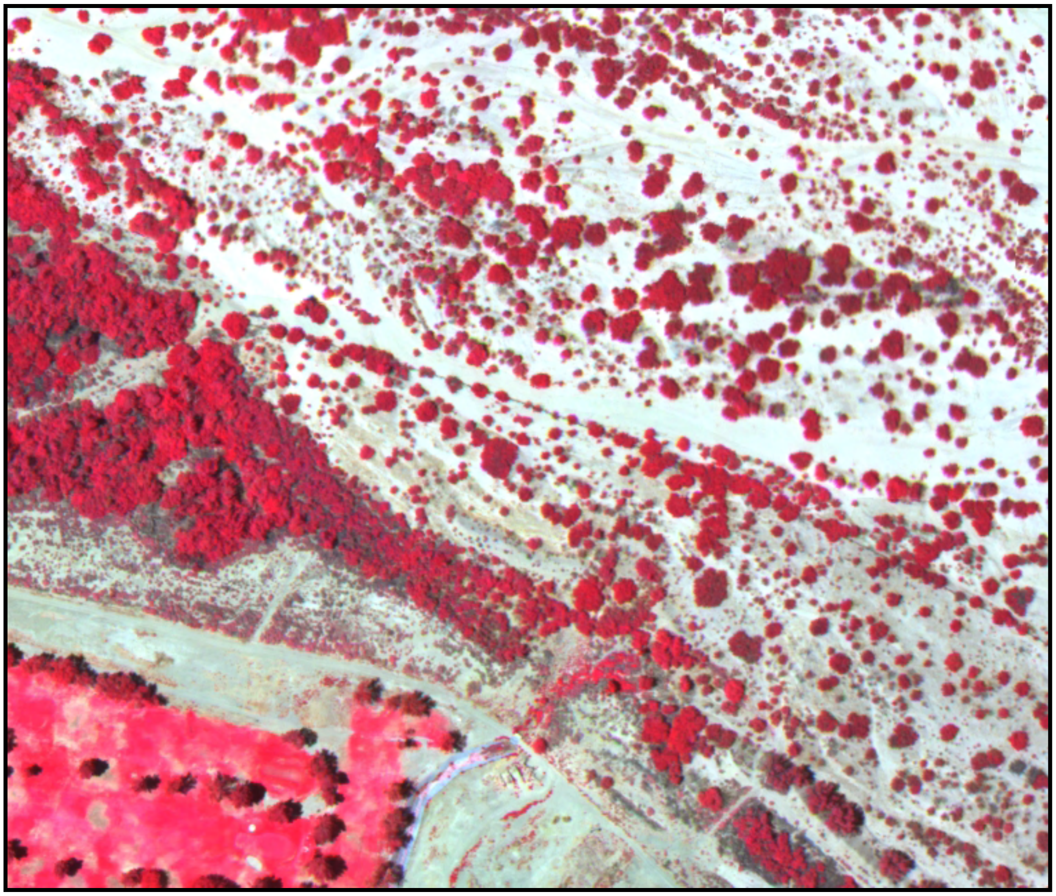

Figure 9. Detail of 3-band multispectral mosaic of Block 1. Vegetation is red.

The multispectral mosaics were sent to the Reclamation Boulder Canyon Operations Office for classification by vegetation type. The eCognition software was used to obtain different surface classes of interest to the Study (see Section 2.3 for further information).

2.2.2 Thermal Infrared Image Processing

The thermal images corresponding to the vegetated floodplain were rectified to the 3-band ortho-mosaic and stitched along the flight lines forming strips that were calibrated using the system calibration to obtain at-surface temperatures. The strips were stitched forming a mosaic of the vegetated floodplain.

The MODTRAN atmospheric transmission model (Berk et al., 1989) was used to correct for atmospheric effects on the imagery as well as the emissivity of the surface. Radiosonde data of temperature and water vapor in the atmospheric profile required to run the model were obtained from radiosondes at a nearby representative airport. Surface emissivity typically varies from 0.9 from a white sandy soil to 0.98 from a full canopy lush vegetation. The emissivity correction followed the method by Brunsell and Gillies (2002) using the fraction of vegetation cover obtained from scaling the Normalized Difference Vegetation Index (NDVI) generated from the calibrated 3-band imagery. The resulting product was an at-surface temperature mosaic at the time of image acquisition. An average time for the center of each mosaicked block of imagery was used for the ET calculations.   Figure 10 shows the thermal IR mosaic for Block 1. The coolest temperatures are in purple and dark blue occurring at a water body, the alfalfa field and portions of the golf course. Most of the saltcedar are in light blue showing cooler temperatures due to transpiration while most of the remaining sparser vegetation is in green. Bare soils are very hot in yellow and orange with temperatures reaching the upper 50 degrees Celsius.

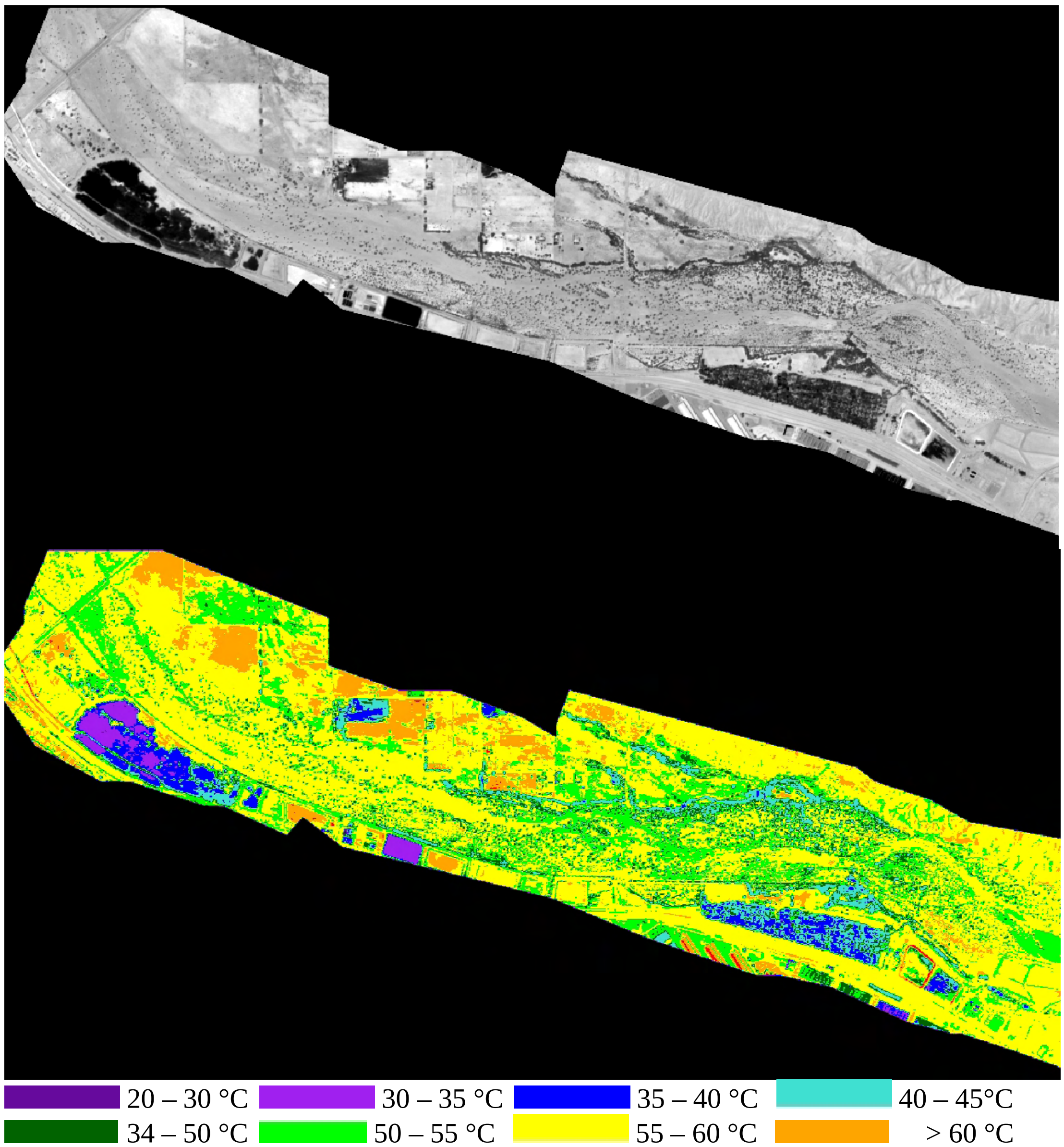

Figure 10. Calibrated Thermal IR mosaic of Block 1 (see Figure 5) in the Baja subarea, in grayscale (top) and colorized according to temperature ranges (bottom).

2.2.3 Lidar Data Processing

Lidar point clouds were created by combining GPS/Inertial Measurement Unit trajectory data with lidar scanner data using proprietary system-specific software. The points were then classified using custom macros developed for differentiating vegetation, buildings, bare-earth, and points generated by system noise. This was supplemented with hand classifications in areas where feature types were mixed together (e.g. where trees overhang buildings). As a part of this process, the classification algorithm was custom-tuned to Mojave River terrain using visualization of results in representative areas. The point data tiles were delivered in the LAS v.1.2 file format. A sample plot of one of these tiles, colored blue to red by elevation, is shown in Figure 11. Note the subtleties in the channel patterns of the Mojave River apparent in the Figure.

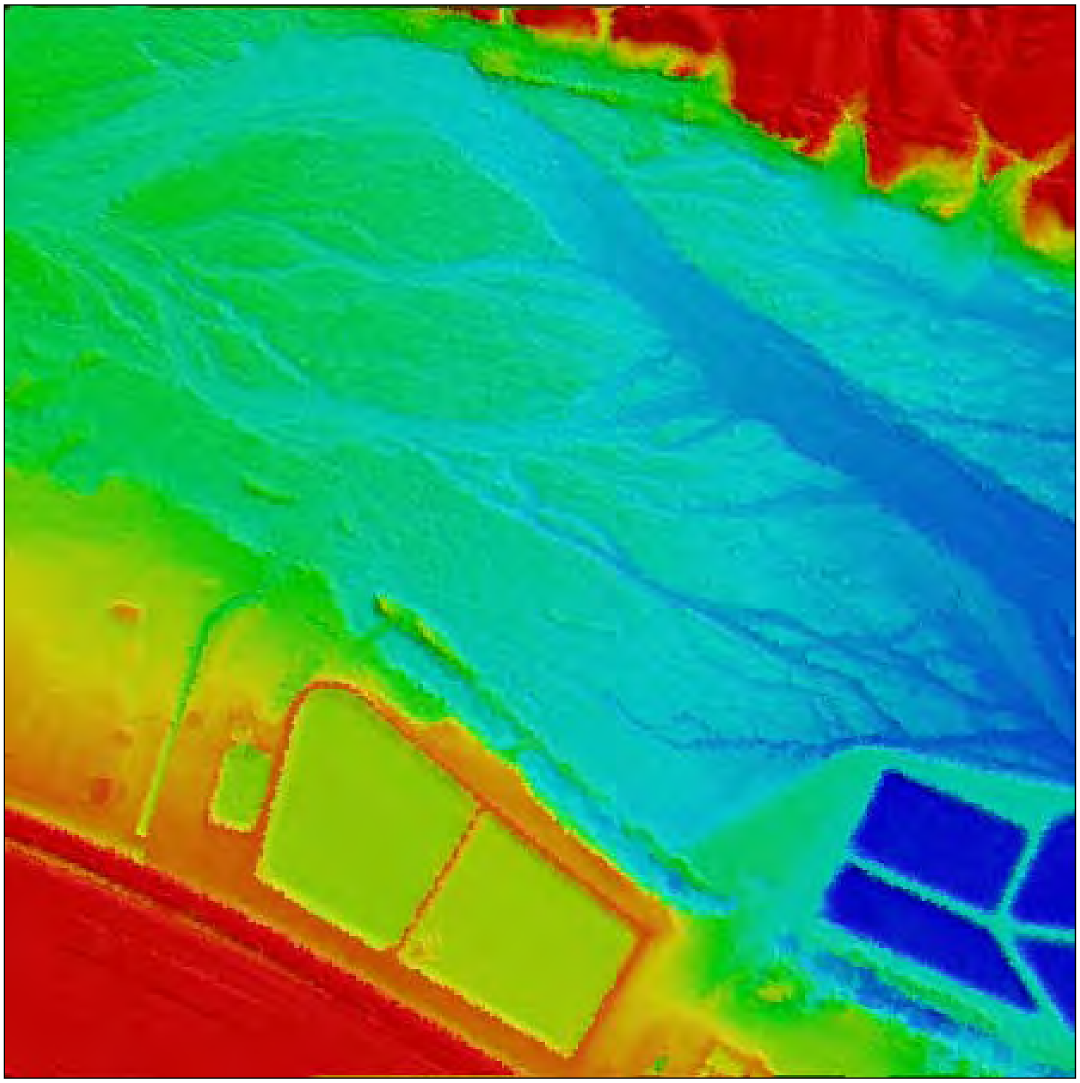

Figure 11. Example plot and individual lidar tile delivered in LAS v.1.2 format (blue colors are lower elevations while red colors are higher elevations). See lower right corner of images in Figure 10 for reference.

A digital elevation model (DEM) compatible with ArcGIS was subsequently created from the randomly distributed lidar points. This was created and delivered at a cell size of 1 square meter. This DEM was derived only using points classified as bare earth so bridges and other structures crossing the Mojave River were removed. The DEM tiles were delivered in the ESRI Binary Grid file format.

The classified point cloud vegetation returns were used to develop a canopy height layer on a 1-meter grid basis, for use in the two energy balance models tested. Figure 12 shows the lidar point cloud profile for a section of Block 1 above the corresponding multispectral image.

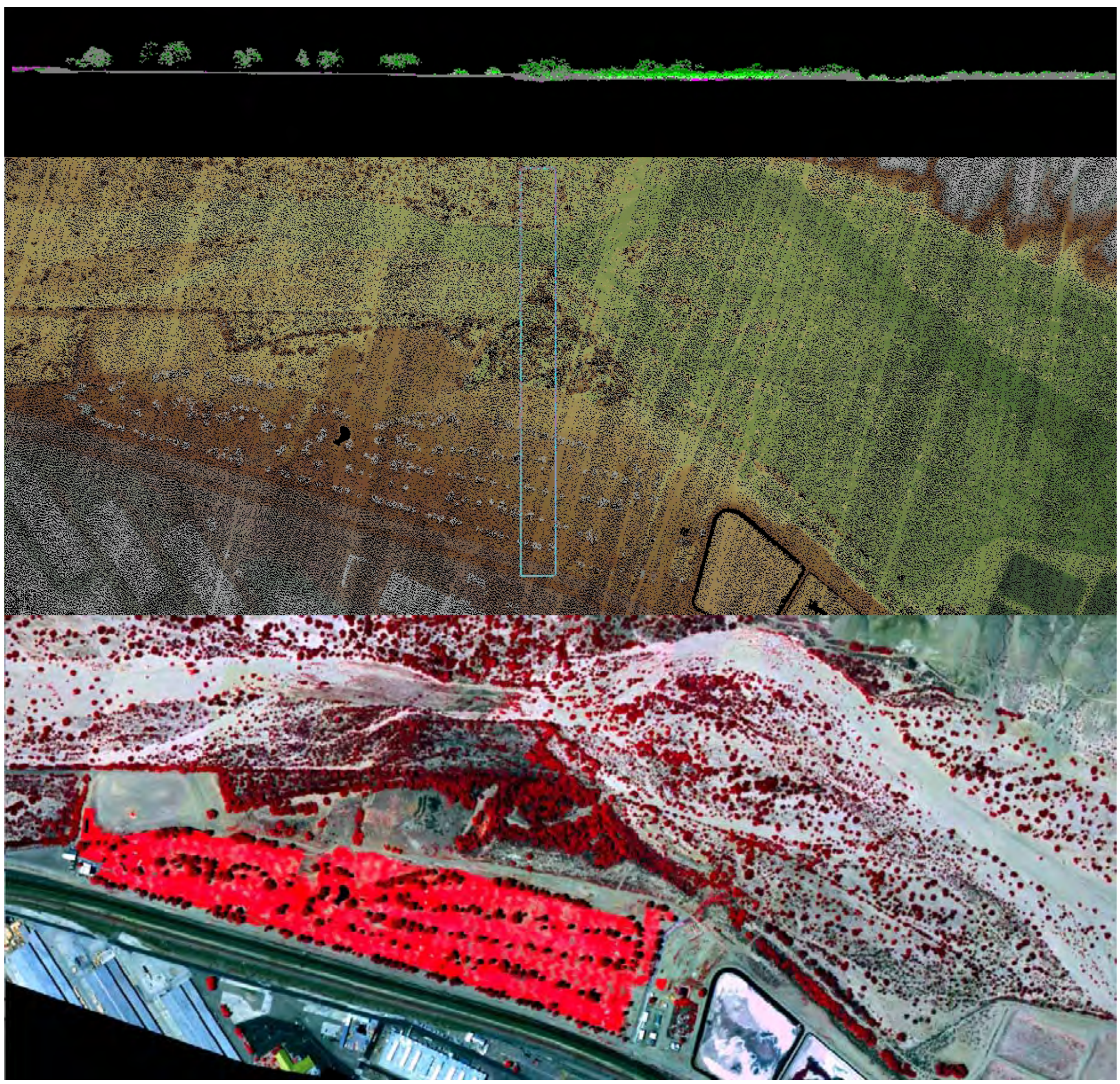

Figure 12. Lidar point cloud profile (top) shown on a section of block 1 lidar (middle) and corresponding multispectral image (bottom).

After model comparison analysis, the Two-Source model with lidar-based canopy heights was chosen to estimate ET for all image blocks along the Mojave River as it runs faster than the SEBAL model, was formulated to work in sparse vegetative environments and does not depend on the subjective process of selecting a hot and cold pixel in the image as SEBAL does.

2.2.4 Groundwater Data Processing

ArcGIS 3D Analyst's Raster interpolator was used to create a raster surface of the USGS groundwater elevations. Similarly, raster surfaces of USU's 2010 lidar-derived surface contour data were generated. Using ArcGIS 3D Analyst's Functional Surface – Surface Spot tool, the USGS depth to groundwater measurements were subtracted from USU's lidar surface elevations in order to derive spot groundwater elevation values within the floodplain of the Mojave River Study Area. Each of the wells within the study area were assigned spot groundwater elevations, as shown Table 2.

Table 2. Groundwater elevation changes for Mojave River Study Area wells.

ID Number	State Well ID [1]	Measurement Date [2]	LiDAR Surface 2010 [3]	Depth to GW 2010 [4]	GW Elevation 2008 [5]	GW Elevation 2010 [6]	GW Elevation Change 2010 - 2008 [7]
0	003N004W12Q002S	3/12/2008	2989	97	2891	2892	1
1	003N004W12G002S	4/11/2008	2973	71	2902	2902	0
3	004N004W36R001S	3/1/2008	2925	29	2881	2896	15
4	004N004W36Q001S	3/1/2008	2923	33	2877	2890	13
5	004N003W31L006S	3/12/2008	2921	46	2872	2875	3
6	004N003W31L007S	3/12/2008	2921	53	2864	2868	4
7	004N003W31L008S	3/12/2008	2921	54	2865	2867	2
8	004N003W31L009S	3/12/2008	2921	51	2867	2870	3
9	004N004W36G003S	3/1/2008	2935	86	2839	2849	10
21	004N003W30D005S	3/12/2008	2897	71	2819	2826	7
22	004N003W30A006S	4/10/2008	2895	69	2824	2826	2
23	004N003W19G002S	3/7/2008	2886	74	2808	2812	4
24	004N003W19G003S	3/7/2008	2886	75	2808	2811	3
25	004N003W19G004S	3/7/2008	2886	69	2813	2817	4
26	004N003W19G005S	3/7/2008	2886	28	2844	2858	14
27	004N003W19G006S	3/7/2008	2886	27	2852	2859	7
28	004N003W19M001S	3/12/2008	2905	94	2808	2811	3
49	004N004W01C002S	3/12/2008	2825	32	2790	2793	3
50	004N004W01C003S	3/12/2008	2825	54	2769	2771	2
51	004N004W01C004S	3/12/2008	2825	51	2771	2774	3
52	004N004W01C005S	3/12/2008	2825	21	2784	2804	20
53	005N004W25Q001S	3/10/2008	2794	17	2771	2777	6
54	005N004W25N001S	4/7/2008	2791	39	2749	2752	3
56	005N004W23R003S	3/12/2008	2775	20	2753	2755	2
57	005N004W23R004S	3/12/2008	2775	12	2762	2763	1
58	005N004W23R005S	3/12/2008	2775	15	2762	2760	-2
59	005N004W23A002S	3/1/2008	2783	38	2723	2745	22
63	005N004W15K001S	3/10/2008	2747	6	2731	2741	10
65	005N004W14D001S	3/10/2008	2730	17	2654	2713	59
66	005N004W14D002S	3/10/2008	2730	5	2709	2725	16
67	005N004W14D003S	3/10/2008	2730	13	2713	2717	4
68	005N004W14D004S	3/10/2008	2730	14	2715	2716	1
69	005N004W10N004S	3/1/2008	2875	156	2715	2719	4
71	005N004W11N004S	3/1/2008	2783	18	2700	2765	65
75	005N004W03P003S	4/10/2008	2705	10	2694	2695	1
76	006N004W33N001S	3/10/2008	2681	10	2670	2671	1
77	006N004W34M012S	3/1/2008	2711	41	2665	2670	5
79	006N004W34M010S	3/1/2008	2729	57	2669	2672	3
80	006N004W34E002S	3/1/2008	2737	61	2676	2676	0
81	006N004W30R001S	3/10/2008	2650	15	2629	2635	6
82	006N004W30R002S	3/10/2008	2650	15	2630	2635	5
83	006N004W30R003S	3/10/2008	2650	12	2635	2638	3
85	006N004W29M001S	3/12/2008	2647	11	2636	2636	0
86	006N004W30J005S	3/10/2008	2642	9	2632	2633	1
90	006N004W30D010S	3/20/2008	2698	79	2617	2619	2
91	006N004W19K001S	4/21/2008	2621	9	2610	2612	2
96	006N004W19C008S	4/21/2008	2611	13	2575	2598	23
97	006N005W13G008S	3/10/2008	2611	1	2609	2612	3
98	006N005W12P002S	4/22/2008	2620	22	2597	2598	1

ID Number	State Well ID [1]	Measurement Date [2]	LiDAR Surface 2010 [3]	Depth to GW 2010 [4]	GW Elevation 2008 [5]	GW Elevation 2010 [6]	GW Elevation Change 2010 - 2008 [7]
99	006N005W12K001S	3/10/2008	2592	4	2588	2588	0
100	006N005W12H001S	3/20/2008	2581	14	2565	2567	2
101	006N005W12G004S	3/10/2008	2570	4	2564	2566	2
102	006N005W12G001S	3/10/2008	2573	3	2571	2570	-1
104	006N005W01A006S	3/10/2008	2546	24	2521	2522	1
105	006N005W01A007S	3/10/2008	2546	23	2521	2523	2
106	006N005W01A008S	3/10/2008	2546	23	2522	2523	1
109	006N005W01C001S	3/6/2008	2547	1	2543	2546	3
110	006N005W01C002S	3/6/2008	2547	1	2543	2546	3
116	007N005W25K006S	4/21/2008	2521	10	2510	2511	1
118	007N005W24R005S	3/10/2008	2505	66	2437	2439	2
119	007N005W24R007S	3/10/2008	2505	28	2476	2477	1
120	007N005W24R008S	3/10/2008	2505	9	2494	2496	2
121	007N005W24R013S	3/10/2008	2507	6	2500	2501	1
122	007N005W24R012S	3/10/2008	2510	26	2483	2484	1
123	007N005W24R011S	3/10/2008	2509	26	2482	2483	1
124	007N005W24R009S	3/10/2008	2505	5	2499	2500	1
128	007N005W13H001S	3/10/2008	2475	13	2461	2462	1
129	007N005W13H001S	3/10/2008	2475	13	2461	2462	1
130	007N005W13H002S	3/10/2008	2475	4	2471	2471	0
131	007N005W13H003S	3/10/2008	2476	4	2472	2472	0
133	007N004W06N001S	3/6/2008	2489	33	2457	2456	-1
135	008N004W29E003S	3/6/2008	2409	16	2393	2393	0
136	008N004W29E004S	3/6/2008	2409	16	2394	2393	-1
137	008N004W29E005S	3/6/2008	2409	15	2395	2394	-1
138	008N004W29E006S	3/6/2008	2409	12	2397	2397	0
139	008N004W21M001S	3/6/2008	2389	10	2378	2379	1
140	008N004W21M002S	3/6/2008	2389	9	2380	2380	0
141	008N004W21M003S	3/6/2008	2389	5	2383	2384	1
142	008N004W21M004S	3/6/2008	2389	7	2381	2382	1
144	008N003W07H003S	4/24/2008	2319	25	2296	2294	-2
145	008N003W08B002S	4/24/2008	2306	15	2293	2291	-2
146	008N004W12C001S	3/6/2008	2352	41	2313	2311	-2
148	008N003W04A007S	3/6/2008	2274	17	2259	2257	-2
149	009N003W34N006S	4/24/2008	2265	11	2255	2254	-1
150	009N003W34D003S	3/25/2008	2268	28	2241	2240	-1
153	009N003W22J004S	3/6/2008	2233	68	2184	2165	-19
159	009N003W23D002S	3/6/2008	2225	64	2174	2161	-13
160	009N003W23C001S	3/6/2008	2222	71	2167	2151	-16
161	009N001E20B003S	4/29/2008	2047	129	1921	1918	-3
162	009N003W14N001S	3/6/2008	2225	64	2175	2161	-14
164	009N001W13H002S	3/27/2008	2007	27	1987	1980	-7
165	009N001E16F001S	3/4/2008	1963	148	1822	1815	-7
166	009N001E16F002S	3/4/2008	1963	148	1822	1815	-7
167	009N001E16F003S	3/4/2008	1963	148	1822	1815	-7
168	009N001E16F004S	3/4/2008	1963	149	1820	1814	-6
169	009N001E15H001S	3/4/2008	1941	157	1789	1784	-5
171	009N001W12N004S	3/4/2008	2004	28	1982	1976	-6
172	009N001W12N005S	3/4/2008	2004	22	1988	1982	-6
173	009N001W12N006S	3/4/2008	2004	22	1988	1982	-6
174	009N001W12N007S	3/4/2008	2004	22	1988	1982	-6
176	009N001W10J012S	3/11/2008	2033	17	2017	2016	-1

ID	State Well	Measurement	LiDAR Surface	Depth to GW	GW Elevation		GW Elevation
177	009N001W10J013S	3/4/2008	2033	17	2016	2016	0
178	009N001W10J014S	3/4/2008	2033	16	2020	2017	-3
179	009N001W10J015S	3/4/2008	2033	16	2020	2017	-3
180	009N001W12L002S	3/4/2008	2007	18	1993	1989	-4
181	009N001W12L004S	3/4/2008	2007	21	1993	1986	-7
182	009N001W12L005S	3/4/2008	2007	20	1994	1987	-7
183	009N001W11K012S	3/4/2008	2019	8	2011	2011	0
184	009N001W11K013S	3/4/2008	2019	12	2009	2007	-2
185	009N001W11K014S	3/4/2008	2019	10	2011	2009	-2
186	009N001W11K015S	3/4/2008	2019	10	2011	2009	-2
187	009N001E10Q002S	3/4/2008	1950	167	1788	1783	-5
188	009N001E10Q003S	3/4/2008	1950	167	1788	1783	-5
189	009N001E10Q004S	3/4/2008	1950	167	1788	1783	-5
190	009N001W09D005S	3/4/2008	2086	19	2070	2067	-3
191	009N001W09D006S	3/4/2008	2086	26	2060	2060	0
192	009N001W09D007S	3/4/2008	2086	38	2049	2048	-1
193	009N001W09D008S	3/4/2008	2086	50	2037	2036	-1
194	009N001W04R002S	3/4/2008	2047	12	2038	2035	-3
195	009N001W04R003S	3/4/2008	2047	13	2036	2034	-2
196	009N001W04R004S	3/4/2008	2047	13	2036	2034	-2
197	009N002W05N007S	3/25/2008	2180	72	2115	2108	-7
198	009N003W01R005S	3/6/2008	2195	73	2131	2122	-9
199	009N003W01R006S	3/6/2008	2195	73	2127	2122	-5
200	009N003W01R007S	3/6/2008	2195	73	2132	2122	-10
201	009N002W05N008S	3/6/2008	2182	71	2119	2111	-8
202	009N002W06P002S	3/6/2008	2187	62	2136	2125	-11
203	009N002W06P001S	3/6/2008	2183	63	2130	2120	-10
204	009N002W06M007S	3/6/2008	2187	68	2130	2119	-11
205	009N002W06L011S	3/6/2008	2183	67	2125	2116	-9
206	009N002W06L012S	3/6/2008	2183	65	2128	2118	-10
207	009N002W06L013S	3/6/2008	2183	66	2128	2117	-11
208	009N002W06L014S	2/4/2008	2183	0	2133	2183	50
209	009N001W04M005S	3/4/2008	2072	35	2041	2037	-4
210	009N001W04M006S	3/4/2008	2072	35	2041	2037	-4
211	009N001W04M007S	3/4/2008	2072	35	2041	2037	-4
212	009N002W01F001S	3/16/2008	2122	70	2061	2052	-9
213	009N002W01F002S	3/16/2008	2122	70	2060	2052	-8
214	009N002W06H006S	3/6/2008	2176	71	2112	2105	-7
215	009N002E03K005S	3/4/2008	1853	74	1781	1779	-2
216	009N002E03K006S	3/4/2008	1853	74	1782	1779	-3
217	009N002E03K007S	3/4/2008	1853	75	1782	1778	-4
218	009N002E03K008S	3/4/2008	1853	74	1782	1779	-3
220	009N002W03E001S	3/4/2008	2142	61	2089	2081	-8
221	009N002W03E002S	3/4/2008	2142	62	2089	2080	-9
222	009N002W03E003S	3/4/2008	2142	61	2090	2081	-9
223	009N002W02E001S	3/4/2008	2135	61	2082	2074	-8
224	009N002W01A002S	3/4/2008	2102	52	2059	2050	-9
225	009N002E03G006S	3/4/2008	1843	134	1713	1709	-4
226	009N002E03G007S	3/4/2008	1843	134	1713	1709	-4
227	009N002E03G008S	3/4/2008	1843	132	1715	1711	-4
228	009N002E03G009S	3/4/2008	1843	131	1716	1712	-4
229	009N002W02B005S	3/4/2008	2122	63	2070	2059	-11

ID Number	State Well ID [1]	Measurement Date [2]	LiDAR Surface 2010 [3]	Depth to GW 2010 [4]	GW Elevation 2008 [5]	GW Elevation 2010 [6]	GW Elevation Change 2010 - 2008 [7]
233	010N001W32Q004S	3/4/2008	2076	38	2046	2038	-8
234	010N001W31L007S	3/16/2008	2096	44	2061	2052	-9
235	010N001W32F012S	3/4/2008	2086	43	2051	2043	-8
238	010N003E26Q001S	5/1/2008	1763	64	1698	1699	1
239	010N003E27J001S	3/3/2008	1751	46	1709	1705	-4
240	010N003E27J002S	3/3/2008	1751	47	1706	1704	-2
241	010N003E27J003S	3/3/2008	1751	48	1705	1703	-2
242	010N003E27J004S	3/3/2008	1751	48	1705	1703	-2
245	010N003E25A002S	5/1/2008	1714	19	1696	1695	-1
246	010N004E19N004S	3/3/2008	1703	11	1694	1692	-2
247	010N004E19N003S	4/7/2008	1703	5	1699	1698	-1
248	010N004E19N002S	4/7/2008	1703	2	1699	1701	2
249	010N004E19M006S	3/3/2008	1707	7	1701	1700	-1
250	010N004E19M002S	3/3/2008	1717	13	1705	1704	-1
251	010N004E20D001S	3/26/2008	1737	166	1571	1571	0
252	010N004E11E001S	5/2/2008	1611	18	1594	1593	-1
254	010N004E11C001S	5/2/2008	1601	26	1577	1575	-2

Footnotes:

1. Well identifier as listed in the USGS National Well Information System.
2. Well Depth to GW measurements taken in March/April 2008; same time period for 2010 measurements.
3. Land surface elevations from high-accuracy LiDAR, provided by Utah State University, June 2010.
4. Depth to GW calculations from USGS-NWIS. Measurements taken in 2008 and 2010 were subtracted from the LiDAR surface to derive GW elevations. Only 2010 Depth to GW measurements are shown.
5. Groundwater elevations calculated from high-accuracy LiDAR (2010), minus Depth to GW for 2008 and 2010.
6. Ibid.
7. Negative (-) numbers indicate lowering GW elevations between 2008 and 2010.

2.2.5 Area of Interest Delineation

As the main data output needed from this Study is the evapotranspiration by vegetation species with access to groundwater within and near the floodplain, it was necessary to limit the calculation of ET statistics to the river bottom, the riparian zone and upland areas immediately adjacent to the floodplain. As the acquired lidar data and multispectral and thermal imagery covered areas beyond the floodplain, an Area of Interest (AOI) polygon was hand digitized over the multispectral ortho-mosaics to delineate the vegetated areas in the floodplain and adjacent uplands while excluding urban areas and upland areas at higher elevations removed from the floodplain (Figure 13). The AOI served as a guide for processing the thermal infrared imagery and classification of the multispectral imagery into vegetation types and cover density classes, which were input into the ET modeling.

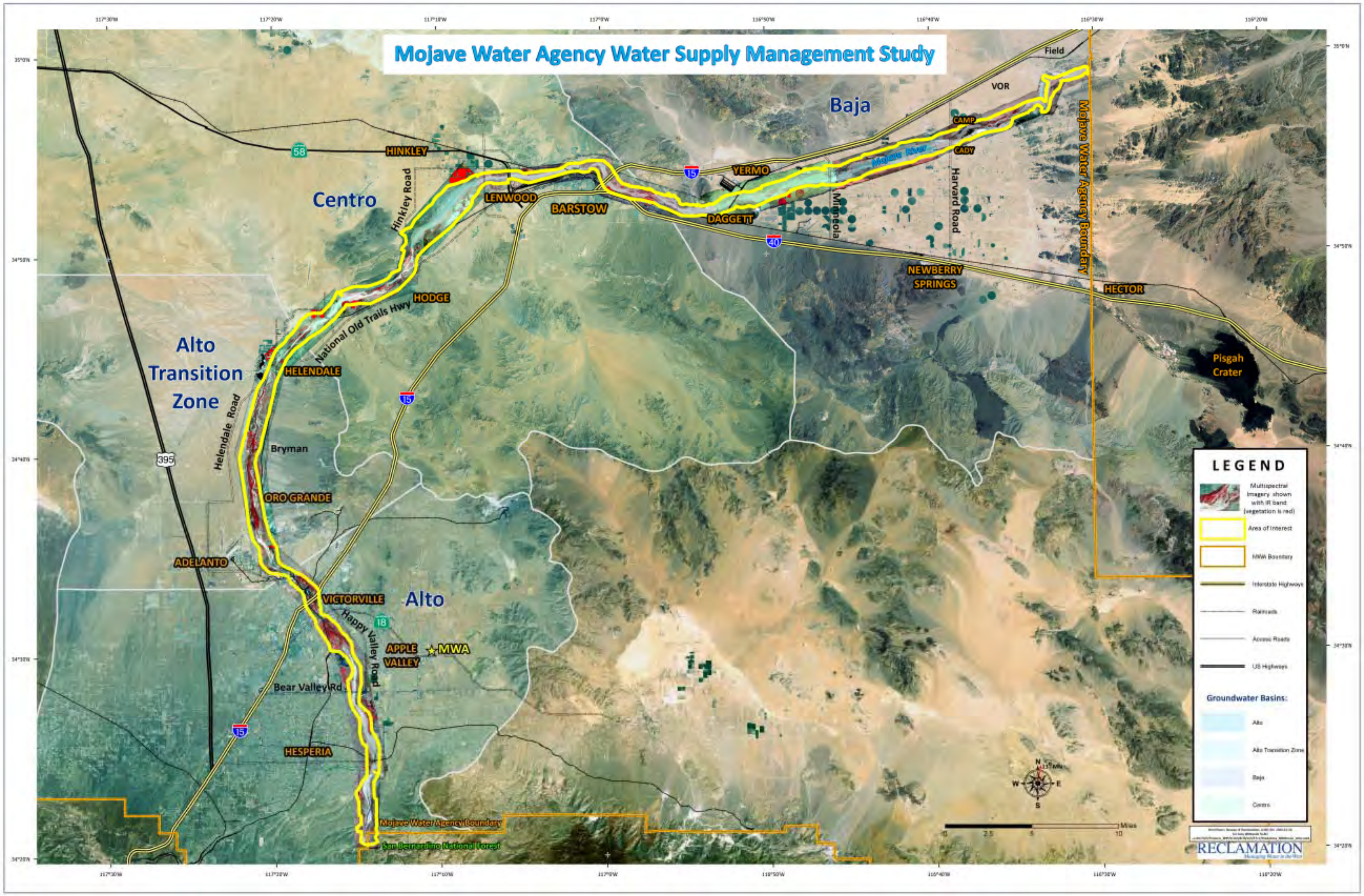

Figure 13. Area of Interest (AOI) polygon of the Mojave River Floodplain used for the evapotranspiration calculation and summary statistics.

2.3 Classification of Vegetation Resources

Vegetation was classified within the AOI for 2007 and 2010 (see Section 3.1 figures). The 2010 classification was completed using calibrated 3-band multispectral image ortho-mosaics acquired by USU. The 2007 classification was completed using 3-band, ortho-rectified multispectral imagery provided by MWA.

Both image sets were acquired during the summer of each respective year. It should be noted that there are certain errors inherent in mapping vegetation as a function of the nature of the vegetation as well as the pixel resolution of the imagery being used. Typically, vegetation such as desert scrub, that has a low leaf area index, is more difficult to differentiate in multispectral imagery. Additionally, any single plants or groups of plants that are close to or less than the size of the pixel resolution of the imagery are also difficult to differentiate. Since desert scrub communities tend to be single small plants in sparse stands, it is probable that there may be significant error in the classification with respect to this vegetation class. Additionally, small, individual saltcedar smaller than the pixel resolution of 1 meter were not captured in the classification.

ERDAS Imagine software was used to pre-process the MWA-supplied 2007 imagery and the 2010 imagery acquired by USU. This preprocessing was completed so that both image sets had the same pixel resolution of 1 meter, were in the same Universal Transverse Mercator (UTM) geographic projection, and were both digital integer (non-floating point) images.

For 2007 imagery, 10 processing areas were created by mosaicking smaller image tiles together and masking the imagery to the AOI polygon. For 2010 imagery, 19 processing areas were created and masked to the AOI polygon. Multiple processing areas were required primarily as a function of image processing file size limitations. Because project scheduling required that 2007 image processing begin before 2010 imagery was acquired, image processing areas could not be the same for each calendar year.

Imagery was imported into Definiens eCognition, object-based hierarchical classification software, to classify vegetation and surface types (Table 3). Part A is a list of vegetation canopy closure (percent of vegetative cover as viewed from above) classes. These classes were mapped independently of vegetation type. Part B is a list of mapped vegetation types. For 2007 and 2010 imagery, eCognition software was used to create objects (aka polygons) at appropriate scales to represent boundaries of vegetation communities for vegetation type mapping, as well as stand boundaries for vegetation canopy closure mapping.

Table 3. List of vegetation classes.

Part A: Canopy Closure Classes	
CC_LT_10	less than 10% canopy closure
CC_10_20	canopy closure 10-20%
CC_20_40	canopy closure 20-40%
CC_40_60	canopy closure 40-60%
CC_60_80	canopy closure 60-80%
CC_80_100	canopy closure 80-100%
Part B: Vegetation Type and Land Cover Classes	
DS	Desert Scrub: includes xerophytes of the area, whether in upland or riparian elevations. Examples include *Chilopsis linearis* (bow willow), *Linneara tridentate* (creosote), *Atriplex* spp, and various grass spp.
CW	Cottonwood/willow: includes *Populus fremontii* (cottonwoods), *Salix goodingii* (willow)
CO	Conifer (*Juniperus* spp, *Pinus* spp)
MS	Mesquite (*Prosopsis* spp)
SC	Saltcedar (*Tamarix ramosissima and Tamarix* spp)
MP	Mesophytes: found in the riparian elevation. Includes grasses *Typha* spp, *Scirpus* spp, *Phragmites* spp, and various broadleaved spp.
AR	Arundo (*Arundo donax*)
LN	Low NDVI vegetation, also referred to as VD, decadent vegetation
WATER	River, stream, pond, lake
Unclassified	Bare earth (<10% veg), buildings, roads, or areas not containing listed classes

Vegetation was classified at two levels:

1. Fine (small) polygons were generated to capture boundaries of individual trees or smaller areas of vegetation. These polygons were attributed with a vegetation species or community class label.

2. Coarser (larger) polygons were then aggregated from the smaller polygons to represent vegetation stand boundary areas as a function of vegetation canopy closure. These polygons were attributed with a canopy closure label. It should be noted that these polygons can contain more than one species if multiple species exist together in a dense stand of vegetation. Vegetation stand boundaries are desirable for ET estimates, since these estimates differ as a function of vegetation density.

Vegetation classes were assigned to these polygons based on a variety of variables including the NDVI and Infrared/Red band ratios, spectral brightness, canopy texture, maximum mean band difference, and visual interpretation. Airborne video of the floodplain was acquired in 2010 by Reclamation, providing additional data for visual interpretation of invasive species (primarily saltcedar) and native species. Russian olive and Arundo were located by overlaying a MDRCD supplied point dataset on the imagery. Presence or absence of the Russian olive and Arundo was determined by reviewing spectral infrared imagery within polygons coincident with MDRCD point locations. Coverage of Russian olive was minimal and only found in the Alto (2.71 acres) and Alto Transition (0.02 acres) subareas; further analysis of this species was not conducted. Post classification editing was also done in ArcMap to improve accuracies. This was a final edit phase using the same data sources above.

Saltcedar areas were isolated and canopy crown closure classes were assigned to saltcedar polygons based on stand-boundary crown closure classes (from step 2 described above). In addition, a saltcedar change map (See Section 3.1 figure) was created by differencing the saltcedar polygons between the 2007 and 2010 classification layers, identifying areas of change in saltcedar.

Once complete, the polygon layers were converted to raster format files and delivered to USU to be used in the estimation of evapotranspiration.

2.4 Estimation of Spatial ET Using Energy Balance Models

Two ET models were evaluated for use in this study, namely the Surface Energy Balance for Land Model (SEBAL) and the Two-Source model. The spatial ET was estimated for 2010 imagery using both the calibrated shortwave 3-band multispectral imagery and the calibrated thermal imagery. Both models were tested on Block 1 and 2 imagery, as described in Section 3, and the Two-Source model was chosen for this Study. A short description of these models and how they were used is given below with a detailed results analysis in Section 3.3. Both energy balance models provide estimates of the different surface energy fluxes: the net radiation (Rn), the soil heat flux (G), the sensible heat flux (H) and the latent heat flux (LE), which represent instantaneous values at the time when the images were taken. The instantaneous LE represents an estimate of the instantaneous ET, and is extrapolated to daily ET values by applying the reference ET fraction (ETrf) method (Chavez et al., 2008) which requires the input of the instantaneous (ETai) and daily reference evapotranspiration (ETo). These values were obtained from the California Irrigation Management Information System (CIMIS) station Barstow (station ID 131) located in a central location of the study area.

The two models were first tested on imagery from Blocks 1 and 2 to examine model performance and the consistency of the results, vis-à-vis expected evapotranspiration amounts from some of the existing vegetation in the imagery.

2.4.1 SEBAL Model

Actual evapotranspiration (ETa) was spatially estimated over 2 blocks covering the Baja subarea of the Mojave River using the SEBAL model (Bastiaanssen et al., 1998). This model was developed to be used with lower resolution satellite imagery so modifications to the model, described below, were needed in order for it to be used with high resolution airborne imagery.

Net radiation (Rn) was estimated in the SEBAL model by subtracting outgoing from incoming short and long wave radiations from the surface:

$$Rn = (1 - \alpha)\, Rs + {}_{Rlin} - {}_{Rlout}$$

Where α is the surface albedo (or reflectance in the shortwave part of the spectrum), Rs is incoming solar radiation, $_{Rlin}$ is the incoming longwave radiation emitted by the atmosphere and $_{Rlout}$ is the outgoing longwave radiation emitted by the surface according to its temperature.

To estimate G, the ratio of G/Rn was calculated for every pixel using an empirical equation based on the NDVI. This ratio was then multiplied by the Rn of that pixel to obtain a spatial layer of G. Finally, H was approximated by selecting two anchor points, known as the cold and hot pixels. These pixels represent the boundary condition, where the former is a wet, well irrigated vegetated surface (e.g. alfalfa), and the latter is a dry, bare agricultural soil.

After estimating three out of four main components of the surface energy balance, the LE was estimated as the residual of the energy balance equation (LE = Rn – H – G). LE fluxes were then converted to instantaneous actual evapotranspiration (ETai) by dividing by the latent heat of vaporization. Modeled spatial ETai is an instantaneous value, due to the fact that the airborne imagery is acquired over a short time period and thus is approximately a snapshot in time. These values were scaled up to daily values using the reference evapotranspiration fraction obtained by dividing ETai by the instantaneous reference evapotranspiration (ET_0i). ET_0i was obtained from the Barstow weather station. The reference ET fraction (ETrf) is assumed to be constant during daylight hours. Daily spatial actual evapotranspiration (ETa) was estimated by multiplying this ET fraction layer by daily reference evapotranspiration (ETo) values obtained from the same weather station.

The following modifications were made to run SEBAL with high resolution imagery. In SEBAL, at-surface albedo is usually modeled based on top-of-atmosphere albedo estimated using band-specific solar exo-atmospheric coefficients, by assuming a constant value (0.03) for average path-radiance albedo and by approximating atmospheric transmissivity from surface elevation. In running SEBAL over the Mojave floodplain, at-surface albedo was estimated using a version of the "Brest & Goward" equation adapted to be used with imagery from the USU airborne system:

$$A = 0.512\ (REDr) + 0.418\ (NIRr)$$

Where REDr and NIRr are the red and near-infrared band reflectance respectively.

Surface emissivity was estimated using Brunsell and Gillies (2002) a different method than the one used in the original SEBAL model which works better for high resolution airborne imagery. Instead of selecting only one hot and cold pixel for estimating H, an AOI polygon (area $\approx$ 900 m^2) the approximate size of a Landsat TM 30 m pixel was defined for each of hot and cold surfaces and the pixels within averaged. This was done to represent the scale of the energy balance processes and avoid any biases in the cold pixel estimation due to shadows.

2.4.2 Two-Source Model

The considerable number of methods described in the scientific literature aimed at improving the estimation of spatial ET using remote sensing has resulted in the development of a group of land surface energy models called Soil-Vegetation Atmosphere Transfer (SVAT) models (Crow et al. 2005). The core of these models is based on applying the energy balance of surface fluxes and/or water balance. There are two different modeling approaches under SVAT, thermal remote sensing (RS-SVAT) and coupled water and energy balance (WEB-SVAT) (Crow et al. 2005). In this Study, we applied one of the RS-SVAT models, namely the Two-Source model (Norman et al. 1995) which utilizes remotely sensed radiometric surface temperature to estimate different surface energy fluxes. There are many RS-SVAT models available in the literature such as the SEBI model by Menenti and Choudhury (1993) and the METRIC model by Allen et al. (2005) (a variation of SEBAL); however, the Two-Source model was selected to apply over the Mojave River AOI due to the significant surface heterogeneity in vegetation density and limited water availability. The Two-Source model was originally designed to handle such conditions and has shown reliable performance in numerous applications. It has recently been extensively reviewed for improved performance over a wide range of heterogeneity and different climate regions (Kustas and Norman, 2000; Li et al. 2005).

The Two-Source model version used in this study is the parallel resistance formulation of Norman et al. (1995). The main concept behind this formulation is that it separates the surface into soil and canopy components and applies the energy balance equation to each component independently in order to estimate the different energy fluxes. Then, at a level above the ground surface called the air-canopy interface, the energy fluxes of each component are added to represent the total surface energy fluxes, as shown in Figure 14.

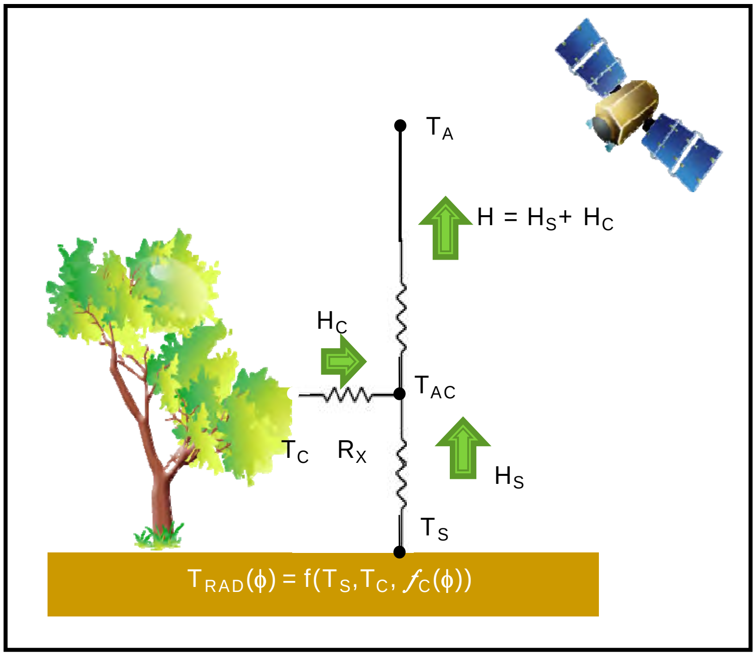

Figure 14. Schematic diagram for the Two-Source model.

One of the recent modifications to the Two-Source model concerns the decomposition of the net radiation in which the physically based model developed by Campbell and Norman (1998) is utilized to estimate the soil and canopy components of the net radiation (Kustas and Norman, 2000; Li et al. 2005). The soil and canopy components of the net radiation are estimated as Rns=Lns+τs(1-αs)S and Rns=Lns+(1-τs)(1-αc)S, respectively, where S represents the solar radiation, Tc the canopy transmittance to solar radiation, αs and αc are the canopy and soil components albedo, and Lnc and Lns the canopy and the soil components of the longwave radiation. The G is calculated as a percent of the soil component of the net radiation Rns. The canopy (Hc) and soil (Hs) sensible heat flux components are calculated as Hc=ρCp[Tc-Tac]/Rx and Hs=ρCp[Ts-Ta]/Rs, respectively, with Ts, Tc, and Tac as the soil, canopy, and air-canopy interface temperatures, respectively, Rs the resistance to heat flow in the boundary layer immediately above the soil surface, Rx the total boundary layer resistance of the complete canopy leaves resistance, ρ the air density, and Cp the specific heat of air. The latent heat flux is the summation of the soil and canopy components latent heat flux LEs and LEc. These different flux components are estimated using Monin-Obukhov similarity theory.

The estimated surface energy fluxes represent an instantaneous value at the time of that specific scene. The daily ET is obtained by extrapolating using the reference evapotranspiration fraction method based on the instantaneous and daily reference (ETai and ETo, respectively) as was performed with the SEBAL model.

2.5 Seasonal Estimates of Evapotranspiration

In order to calculate the 2010 vegetation ET values for the entire growing season, the evapotranspiration fraction layer that was estimated from the instantaneous flux value was used to extrapolate evapotranspiration to seasonal values assuming that the saltcedar and other vegetation types were at peak vegetative cover when the imagery was acquired at the end of June 2010. Using the classified vegetation layer obtained from the 3-band multispectral mosaic, the total area of saltcedar and other vegetation species of interest was estimated within the AOI zone and used to calculate the corresponding average ETrf for the different species within the AOI polygon.

A crop coefficient curve (Kc) was constructed for each vegetation type using the average ETrf (as the plateau portion of the Kc curve and assuming a date for the green-up of vegetation starting from a value of 0.15 until a date that the average ETrf is reached and that the senescence started on a particular date in the fall and that the Kc decreased to a value of 0.15 at the end of a specified period). Kc was assumed to remain at the constant value estimated from SEBAL and/or the Two-Source model during the plateau period. This seasonal ET calculation described above was conducted for most vegetation classes in the floodplain, namely saltcedar, cottonwood/willow, mesquite, desert scrub and low NDVI using the dates shown in Table 4. Further seasonal ET statistics were also estimated by canopy closure class for saltcedar using a similar method. All seasonal estimates were summarized by groundwater subarea. Total volume of water used by each vegetation class was estimated by multiplying the average ET depth by the total area of each vegetation class.

ET was estimated for the 2007 season using the “Kc” curves constructed for the different vegetation types with the 2010 remote sensing estimates of ET. Average Kc curves for each groundwater subarea were used with reference ET data for 2007 along with the classified areas by vegetation type from the 2007 imagery to obtain volume of water use by vegetation type.

Table 4. Main phenological dates used to construct the seasonal “Kc” curves for different vegetation types.

Phenology Dates	Code	Greenup Begins	Peak ET	Senescence Begins	Senescence Ends
Saltcedar (Tamarisk)	SC	3/1	5/1	9/1	11/1
Mesquite	MS	4/1	5/15	8/1	9/15
Cottonwood	CW	4/1	5/15	9/15	11/1
Desert Scrub	DS	3/1	4/15	7/1	8/1
Low NDVI	LN	4/1	5/15	8/1	9/15
Mesophytes	MP	4/1	5/15	7/1	8/1
Conifer	CO	3/1	5/15	10/1	11/15
Arundo	AR	4/1	6/1	10/1	11/1

2.6 Water Cost Methodology

Water use reduction by non-native vegetation is often difficult to quantify in terms of return flows or changes in groundwater. This is largely due to the complexity of ground/surface water interactions, difficulties in accounting for multiple and diverse ground water uses, the temporal delay (sometimes decades) between changes in the system and measureable effects, and variability in measurements. However, it is possible to quantify the amount of water transpired by vegetation (as performed in this Study) and water used by non-native species can be seen as a non-beneficial use of a scarce resource. Costs are presented as general and theoretical amounts to give some quantifiable measure to the water transpired by vegetation, but the amount of water saved does not necessarily correlate to the amount of water transpired. Any dollar figure associated with ET is arbitrary to a certain extent because removal of vegetation and subsequent reductions in ET do not result in immediate additions of water to the system and/or additions equal to the estimated ET.

There are two ways in which costs associated with elimination of evapotranspiration can be assessed. First, the economic gain from delivering the transpired water to customers can be calculated based on current or historical prices. The second method is to estimate the reduction in costs necessary to acquire the rights to the same amount of water lost to ET. This second approach is used for the purposes of this study per discussions with the Mojave Water Agency regarding current procedures in which they acquire and deliver water.

In 2007, acquisition of the rights to an acre-foot of water required the MWA to allocate a capital investment of $3,300 plus an annual fixed charge from Department of Water Resources of $180 per acre-foot. In addition, for each "wet" acre-foot of water, 1.67 acre-feet are actually added to the contract due to only approximately 60% of the water being considered reliably delivered due to wet/dry year constraints and operational/environmental limits. The total cost to acquire an acre-foot of water in 2007 was $5,395 (3,330 + 180 ÷ 0.6). Total costs per acre-foot of water in 2010 and 2011 were similarly calculated incorporating increases in capital investment and other charges at $10,050 and $10,221 per acre-foot, respectively. As the cost of acquiring one acre-foot of water almost doubled between 2007 and 2011, the ET of saltcedar would have to be halved between these years in order to have comparable cost estimates. To have a reasonable comparison of costs between years, 2011 costs are presented for both years.

Costs of water lost to ET of other species were also generated for general comparative purposes. Desert scrub was excluded from these estimates, as vegetation in this class are shallow rooted and rely on precipitation. They do not access groundwater supplies, and although local precipitation contributes to groundwater, the degree to which it does so is undeterminable within the scope of this Study. Therefore, assignment of cost estimates to the water lost through ET of the species within desert scrub class is deemed highly inaccurate.

3.0 Results and Discussion

3.1 Vegetation Classification and Change Detection

Figure 15 shows an example of fine (smaller) polygons (blue boundaries) generated in eCognition software for mapping vegetation at the species or community level. This level accommodates differentiating single trees (round red areas in Figure 16). It should be noted that isolated individual trees or shrubs equal to or smaller than the image resolution of 1 meter, are typically too small to differentiate. This probably occurred with desert scrub and small saltcedar.

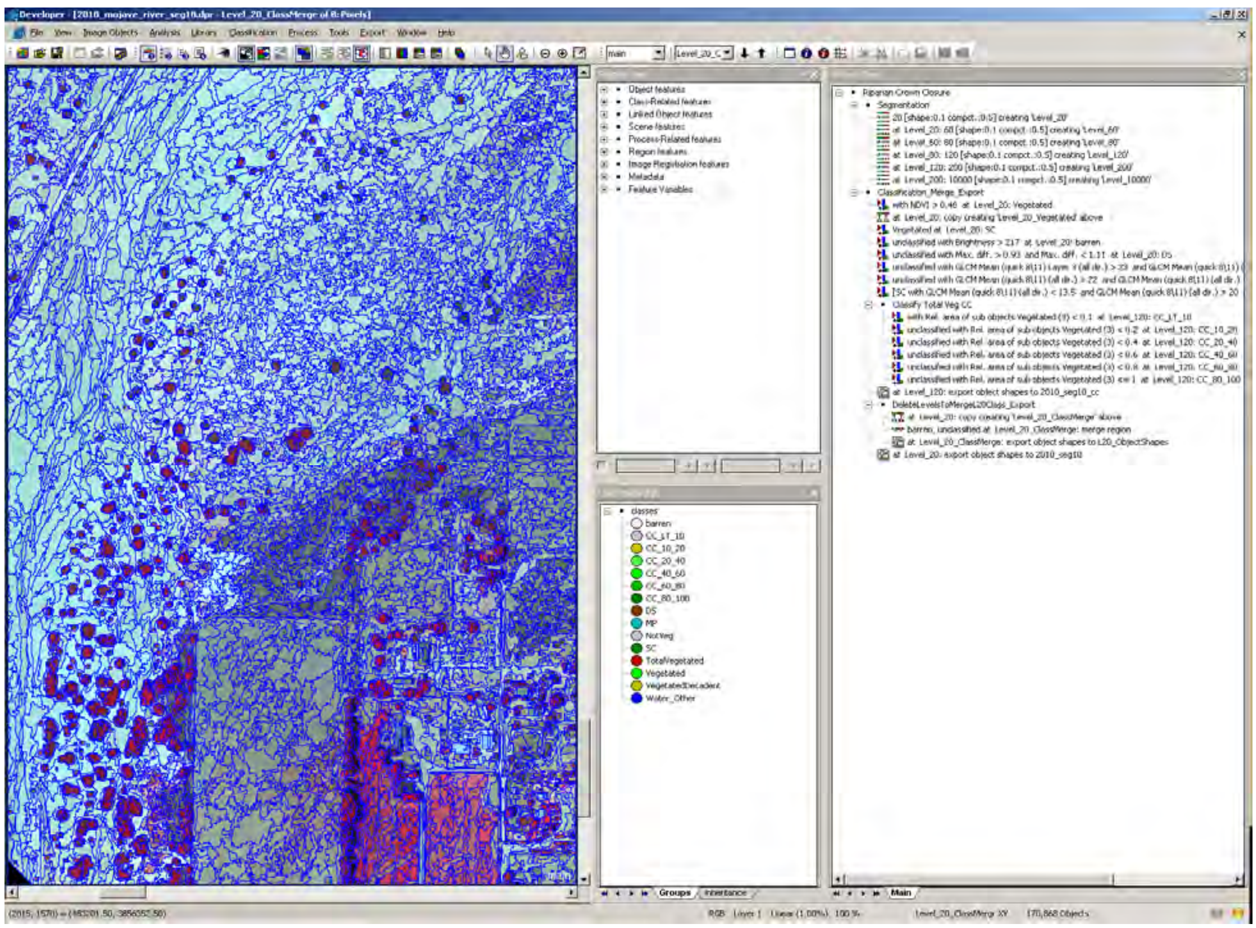

Figure 15. eCognition interface showing fine polygon boundaries (blue) over color infrared imagery for the 2010 classification.

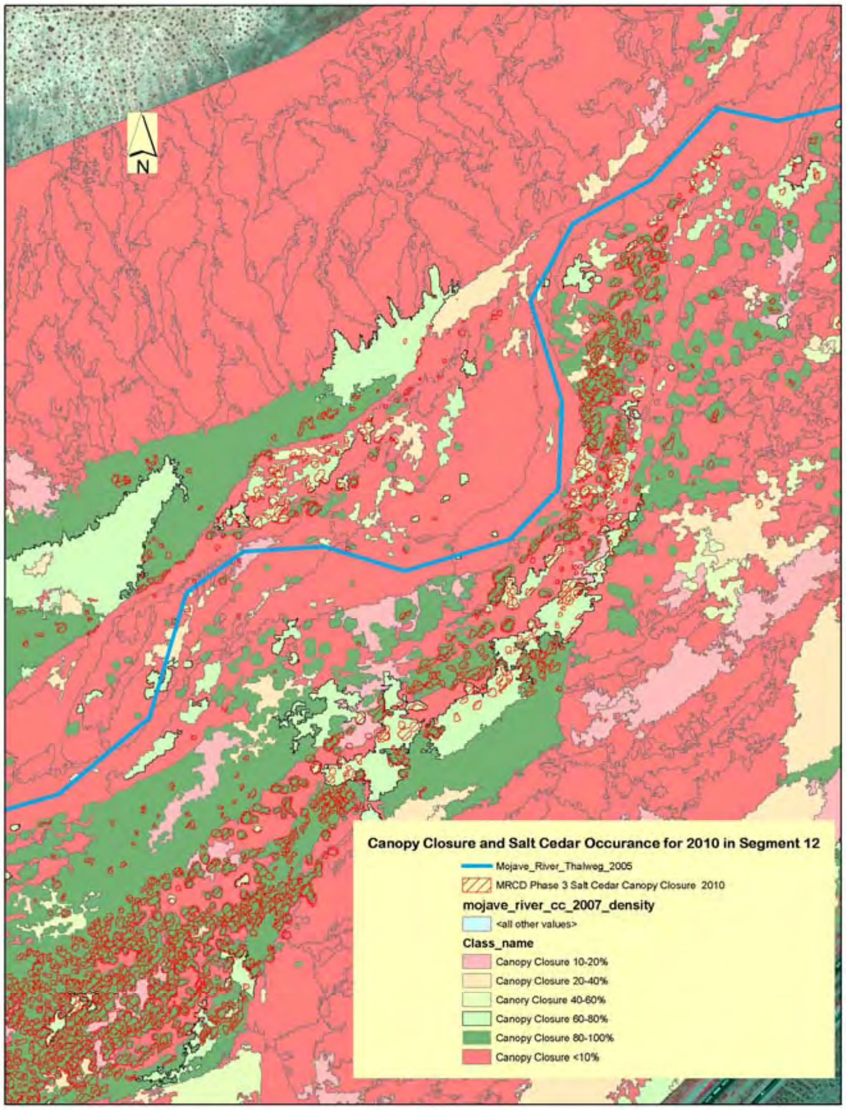

Figure 16. Canopy Closure map with 2010 saltcedar polygons overlaid in red outline

After classification and editing were completed, data was exported into ESRI ArcMap feature class layers (FC) within the ArcMap geodatabase (GDb) environment. Figures 17 and 18 show the 2007 and 2010 classifications. The figures are printed in a larger size in the Appendix of this report and are available as GIS digital files at the Mojave Water Agency to allow viewing of the data at appropriate scales. The same applies to Figure 19.

Figure 19 shows changes in saltcedar presence between 2007 and 2010. Polygons classified as saltcedar were selected from the FC to create FC layers of saltcedar by subarea. The saltcedar FC polygons were merged with the canopy closure FC in order to assign stand-based crown closure values to each saltcedar area. Acreage was then calculated for saltcedar canopy closure classes. Most reduction occurred in the Alto and Alto Transition subareas, where MDRCD efforts began.

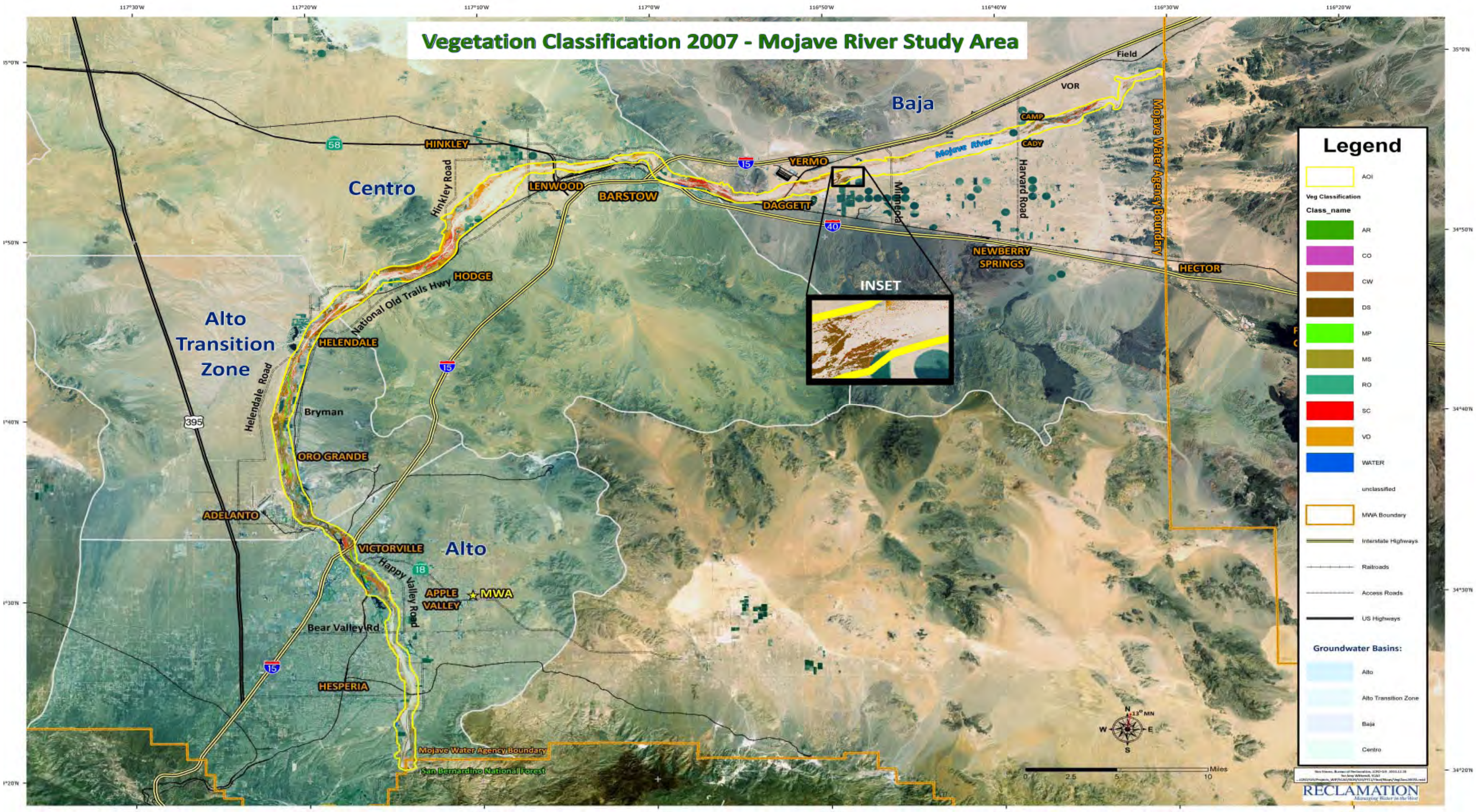

Figure 17. 2007 Vegetation Classification

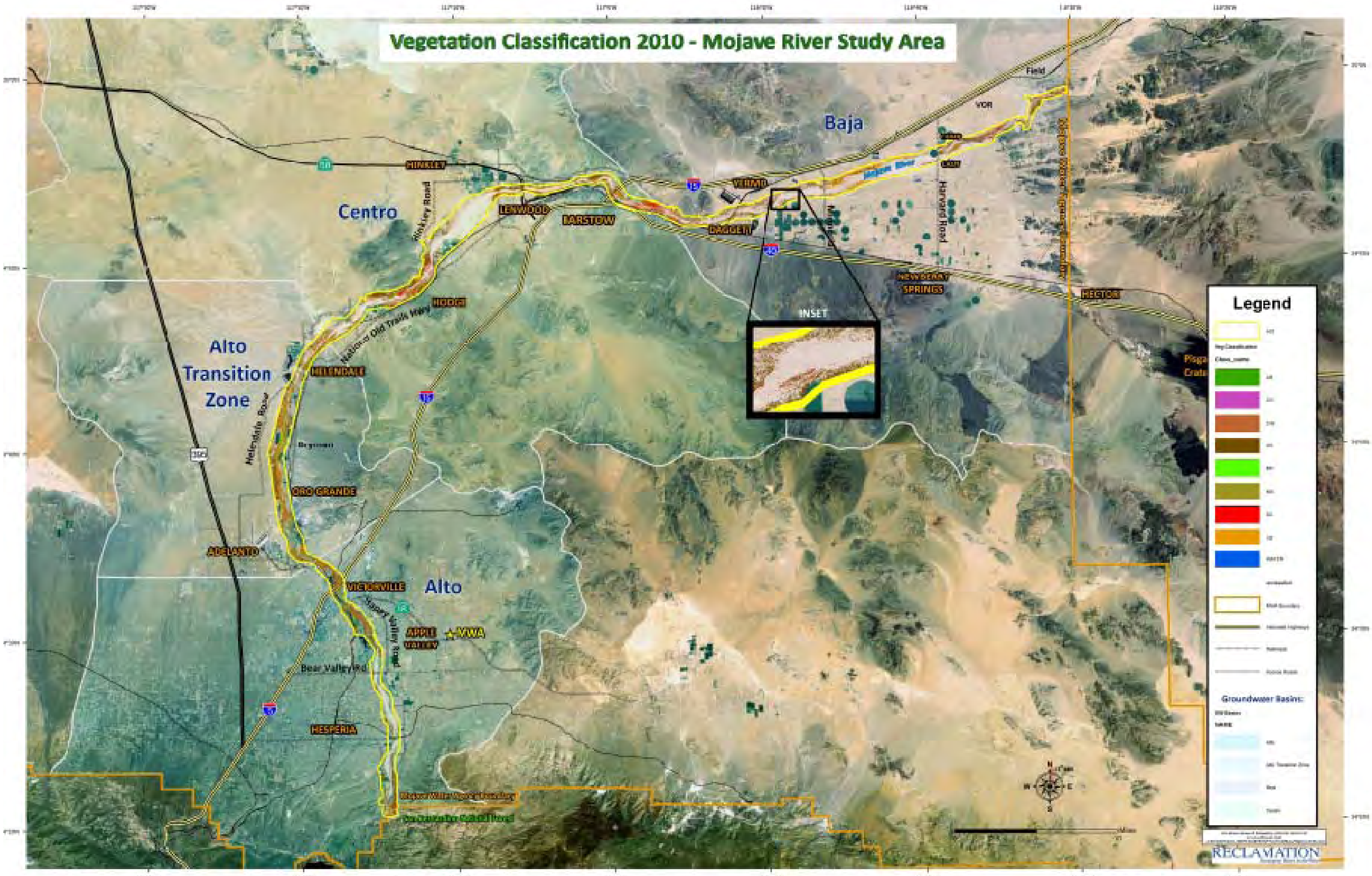

Figure 18. 2010 Vegetation classification

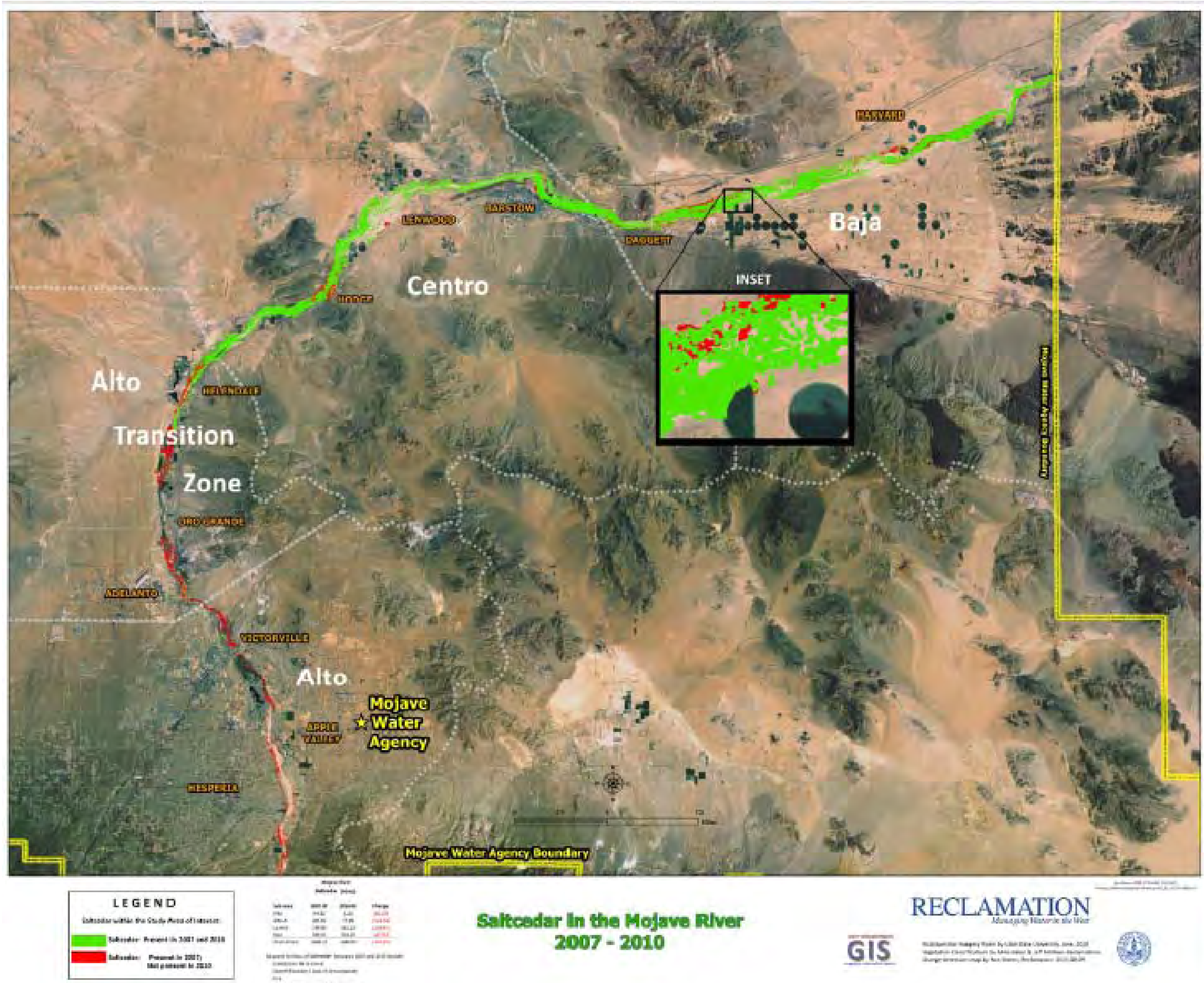

Figure 19. Saltcedar change layer showing areas of saltcedar present in 2007 and 2010.

Figure 20 shows a close-up of saltcedar in 2007 which is no longer present in 2010 (green outlines), and saltcedar present in both 2007 and 2010 (red crosshatch). Red crosshatch areas were not removed by MDRCD due to lack of landowner approval and erosion concerns.

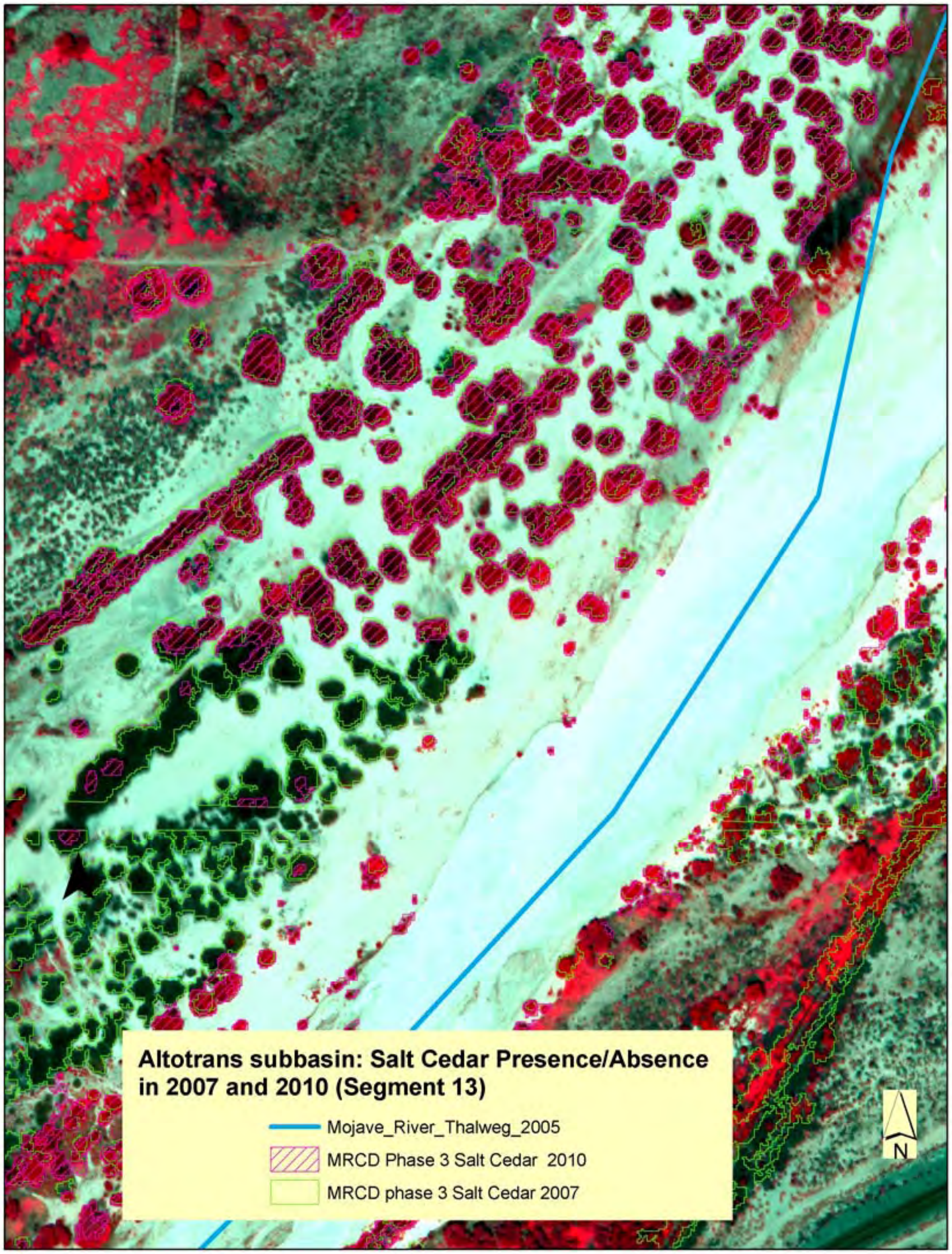

Figure 20. Saltcedar in 2007 which is no longer present in 2010 (green outlines), and saltcedar present in both 2007 and 2010 (red crosshatch).

Canopy closure, vegetation class and saltcedar canopy closure layers for 2007 and 2010 were divided into the four subareas and acreage values were calculated. These layers were exported into raster formats and provided to USU for ET calculations and statistics. Figure 21 shows an example of the raster format data provided to USU.

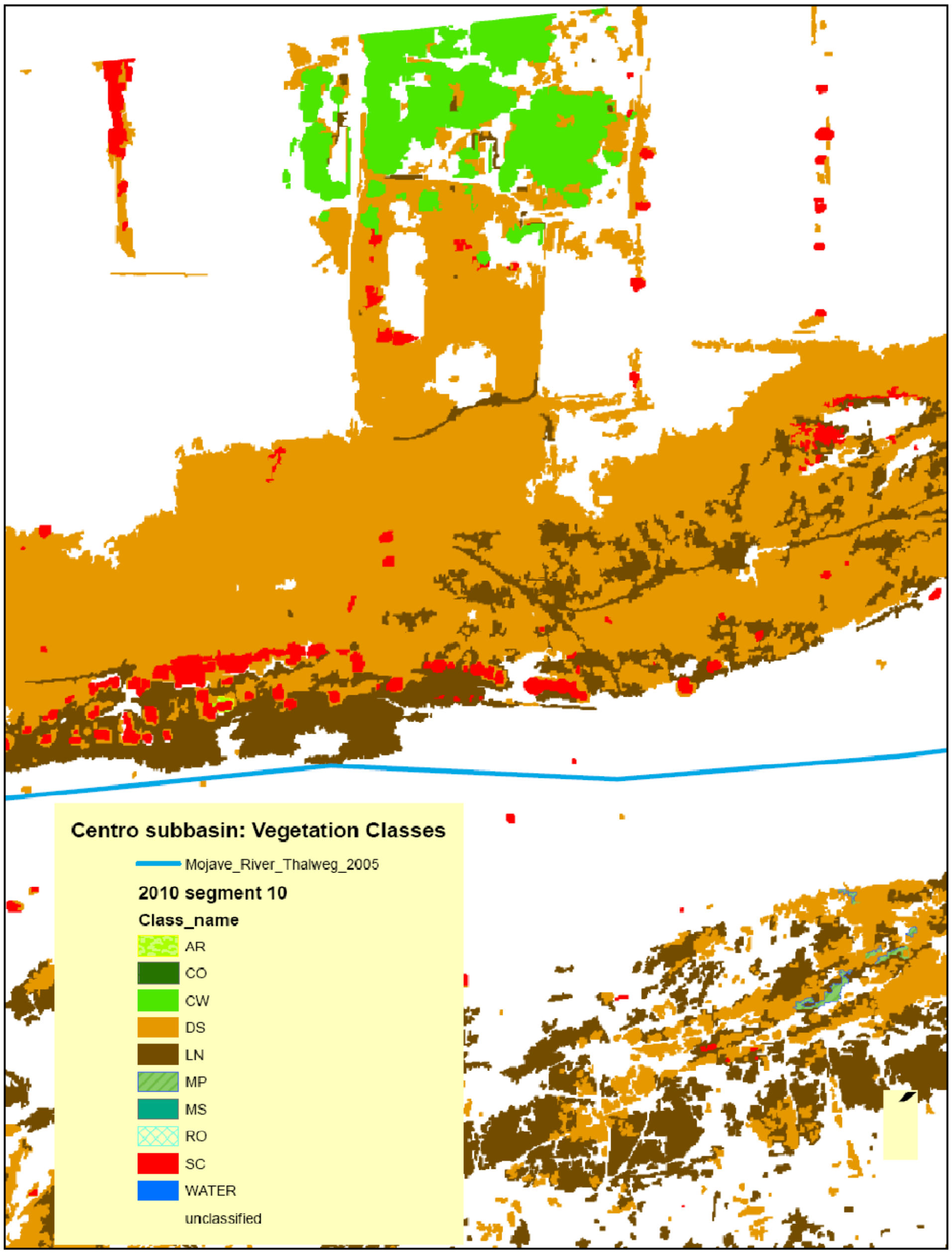

Figure 21. Vegetation classification in raster format.

Federal Geographic Data Committee (FGDC) standard metadata was created for each feature class. Metadata contains methodology-lineage and attribute descriptions. Final vegetation feature class boundaries were merged based on vegetation class to simplify the data and reduce file size.

3.2 Evapotranspiration model evaluation

The two remote sensing based energy balance models, SEBAL and Two-Source model, were tested on Blocks 1 and 2 to determine which model to use for the ET estimation on the entire project area. The differences between the models were described in sections 2.4.1 and 2.4.2.

Figure 22 shows the daily ET map for a portion of Block 1 obtained using the SEBAL model.

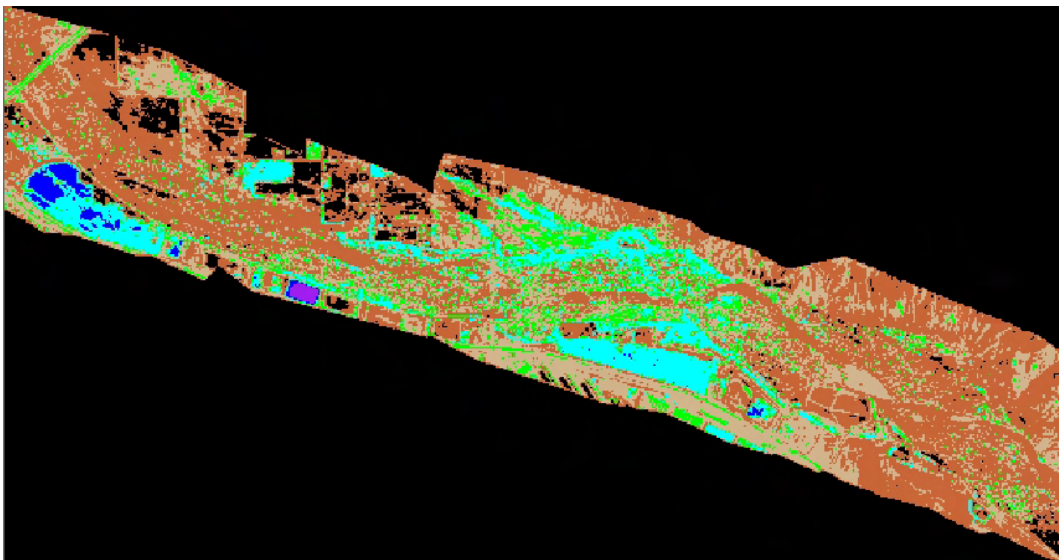

0–1 mm/day 1–2 mm/day 2–3.3 mm/day
3.4–7.1 mm/day 7.1–8.9 mm/day >9 mm/day

Figure 22. Daily ET map of a portion of Block 1 resulting from the SEBAL model.

Of the two blocks (Blocks 1 and 2) initially processed covering a portion of the Baja subarea, Block 1 contains the densest stands and largest surface area of saltcedar. The daily ET in this image varied between a high of over 9 mm/day for the water bodies (purple), 7.1 mm/day to 8.9 mm/day corresponding to alfalfa and well watered trees in the golf course (dark blue), 3.3-7.1 mm/day corresponding to the golf course grass and most saltcedar trees (light blue), 2 – 3.3 mm/day corresponding to sparse saltcedar and other riparian trees and shrubs (green), light brown corresponding to sparse desert scrub with ET varying between 1 – 2 mm/day, and dark brown corresponding to bare soil which varied between 0 – 1 mm/day. The daily reference ET on June 29th when Block 1 was flown was 7.1 mm/day. The ET estimates over grass and alfalfa are reasonable when compared to the grass reference ET resulting in alfalfa values approximately 20% higher than the grass reference ET. Saltcedar ET estimates were less than grass reference ET. Similar saltcedar ET results were measured with Bowen ratio systems at the Cibola National Wildlife Refuge in southern California along the Colorado River (Taghvaeian, 2011).

The daily ET values initially estimated with the Two-Source model were similar, but slightly lower (within 6%) for saltcedar compared to the SEBAL results. The models provide different results due to different parameterizations and the way they model the land-atmosphere interaction and obtain vegetation height for the estimation of the aerodynamic resistance. The SEBAL model is a one layer model, developed originally for irrigated areas. Thus it does better in dense vegetation with good water availability. Some of the empirical relationships within the model, such as canopy height, assume agricultural crops and thus lower canopy heights vis-à-vis the NDVI. This affects the estimation of the aerodynamic resistance parameter and ultimately the estimates of sensible heat fluxes.

The Two-Source model is a two layer model and is well suited for the sparse and heterogeneous ecosystem encountered along the Mojave River. The model was developed to be used with satellite imagery at much lower spatial resolutions than the 1-m thermal pixels used for this effort. The model was adapted for use with the high spatial resolution imagery and adjusted to benefit from the more accurate canopy heights derived from lidar. The parallel version of the Two-Source model was applied in this Study.

Daily reference ET values from the CIMIS weather stations for the 2007 and 2010 growing seasons were used with the 2010 saltcedar coverage data in order to compare the models. The results for estimated seasonal saltcedar ET for the SEBAL and Two-Source models are summarized in Tables 5 and 6 below for modeled canopy height and lidar derived height. The results were very similar among the years and the small differences due to the variability in seasonal reference ET from year-to-year. These assume saltcedar coverage and density are unchanged from 2010 data.

In order to improve the estimates, canopy heights were incorporated from the lidar data in the model runs. Both models were run on Block 1 twice: the first time with the model parameterizations for estimating vegetation canopy height and a second time using the lidar derived canopy vegetation height product.

The SEBAL results were about 6% higher than the Two-Source model results using the modeled canopy height. With the inclusion of lidar-derived canopy heights, the results of both models converged with differences of less than 0.01%.

Table 5. Comparison of seasonal saltcedar ET results (in millimeters of water) for the SEBAL and Two-Source models, Block 1, using modeled canopy height

	2010			**2007**	
	SEBAL	TSM		SEBAL	TSM
Total ET (mm)					
March to May	107	102		112	107
May to September	533	503		509	480
September to November	230	216		226	212
Total ET (mm)	**870**	**820**		**847**	**799**
Reference ET (grass)	1589	1589		1561	1561

Table 6. Comparison of seasonal saltcedar ET results for the SEBAL and Two-Source models, Block 1, using canopy height derived from lidar

	2010			**2007**	
	SEBAL	TSM		SEBAL	TSM
Total ET (mm)					
March to May	104	104		109	109
May to September	514	515		491	492
September to November	221	222		217	217
Total ET (mm)	**838**	**840**		**816**	**818**
Reference ET (grass)	1589	1589		1561	1561

The calculated area of saltcedar canopy in the riparian/floodplain zone in Block 1 was 926,622 m^2 or 229 canopy acres. Based on the total ET for saltcedar estimated using the SEBAL model along with the area, a total volume of 776,811 m^3 (205,211,660 gallons) of water use for 2010 was calculated. This is equivalent to 630 acre-feet of water. The Two-Source model estimated 631 acre-feet for the same season. As a result of this comparative analysis between the two energy balance models, it was concluded that both models were performing with a high level of confidence.

The Two-Source model was determined to be a better choice for the Mojave River for several reasons: it is faster to run, was formulated to work with sparse heterogeneous environments and does not depend on the sometimes subjective process of selecting a hot and cold pixel in the imagery. It was chosen to run on the entire AOI.

ET results for the Two-Source model applied to 2010 Block 2 imagery using reference ET values from 2007 and 2010 and lidar-based canopy heights are presented in Table 7.

Table 7. Seasonal saltcedar ET results for the Two-Source model, Block 2 using canopy height derived from lidar.

	2010	**2007**
Total ET (mm)		
March to May	96	101
May to September	465	445
September to November	198	194
Total ET (mm)	**759**	**740**
Reference ET (grass)	1589	1561

There was much less saltcedar in Block 2 with an area of 56 acres and an average ETrf of 0.48 estimated with the Two-Source model. An approximate volume of 45,705,223 gallons of water use in Block 2 was estimated for 2010 equivalent to 140 acre-feet. It appears that the saltcedar in this section of the river, in addition to being sparser, is using less water than the saltcedar in the Block 1 section upstream, which could be due to depth to the water table. This is corroborated with an analysis of the depth to groundwater in Figure 23, obtained from lidar-based ground elevations and measured depths to groundwater at different wells provided by the U.S. Geological Survey. Green, blue, and white symbols represent wells where groundwater has risen between 2007 and 2010, while red, pink, and orange symbols represent wells where groundwater levels have dropped in the same period. Sizes of the symbols are proportional to the depth to groundwater and vary between 2 and 100 feet. Depth to groundwater is greater in wells from Block 2 (125 to 155 feet) than in Block 1 (12 to 28 feet) on the western border of the Baja basin and affect the lower ET values as well as the sparser cover of saltcedar.

Saltcedar ET values in general decreased in the downstream direction as indicated by the peak ET Kc values (ETrf) shown in Table 8, except for Block 5 where ET values showed an increase. Block 5 also has a higher saltcedar area and lower depth to groundwater indicating that there is a strong relationship between water availability with the presence and density of saltcedar.

Table 8. Saltcedar crop coefficients by Block in the Baja basin used in the estimation of seasonal ET with Two-Source model

	Block 1	**Block 2**	**Block 3**	**Block 4**	**Block 5**	**Block 6**	**Block 7**
Kc							
Initial Kc (March 1)	0.15	0.15	0.15	0.15	0.15	0.15	0.15
Mean Kc (May to Sept.)	0.53	0.48	0.40	0.41	0.48	0.31	0.28
Late Kc (November 1)	0.15	0.15	0.15	0.15	0.15	0.15	0.15

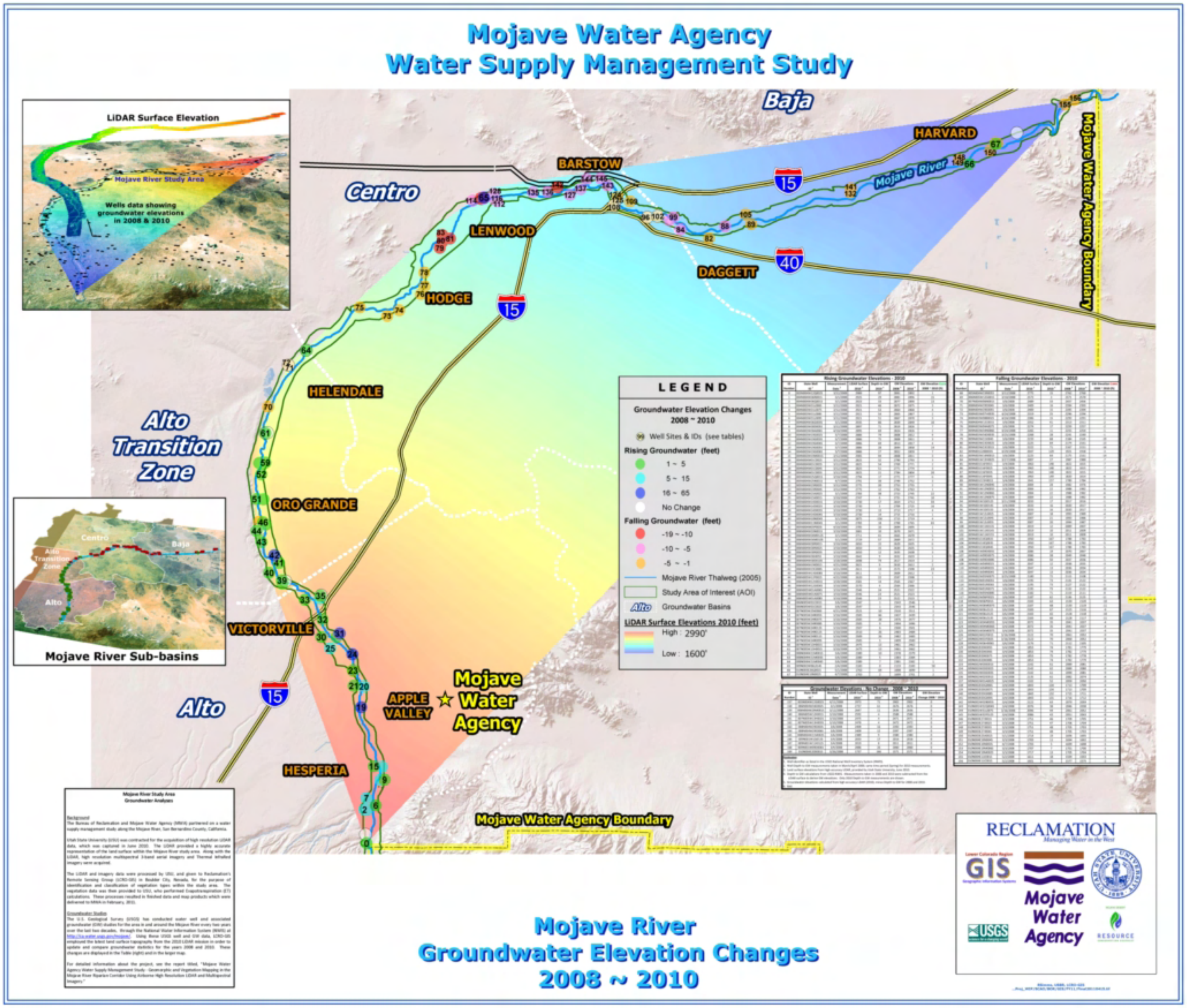

Figure 23. Depth to groundwater in 2010 for wells along the Mojave River floodplain.

3.3 Evapotranspiration model outputs, 2007 and 2010

Saltcedar ET in the Study area decreased by approximately 800 acre-feet between 2007 and 2010. This reduction does not include MDRCD removal efforts after June 2011. In Table 9 below, the Kc coefficients used in the ET modeling are summarized for all subareas, as seen in Sections 3.3.1 to 3.3.4.

Table 9. ET fraction of different vegetation types for the 4 groundwater subareas.

	ALTO							
	SC	**DS**	**CW**	**MS**	**VD**	**MP**	**CO**	**AR**
Initial Greenup Kc	0.15	0.15	0.15	0.15	0.15	0.15	0.15	0.15
Peak Kc	0.49	0.34	0.71	0.36	0.33	0.56	0.36	0.4
Final Senescence Kc	0.15	0.15	0.15	0.15	0.15	0.15	0.15	0.15
	ALTO TRANSITION							
	SC	**DS**	**CW**	**MS**	**VD**	**MP**	**CO**	**AR**
Initial Greenup Kc	0.15	0.15	0.15	0.15	0.15	0.15	0.15	0.15
Peak Kc	0.5	0.27	0.63	0.23	0.33	0.49	0.35	0.41
Final Senescence Kc	0.15	0.15	0.15	0.15	0.15	0.15	0.15	0.15
	CENTRO							
	SC	**DS**	**CW**	**MS**	**VD**	**MP**	**CO**	**AR**
Initial Greenup Kc	0.15	0.15	0.15	0.15	0.15	0.15	0.15	0.15
Peak Kc	0.48	0.23	0.62	0.42	0.25	0.39	0.32	0.66
Final Senescence Kc	0.15	0.15	0.15	0.15	0.15	0.15	0.15	0.15
	BAJA							
	SC	**DS**	**CW**	**MS**	**VD**	**MP**	**CO**	**AR**
Initial Greenup Kc	0.15	0.15	0.15	0.15	0.15	0.15	0	0
Peak Kc	0.47	0.25	0.56	0.27	0.24	0.43	0	0
Final Senescence Kc	0.15	0.15	0.15	0.15	0.15	0.15	0	0

3.3.1 Baja subarea

Table 10 summarizes the seasonal evapotranspiration by saltcedar in both 2007 and 2010 for the Baja subarea. As MDRCD Phase 4 had not commenced at the time of imagery acquisition, reduction in saltcedar ET is likely due to natural causes or classification discrepancies.

Table 10. Evapotranspiration and estimated seasonal water use by saltcedar in the Baja subarea during 2007 and 2010 seasons.

Year	2007	2010
Initial Greenup Kc	0.15	0.15
Peak Kc	0.46	0.46
Final Senescence Kc	0.15	0.15
Total Area (acres)	384	359
ET Greenup Period (mm)	97	92
ET Peak Period (mm)	425	445
ET Senescence Period (mm)	185	185
Total Seasonal ET (mm)	707	722
Volume (m3)	1,099,007	1,047,714
Volume (gallons)	290,326,999	276,776,633
acre-feet	892	844

Table 11 summarizes the seasonal evapotranspiration for the remaining vegetation types in the same years. Cottonwood/willow (CW) resulted in the highest ET rate as represented by the peak period Kc value as well as by the total seasonal ET followed by saltcedar (SC), and mesquite (MS). In terms of volume of water consumed, desert scrub (DS) and low NDVI vegetation (LN) resulted in the highest amounts in 2010, mostly due to the large acreages that both vegetation types occupy in the Baja subarea. Desert scrub is composed of mainly shrubs with shallow roots that depend on precipitation to refill the root zone. Mean precipitation in the region is 110 mm, a third of the 302 mm amount estimated for DS seasonal ET based on an average growth cycle for typical species in this class. In certain years, seasonal ET will be higher if monsoon and/or fall rains occur. This class however represents several desert shrubs with different growth cycles, so the average growth cycle assumed was probably longer than that for the individual plants, resulting in estimated ET significantly greater than the precipitation. Considering that these shrubs have shallow root zones and generally do not extract water from the water table, they were excluded from the comparative cost analysis. Low NDVI vegetation is composed of various species such as saltcedar and mesquite as well as dead vegetation, and had ET rates similar to the desert scrub class with high seasonal water losses due to expansive coverage. These results also show that potential replacement vegetation after saltcedar control such as mesquite and desert scrub mix will not use as much water as saltcedar because they will not reach the same density levels.

Table 11. Evapotranspiration and estimated seasonal water use by vegetation type in the Baja subarea for 2007 and 2010.

	DS	CW	MS	LN	MP	CO	AR
Initial Greenup Kc	0.15	0.15	0.15	0.15	0.15	0	0
Peak Kc	0.25	0.56	0.27	0.24	0.43	0	0
Final Senescence Kc	0.15	0.15	0.15	0.15	0.15	0	0
2007	**DS**	**CW**	**MS**	**LN**	**MP**	**CO**	**AR**
Total Area (acres)	769	16	183	679	1	0	0
ET Greenup (mm)	49	85	51	53	70	0	0
ET Peak Period (mm)	129	537	167	155	155	0	0
ET Senescence (mm)	136	109	178	178	136	0	0
Total Seasonal ET (mm)	313	732	397	386	361	0	0
acre-feet	790	39	238	860	1	0	0
2010	**DS**	**CW**	**MS**	**LN**	**MP**	**CO**	**AR**
Total Area (acres)	2,523	16	95	1,127	2	0	0
ET Greenup (mm)	41	101	58	61	82	0	0
ET Peak Period (mm)	147	546	164	151	169	0	0
ET Senescence (mm)	114	108	193	193	114	0	0
Total Seasonal ET (mm)	302	754	415	405	364	0	0
acre-feet	2,500	40	129	1,499	3	0	0

DS=Desert scrub, **CW**=Cottonwood/willow, **MS**=Mesquite, **LN**=Low NDVI, **MP**=Mesophytes, **CO**=Conifers, **AR**=Arundo.

An analysis of the saltcedar ET by canopy closure shown in Table 12 indicates that at higher densities the ET rates of saltcedar approximate those of cottonwood/willow. ET rates of saltcedar decreased as canopy closure or density decreased, thus control of saltcedar for the purpose of reducing ET is more effective when conducted in higher density classes with larger acreage. This has been implemented by MDRCD efforts by avoiding sporadic, individual plants, especially in erosion-prone areas.

Table 12. Evapotranspiration of saltcedar by canopy density or closure class in 2007 and 2010 for the Baja subarea.

	LT_10	10_20	20_40	40_60	60_80	80_100
Initial Greenup Kc	0.15	0.15	0.15	0.15	0.15	0.15
Peak Kc	0.40	0.43	0.45	0.47	0.49	0.55
Final Senescence Kc	0.15	0.15	0.15	0.15	0.15	0.15
2007	**LT_10**	**10_20**	**20_40**	**40_60**	**60_80**	**80_100**
Total Area (acres)	118	64	45	41	43	71
ET Greenup (mm)	89	94	96	99	103	113
ET Peak Period (mm)	375	404	417	435	460	514
ET Senescence (mm)	161	175	181	190	202	228
Total Seasonal ET (mm)	625	672	694	724	765	855
acre-feet	242	142	103	98	108	199
2010	**LT_10**	**10_20**	**20_40**	**40_60**	**60_80**	**80_100**
Total Area (acres)	125	57	47	42	29	60
ET Greenup (mm)	84	89	91	94	98	108
ET Peak Period (mm)	393	423	437	455	482	538
ET Senescence (mm)	161	175	181	190	202	228
Total Seasonal ET (mm)	638	686	709	739	782	874
acre-feet	261	128	110	102	73	171

LT_10=Less than 10% canopy closure, **10_20**=10-20% canopy closure, etc.

3.3.2 Centro Subarea

Saltcedar ET was higher in the Centro subarea (Table 13) than Baja, with a significantly larger volume of water use due to twice the acreage. In general, depth to groundwater is shallower in the Centro area.

Table 13. Evapotranspiration and estimated seasonal water use by saltcedar in the Centro subarea during 2007 and 2010 seasons.

Year	2007	2010
Initial Greenup Kc	0.15	0.15
Peak Kc	0.50	0.50
Final Senescence Kc	0.15	0.15
Total Area (acres)	751	633
ET Greenup Period (mm)	104	99
ET Peak Period (mm)	465	487
ET Senescence Period (mm)	204	204
Total Seasonal ET (mm)	774	790
Volume (m3)	2,351,576	2,023,410
Volume (gallons)	621,220,566	534,528,276
acre-feet	1,864	1,643

A similar pattern of ET among the different vegetation types can be seen in Table 14, with cottonwood/willow, saltcedar and mesophytes resulting in higher ET amounts. Mesquite showed higher values of ET than in the Baja subarea, possibly a result of shallower water table. Arundo was present in Centro and had a high ET amount, which is not surprising due to being a wetland species with high biomass.

Table 14. Evapotranspiration and estimated seasonal water use by vegetation type in the Centro subarea for 2007 and 2010.

	DS	**CW**	**MS**	**LN**	**MP**	**CO**	**AR**
Initial Greenup Kc	0.15	0.15	0.15	0.15	0.15	0.15	0.15
Peak Kc	0.23	0.62	0.42	0.25	0.39	0.32	0.66
Final Senescence Kc	0.15	0.15	0.15	0.15	0.15	0.15	0.15
2007	**DS**	**CW**	**MS**	**LN**	**MP**	**CO**	**AR**
Total Area (acres)	936	44	7	2,002	27	0	1
ET Greenup (mm)	46	93	69	55	65	93	135
ET Peak Period (mm)	118	594	260	143	140	330	621
ET Senescence (mm)	141	114	185	185	141	68	73
Total Seasonal ET (mm)	306	801	514	383	347	492	830
acre-feet	938	115	12	2,513	31	0	2
2010	**DS**	**CW**	**MS**	**LN**	**MP**	**CO**	**AR**
Total Area (acres)	2,204	58	11	1,284	93	0	1
ET Greenup (mm)	39	109	80	63	76	98	164
ET Peak Period (mm)	135	605	254	139	153	342	628
ET Senescence (mm)	118	112	201	201	118	87	64
Total Seasonal ET (mm)	293	826	535	403	347	526	856
acre-feet	2,115	158	20	1,698	106	0	2

DS=Desert scrub, **CW**=Cottonwood/willow, **MS**=Mesquite, **LN**=Low NDVI, **MP**=Mesophytes, **CO**=Conifers, **AR**=Arundo.

Saltcedar ET by canopy closure class showed a decreasing ET trend with decreasing density, similar to the Baja subarea (Table 15).

Table 15. Evapotranspiration of saltcedar by canopy density or closure class during 2007 and 2010 for the Centro subarea.

	LT_10	10_20	20_40	40_60	60_80	80_100
Initial Greenup Kc	0.15	0.15	0.15	0.15	0.15	0.15
Peak Kc	0.42	0.46	0.47	0.49	0.51	0.55
Final Senescence Kc	0.15	0.15	0.15	0.15	0.15	0.15
2007	**LT_10**	**10_20**	**20_40**	**40_60**	**60_80**	**80_100**
Total Area (acres)	96	163	64	51	76	285
ET Greenup (mm)	193	214	219	228	237	257
ET Peak Period (mm)	362	404	414	432	451	490
ET Senescence (mm)	99	112	115	121	127	140
Total Seasonal ET (mm)	654	730	748	781	815	887
acre-feet	203	382	153	127	197	802
2010	**LT_10**	**10_20**	**20_40**	**40_60**	**60_80**	**80_100**
Total Area (acres)	92	69	84	86	101	203
ET Greenup (mm)	86	93	95	98	101	108
ET Peak Period (mm)	407	450	461	480	500	541
ET Senescence (mm)	168	188	192	201	210	229
Total Seasonal ET (mm)	660	731	748	779	812	878
acre-feet	198	165	207	219	268	585

LT_10=Less than 10% canopy closure, **10_20**=10-20% canopy closure, etc.

3.3.3 Alto Transition

A further increase in saltcedar ET, as seen in the Kc numbers, was observed in the Alto Transition subarea, potentially due to shallower water tables and the presence of surface water in the river (Table 16). A large decrease in saltcedar ET volume (323 acre-feet) was observed from 2007 to 2010 due to the decrease in acreage (123 acres).

Table 16. Evapotranspiration and estimated seasonal water use by saltcedar in the Alto Transition subarea during 2007 and 2010 seasons.

Year	2007	2010
Initial Greenup Kc	0.15	0.15
Peak Kc	0.52	0.52
Final Senescence Kc	0.15	0.15
Total Area (acres)	202	78
ET Greenup Period (mm)	108	102
ET Peak Period (mm)	484	507
ET Senescence Period (mm)	214	214
Total Seasonal ET (mm)	805	823
Volume (m3)	656,917	259,346
Volume (gallons)	173,539,143	68,512,017
acre-feet	534	210

Other vegetation types had similar ET results as the other two subareas downstream (Table 17).

Table 17. Evapotranspiration and estimated seasonal water use by vegetation type in the Alto Transition subarea for 2007 and 2010.

	DS	CW	MS	LN	MP	CO	AR
Initial Greenup Kc	0.15	0.15	0.15	0.15	0.15	0.15	0.15
Peak Kc	0.27	0.63	0.23	0.33	0.49	0.35	0.41
Final Senescence Kc	0.15	0.15	0.15	0.15	0.15	0.15	0.15
2007	**DS**	**CW**	**MS**	**LN**	**MP**	**CO**	**AR**
Total Area (acres)	1,091	390	0	882	346	0	18
ET Greenup (mm)	51	94	46	69	77	99	94
ET Peak Period (mm)	139	604	143	167	176	361	386
ET Senescence (mm)	155	125	204	204	155	75	80
Total Seasonal ET (mm)	345	823	392	440	409	535	560
acre-feet	1,235	1,052	0	1,273	464	1	34
2010	**DS**	**CW**	**MS**	**LN**	**MP**	**CO**	**AR**
Total Area (acres)	1,542	621	1	1,141	304	1	0
ET Greenup (mm)	43	111	52	81	90	105	112
ET Peak Period (mm)	159	615	139	164	192	374	390
ET Senescence (mm)	130	123	221	221	130	95	70
Total Seasonal ET (mm)	332	848	412	465	412	574	572
acre-feet	1,680	1,728	1	1,741	411	2	1

DS=Desert scrub, **CW**=Cottonwood/willow, **MS**=Mesquite, **LN**=Low NDVI, **MP**=Mesophytes, **CO**=Conifers, **AR**=Arundo.

Similar decreases in saltcedar ET with decreasing canopy closure class (Table 18) were observed as with the other two subareas downstream, but with higher ET values overall.

Table 18. Evapotranspiration of saltcedar by canopy density or closure class during 2007 and 2010 for the Alto Transition subarea.

	LT_10	**10_20**	**20_40**	**40_60**	**60_80**	**80_100**
Initial Greenup Kc	0.15	0.15	0.15	0.15	0.15	0.15
Peak Kc	0.45	0.49	0.50	0.51	0.52	0.55
Final Senescence Kc	0.15	0.15	0.15	0.15	0.15	0.15
2007	**LT_10**	**10_20**	**20_40**	**40_60**	**60_80**	**80_100**
Total Area (acres)	10	35	17	21	24	94
ET Greenup (mm)	97	102	104	106	107	113
ET Peak Period (mm)	422	453	462	475	483	515
ET Senescence (mm)	184	198	203	209	213	229
Total Seasonal ET (mm)	703	753	768	790	803	857
acre-feet	22	86	42	55	64	264
2010	**LT_10**	**10_20**	**20_40**	**40_60**	**60_80**	**80_100**
Total Area (acres)	6	5	10	12	16	30
ET Greenup (mm)	92	97	99	101	102	108
ET Peak Period (mm)	442	474	483	497	505	539
ET Senescence (mm)	184	199	203	209	213	228
Total Seasonal ET (mm)	718	770	785	807	821	875
acre-feet	14	12	25	32	42	85

LT_10=Less than 10% canopy closure, **10_20**=10-20% canopy closure, etc.

3.3.4 Alto Subarea

The seasonal ET amounts for saltcedar on the average were lower for the Alto subarea (Table 19). Differences in ET volume (200 acre-feet) between 2007 and 2010 were a result of reduction of saltcedar coverage, likely due to management during this period.

Table 19. Evapotranspiration and estimated seasonal water use by saltcedar in the Alto subarea during 2007 and 2010 seasons.

Year	2007	2010
Initial Greenup Kc	0.15	0.15
Peak Kc	0.48	0.48
Final Senescence Kc	0.15	0.15
Total Area (acres)	85	2.5
ET Greenup Period (mm)	101	96
ET Peak Period (mm)	444	465
ET Senescence Period (mm)	194	194
Total Seasonal ET (mm)	739	755
Volume (m3)	253,639	7,546
Volume (gallons)	67,004,350	1,993,490
acre-feet	210	6

ET from other vegetation types (Table 20) followed a similar pattern as the other subareas with cottonwood/willow consistently resulting in the highest ET values.

Table 20. Evapotranspiration and estimated seasonal water use by vegetation type in the Alto subarea for 2007 and 2010.

Initial Greenup Kc	0.15	0.15	0.15	0.15	0.15	0.15	0.15
Peak Kc	0.34	0.71	0.36	0.33	0.56	0.36	0.40
Final Senescence Kc	0.15	0.15	0.15	0.15	0.15	0.15	0.15
2007	**DS**	**CW**	**MS**	**LN**	**MP**	**CO**	**AR**
Total Area (acres)	450	500	0	658	143	16	15
ET Greenup (mm)	60	104	62	70	85	101	93
ET Peak Period (mm)	175	683	225	211	200	371	381
ET Senescence (mm)	162	130	213	213	162	78	84
Total Seasonal ET (mm)	397	917	500	494	447	551	558
acre-feet	587	1,504	0	1,066	210	29	28
2010	**DS**	**CW**	**MS**	**LN**	**MP**	**CO**	**AR**
Total Area (acres)	1,285	563	0	396	140	28	0
ET Greenup (mm)	51	123	72	81	100	107	111
ET Peak Period (mm)	200	695	220	206	218	384	386
ET Senescence (mm)	136	128	231	231	136	99	73
Total Seasonal ET (mm)	387	946	522	519	454	591	570
acre-feet	1,632	1,748	1	674	208	55	0

DS=Desert scrub, **CW**=Cottonwood/willow, **MS**=Mesquite, **LN**=Low NDVI, **MP**=Mesophytes, **CO**=Conifers, **AR**=Arundo.

The distribution by canopy closure class (Table 21) results were mixed and did not follow the decreasing pattern by density class as the other 3 subareas.

Table 21. Evapotranspiration of saltcedar by canopy density or closure class for 2007 and 2010 in the Alto subarea.

	LT_10	**10_20**	**20_40**	**40_60**	**60_80**	**80_100**
Initial Greenup Kc	0.15	0.15	0.15	0.15	0.15	0.15
Peak Kc	0.47	0.51	0.48	0.48	0.61	0.48
Final Senescence Kc	0.15	0.15	0.15	0.15	0.15	0.15
2007	**LT_10**	**10_20**	**20_40**	**40_60**	**60_80**	**80_100**
Total Area (acres)	9	4	3	5	6	58
ET Greenup (mm)	100	106	101	101	123	101
ET Peak Period (mm)	439	475	447	447	572	447
ET Senescence (mm)	192	209	196	196	256	196
Total Seasonal ET (mm)	731	790	744	744	952	744
acre-feet	22	10	7	12	18	141
2010	**LT_10**	**10_20**	**20_40**	**40_60**	**60_80**	**80_100**
Total Area (acres)	6	5	10	12	16	30
ET Greenup (mm)	95	101	96	96	118	96
ET Peak Period (mm)	460	497	468	468	599	468
ET Senescence (mm)	192	209	196	196	256	196
Total Seasonal ET (mm)	747	807	760	760	973	760
acre-feet	1	2	2	0.1	0.2	0.3

LT_10=Less than 10% canopy closure, **10_20**=10-20% canopy closure, etc.

3.4 Vegetation Re-growth between 2007 and 2010

3.4.1 Changes in vegetation composition and density

3.4.1.1 Saltcedar

Between 2007 and 2010, changes in the species composition, distribution, and density of vegetation in the Mojave River basin occurred as a result of both human manipulation of the environment and natural succession processes. Urban expansion did not significantly affect the area of interest for this study, and changes in surface water were minimal.

Management of saltcedar in the floodplain was conducted annually by the MDRCD starting in 2008. Management began near the Mojave River Forks Dam and continued downstream in phases (Figure 24).

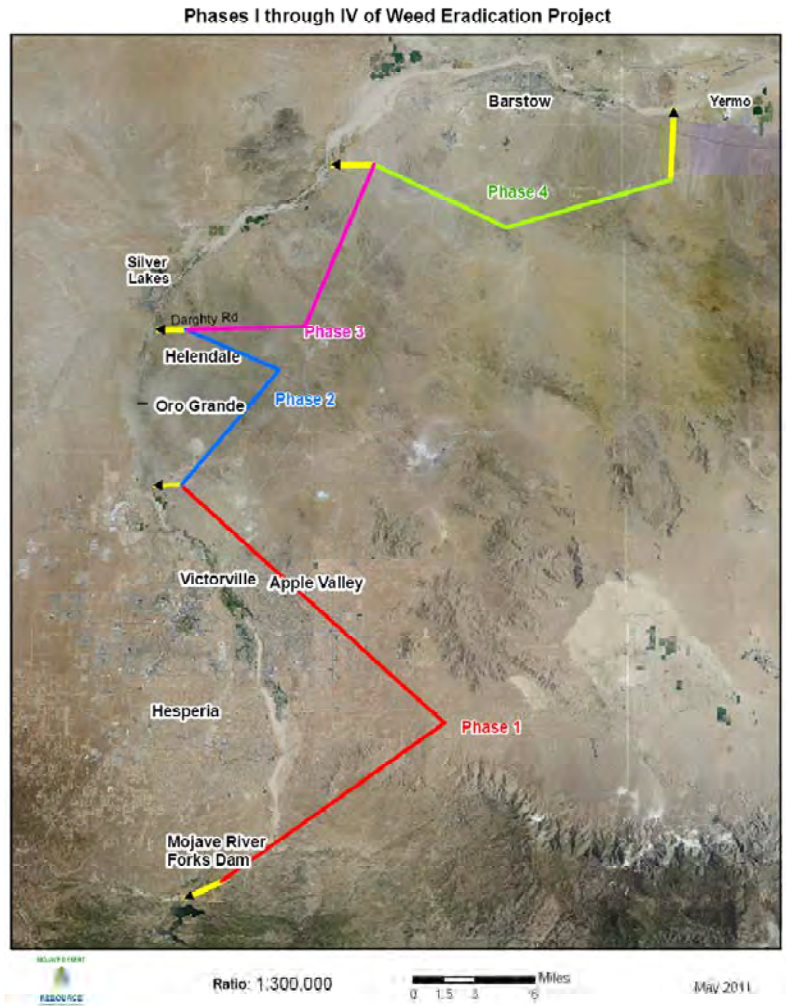

Figure 24. MDRCD saltcedar management phases

Monitoring of saltcedar regrowth and changes in vegetation composition in managed areas was largely anecdotal and no quantitative data exists. Ground-based mapping for invoicing purposes was conducted but did not correlate well with the aerial-based classification. This is likely due to the large areas of relatively small plants that are easily visible from the ground but often difficult to discern from aerial imagery. Therefore, the 2007 classified imagery data could not be used as a baseline to ascertain the changes in saltcedar density or vegetation composition compared to MDRCD phases.

A summary of saltcedar acreage reductions, Table 1 from the Executive Summary, is shown below.

Copy of Table 1. Saltcedar canopy acres, 2007-2010

	--------Saltcedar Canopy acres--------			
Subarea	**2007**	**2010**	**Δ**	**%Δ**
Alto	84.3	2.5	-81.9	-97.1%
Alto Transition	201.0	77.9	-123.1	-61.3%
Centro	732.9	634.1	-98.8	-13.5%
Baja	383.1	358.7	-24.4	-6.4%
MOJAVE BASIN TOTAL ACRES	**1,401**	**1,073**	**-328**	**-23.4%**

Δ=change

Over the entire basin, delineation of saltcedar acreages from aerial imagery resulted in a net reduction of 328 canopy acres between 2007 and 2010. This delineation does not include MDRCD removal efforts after June 2010. All subareas displayed a total reduction in saltcedar infested acres. The largest acreage occurred in the Alto Transition subarea (123 canopy acres, 61% reduction). The largest percent reduction occurred in the Alto subarea (82 canopy acres, 97%). The greatest decreases in canopy closure acres of saltcedar were in the 81-100% canopy-closure class at both the Alto and Alto Transition subareas (total of 122 acres), which contributed the majority of the reductions of saltcedar in these subareas. Large decreases in the Centro subarea were primarily in the 11-20% and 81-100% canopy-closure classes. The Baja subarea exhibited the lowest decline in saltcedar of all the subareas (24 acres) as it had not been managed by the MDRCD prior to imagery capture. Some of the canopy-closure classes increased in acreage, most notably in the Centro subarea (21-60% canopy closure classes increased by a total of 81 acres), but decreases in other classes were high enough that the net change was a 99 acre reduction over the entire subarea. Smaller increases in several of the saltcedar density classes occurred in the Baja subarea as well. Saltcedar classification summaries from 2007 and 2010 by subarea are presented in Table 22.

Table 22. Summary of saltcedar classification, 2007 and 2010, by subarea.

Subarea	Saltcedar density (% foliar cover)	-----------Canopy acres----------- 2007	2010	Δ	%Δ
Alto	1-10	9.27	0.55	-8.71	-94.0%
Alto	11-20	3.75	0.75	-2.99	-79.9%
Alto	21-40	2.74	0.99	-1.75	-63.8%
Alto	41-60	4.96	0.02	-4.94	-99.6%
Alto	61-80	5.73	0.05	-5.69	-99.2%
Alto	81-100	57.87	0.10	-57.77	-99.8%
	Alto Subarea Total Acres	**84.32**	**2.47**	**-81.85**	**-97.1%**
Alto Transition	1-10	9.59	5.95	-3.65	-38.0%
Alto Transition	11-20	34.93	4.77	-30.16	-86.3%
Alto Transition	21-40	16.64	9.81	-6.83	-41.1%
Alto Transition	41-60	21.31	12.16	-9.15	-42.9%
Alto Transition	61-80	24.45	15.68	-8.77	-35.9%
Alto Transition	81-100	94.09	29.51	-64.58	-68.6%
	Alto Transition Subarea Total Acres	**201.02**	**77.88**	**-123.14**	**-61.3%**
Centro	1-10	95.84	91.64	-4.20	-4.4%
Centro	11-20	162.82	68.68	-94.14	-57.8%
Centro	21-40	63.55	84.32	20.78	32.7%
Centro	41-60	50.58	85.74	35.16	69.5%
Centro	61-80	75.53	100.70	25.17	33.3%
Centro	81-100	284.60	203.07	-81.53	-28.6%
	Centro Subarea Total Acres	**732.92**	**634.14**	**-98.78**	**-13.5%**
Baja	1-10	118.11	124.56	6.46	5.5%
Baja	11-20	64.47	56.73	-7.75	-12.0%
Baja	21-40	45.12	47.20	2.08	4.6%
Baja	41-60	41.45	41.87	0.42	1.0%
Baja	61-80	43.13	28.58	-14.55	-33.7%
Baja	81-100	70.77	59.75	-11.02	-15.6%
	Baja Subarea Total Cost	**383.06**	**358.68**	**-24.37**	**-6.4%**
MOJAVE BASIN TOTAL ACRES		**1,401**	**1,073**	**-328**	**-23.4%**

Δ=change

There is potential for removal of approximately1,000 additional acres of saltcedar along the Mojave River, depending on landowner permission and erosion concerns. Some of this removal has already occurred by the MDRCD after June 2010. The additional removal could translate to an additional ET reduction of up to 2,500 acre-feet per year, with Study average ET rate of approximately 2.5 acre-feet/year per acre of saltcedar.

3.4.1.2 Total other vegetation

Overall, total vegetated acres (not including saltcedar) in the Mojave River AOI increased by over 3,900 acres (37%) between 2007 and 2010 Individually, all subareas also increased in total vegetated acres. A summary of all vegetation classes by subarea and year is presented in Table 23.

Table 23. Summary of all vegetation classes by subarea, not including saltcedar, 2007 and 2010.

	Vegetation	-----------Canopy acres-----------			
Subarea	**Class**	**2007**	**2010**	**Δ**	**%Δ**
Alto	AR	15.11	0.11	-15.00	-99.3%
Alto	CO	15.93	28.13	12.20	76.6%
Alto	CW	499.62	563.05	63.43	12.7%
Alto	DS	450.35	1284.64	834.30	185.3%
Alto	MP	143.21	139.60	-3.61	-2.5%
Alto	MS	0.25	0.48	0.23	94.5%
Alto	RO	2.71	0.00	-2.71	-100.0%
Alto	LN	658.28	396.04	-262.24	-39.8%
	Alto Subarea Total Acres	**1785.45**	**2412.05**	**626.60**	**35.1%**
Alto Transition	AR	18.33	0.41	-17.92	-97.8%
Alto Transition	CO	0.38	0.80	0.42	112.4%
Alto Transition	CW	389.86	620.86	231.00	59.3%
Alto Transition	DS	1090.55	1541.58	451.03	41.4%
Alto Transition	MP	346.05	304.03	-42.02	-12.1%
Alto Transition	MS	0.18	0.86	0.69	387.4%
Alto Transition	RO	0.02	0.00	-0.02	-100.0%
Alto Transition	LN	881.81	1141.46	259.65	29.4%
	Alto Transition Subarea Total Acres	**2727.17**	**3610.00**	**882.83**	**32.4%**
Centro	AR	0.67	0.67	0.00	0.0%
Centro	CO	0.10	0.20	0.10	101.5%
Centro	CW	43.69	58.44	14.75	33.8%
Centro	DS	935.72	2204.06	1268.34	135.5%
Centro	MP	27.06	93.43	66.37	245.3%
Centro	MS	7.38	11.16	3.78	51.1%
Centro	LN	2001.84	1284.36	-717.48	-35.8%
	Centro Subarea Total Acres	**3016.46**	**3652.32**	**635.86**	**21.1%**
Baja	CW	16.32	16.23	-0.09	-0.5%
Baja	DS	769.03	2523.18	1754.15	228.1%
Baja	MP	0.59	2.38	1.79	304.6%
Baja	MS	183.23	94.66	-88.57	-48.3%
Baja	LN	678.90	1127.26	448.36	66.0%
	Baja Subarea Total Acres	**1648.07**	**3763.71**	**2115.65**	**128.4%**
MOJAVE BASIN TOTAL ACRES		**9,177**	**13,438**	**4,261**	**46.4%**

3.4.2 Re-treatment costs of re-sprouts and new infestations

Retreatment of saltcedar is almost always necessary, but the degree to which re-sprouts occur can fluctuate. Accordingly, costs of retreatment will vary with plant density as well as control method, site conditions, and other factors. Generally, retreatment costs are less than primary treatment costs for mature stands, although they may be necessary for several years. In cases where sites are reseeded by adjacent saltcedar stands, re-sprouts may be significantly higher. Re-vegetation of managed saltcedar sites is often performed to limit re-growth and re-infestation.

Cost of retreatment is not often specifically addressed in literature. In general, published costs for treatment of saltcedar are extremely variable (between $24 and $5,000 per canopy acre), and is dependent on method and site conditions (Tamarisk Coalition, 2006; U.S. Forest Service, 2004; O'Meara et al., 2010). A more relevant range of costs for retreatment in the Mojave River Basin is evident in those performed in this area between 2007 and 2010. Contracted costs were $200 per canopy acre for extraction and $285 per canopy acre for cut stump for the second retreatment in MDRCD Phase 2. Other costs for retreatment in the Mojave Basin are not available at this time, but are presumed similar.

New infestations are much easier to control than established stands; control efforts are more successful and associated costs typically lower if infestations are caught in early growth stages. Retreatment may still be necessary with new infestations, but again the degree to which it must be applied for long-term management is less than with large and mature stands.

3.4.3 Literature review of re-growth potential

Saltcedar re-sprouts readily from the root crown or from stems or roots in contact with soil (Warren and Turner, 1975; Burke, 1989; Lovich, 2000; Carruthers et al., 2007; McDaniel, 2008). Although much of literature related to saltcedar management has some mention of its re-growth potential, quantification of factors affecting re-growth such as environmental conditions, treatment methods, and timing are not well documented. Presented below is available information regarding the potential of saltcedar to re-sprout after control measures have been taken.

Fire alone is not typically used for control of saltcedar. Some of the most extreme cases of saltcedar re-growth have been observed after stands have burned. Fox et al. (2001) reported a stand of saltcedar, burned in July of 1998, had re-grown in excess of 6 feet by the end of the growing season that same year. Many studies have noted that saltcedar is highly adapted to fire and re-growth following burns are rapid and may actually increase in density (Barranco, 2001; Busch, 1995; Duncan, 1997).

Saltcedar has been reported to re-sprout from chemical and mechanical treatments as well. In a study by Hatler and Hart (2009), significant re-growth of saltcedar occurred 4 years after chemical treatment (imazapyr), was at 25% of the pre-treatment canopy cover 5 years after treatment, and half of the treated trees showed some signs of growth. McDaniel and Taylor (2003) compared re-sprouting in chemically and mechanically controlled saltcedar stands. At the chemically treated site, they observed limited re-growth of saltcedar one year after application of a tank mixture of imazapyr and glyphosate (2 plants re-sprouted out of 2,840 surveyed). Two years after initial treatment, 39 re-sprouts were found, at which point the site was burned in order to remove standing dead material. One year later, even more re-sprouts were present than before the burn (7% re-sprouted). Numbers of re-sprouts continued to increase over the next two years, at which point the study was concluded. At the mechanically treated sites, saltcedar plants were bladed and sub-surface material was removed by plowing and root-raking. Plant debris was stacked and burned after removal. McDaniel and Taylor (2003) found 30% of the trees had re-sprouted three years after mechanical treatment. A second root-raking was then performed, after which only 3% of the trees re-sprouted. Re-sprouts at the mechanically controlled site increased over the next two years of observations, but total numbers remained relatively low.

Other documents have made reference to the general ability of saltcedar to re-sprout after disturbance by management efforts (Carruthers et al., 2007; National Park Service, 2005; U.S.G.S. 2010). Although the fact that re-growth is common in saltcedar is pervasive to the point of common knowledge, specific relationships between the timing and density of re-sprouting and methods of control, site characteristics, and other pertinent variables are not well understood.

3.5 Value of Water Lost to Non-Native Plant Usage

Water cost estimates are calculated by multiplying the acre-feet of water lost to ET by a constant number ($10,221). Relative differences and trends are identical for both ET and costs.

Estimated costs of water lost to ET from saltcedar by subarea and canopy closure class are presented in Tables 24-25. Total costs in this category over the entire basin were reduced from $35.8 million to $27.6 million between 2007 and 2010, a 23% decrease. The largest ET losses in 2007 were in the 81-100% canopy closure class ($14.4 million). This canopy closure class also experienced the largest decline in ET costs in 2010 (-$5.8 million). Proportionately, the 11-20% canopy closure class had the highest reduction at 51% (from $6.3 in 2007 to $3.1 million in 2010). In other canopy closure classes, costs declined slightly (1-10% and 61-10%) or increased slightly (21-40% and 41-60%) between 2007 and 2010 across the basin.

Between the individual subareas, water losses to saltcedar ET in 2007 in Alto had the lowest overall costs at $2.1 million and Centro the highest at $19.1 million, with Alto Transition and Baja intermediate at $5.5 and $9.1 million, respectively.

The 81-100% canopy closure class contributed to the majority of the 2007 costs in all subareas with the exception of Baja, in which the 1-10% class exhibited the highest cost. Declines in 2010 costs from 2007 varied significantly between the subareas. In Alto, costs were reduced almost entirely (97%), accounting for $2.1 million less associated with ET water loss in 2010 than in 2007. The Centro subarea only experienced a 12% reduction in costs between 2007 and 2010, but still contributed to a significant decline (-$2.3 million). Alto Transition costs were cut by more than half (61%) between 2007 and 2010, and contributed the largest cost reduction of the subareas. Baja exhibited the least reduction of costs both total (-$489,921) and proportionate (5% decline).

On a per-acre basis, costs would be expected to increase with canopy closure. This trend held true in all subareas for both 2007 and 2010 with the exception of Alto. In 2007, costs were generally in the range of $20,000 to $25,000 per acre at 1-10% canopy closure, and ramped up to $25,000 to almost $30,000 per acre at 81-100% canopy closure. Ranges within subareas were similar in 2010, which is reasonable as hydraulic, climatic, and other factors affecting ET are expected to be reasonably stable within subareas.

In the Alto subarea, costs per acre spike in the 11-20% canopy closure class, then drop down and are relatively similar in the 21-40% and 41-60% class. At 61-80% canopy closure, saltcedar in Alto had a higher per-acre cost than any other canopy closure class in any of the subareas for both 2007 and 2010. Costs per acre drop down again at the highest canopy closure class and are similar again to the 1-10% and 41-60% canopy closure classes. This is likely a factor of moderately high ET associated with this canopy cover class over relatively small acreages. Because these trends are similar for both 2007 and 2010, it is possible that these trends are real and not a product of ET estimation errors. An explanation for this deviation from the generally accepted positive relationship between canopy closure and ET/costs per acre is difficult to determine. Potential rationale could be: Understory or small saltcedar plants contributing to the ET of the 21-40% and 61-80% closure classes that are difficult to discern or unobservable from aerial imagery; variation in climatic, groundwater, or other factors contributing to ET; and/or newly established stands of saltcedar with variable canopy closure in the Alto subarea.

Table 24. Estimated costs of water lost to ET of saltcedar by subarea and density class, 2007.

Subarea	Saltcedar density (% canopy closure)	---------Water cost of ET--------- Total	Per acre
Alto	1-10	$227,303	$24,521
Alto	11-20	$99,305	$26,499
Alto	21-40	$68,386	$24,961
Alto	41-60	$123,769	$24,962
Alto	61-80	$183,014	$31,919
Alto	81-100	$1,444,653	$24,962
	Alto Subarea Total Cost	**$2,146,431**	**$25,455**
Alto Transition	1-10	$226,050	$23,562
Alto Transition	11-20	$882,243	$25,259
Alto Transition	21-40	$428,559	$25,754
Alto Transition	41-60	$564,780	$26,499
Alto Transition	61-80	$658,676	$26,936
Alto Transition	81-100	$2,702,350	$28,721
	Alto Transition Subarea Total Cost	**$5,462,658**	**$27,175**
Centro	1-10	$2,077,860	$21,680
Centro	11-20	$3,906,928	$23,995
Centro	21-40	$1,560,437	$24,556
Centro	41-60	$1,293,468	$25,573
Centro	61-80	$2,011,727	$26,635
Centro	81-100	$8,201,958	$28,819
	Centro Subarea Total Cost	**$19,052,378**	**$25,995**
Baja	1-10	$2,475,481	$20,960
Baja	11-20	$1,452,741	$22,533
Baja	21-40	$1,050,273	$23,275
Baja	41-60	$1,006,217	$24,274
Baja	61-80	$1,107,131	$25,669
Baja	81-100	$2,029,644	$28,680
	Baja Subarea Total Cost	**$9,121,488**	**$23,812**
MOJAVE BASIN TOTAL COST		**$35,782,955**	**$25,535**

Table 25. Estimated costs of water lost to ET of saltcedar by subarea and density class, 2010.

Subarea	Saltcedar density (% canopy closure)	Water cost of ET Total	Per acre
Alto	1-10	$13,899	$25,048
Alto	11-20	$20,389	$27,076
Alto	21-40	$25,261	$25,500
Alto	41-60	$510	$25,480
Alto	61-80	$1,524	$32,630
Alto	81-100	$2,653	$25,500
	Alto Subarea Total Cost	**$61,073**	**$24,733**
Alto Transition	1-10	$143,096	$24,065
Alto Transition	11-20	$123,056	$25,804
Alto Transition	21-40	$258,026	$26,312
Alto Transition	41-60	$329,275	$27,075
Alto Transition	61-80	$431,663	$27,523
Alto Transition	81-100	$866,191	$29,353
	Alto Transition Subarea Total Cost	**$2,151,305**	**$27,625**
Centro	1-10	$2,028,547	$22,137
Centro	11-20	$1,683,356	$24,509
Centro	21-40	$2,115,180	$25,084
Centro	41-60	$2,240,004	$26,126
Centro	61-80	$2,740,417	$27,214
Centro	81-100	$5,980,946	$29,453
	Centro Subarea Total Cost	**$16,788,450**	**$26,474**
Baja	1-10	$2,665,439	$21,398
Baja	11-20	$1,305,315	$23,010
Baja	21-40	$1,122,010	$23,771
Baja	41-60	$1,038,153	$24,795
Baja	61-80	$749,450	$26,225
Baja	81-100	$1,751,199	$29,310
	Baja Subarea Total Cost	**$8,631,567**	**$24,064**
MOJAVE BASIN TOTAL COST		**$27,635,558**	**$25,751**

Estimates of the cost of water lost through ET by vegetation other than saltcedar are presented in Tables 26-27. Total costs in this category over the entire basin were $96.8 million in 2007 and $104.5 million in 2010. The majority of these costs were attributed to vegetation with low NDVI values ($58.4 and $57.4 million in 2007 and 2010, respectively).

Overall, changes in costs between 2007 and 2010 were relatively minimal. Conifers and mesophytes both exhibited minor increases in costs, although proportionately the increase in conifer costs was substantial (90%). Arundo and mesquite had reduced costs of $616,349 and $1 million (declines of 95% and 40%), respectively.

In examination of the individual subareas, vegetation with low NDVI values significantly decreased ET water loss costs in the Alto and Centro subareas (-$4 million [37%] and -$8.3 million [32%], respectively.) However, these decreases were largely offset by similar increases in the Alto Transition (+$4.8 million, 37%) and Baja (+$6.5 million, 74$) subareas. Absolute cost changes of water lost to ET were relatively small across all other vegetation categories and subareas

On a per-acre basis, all vegetation classes had lower costs than saltcedar with the exception of cottonwood/willow in all subareas and arundo in Centro for both 2007 and 2010. Costs were generally lowest in the mesophytes (MP), mesquite (MS), and low NDVI (LN) classes. Vegetation classes are relatively consistent between subareas and years, indicating that per-acre costs are relatively stable as would be expected in similar climatic and geomorphologic zones. The high per-acre costs observed with arundo in the Centro subarea are from a small stand of plants (less than half an acre) that are likely in saturated soils and may be adjacent to open water, which may have biased the ET calculations. This anomaly did not have a significant impact on the overall basin cost estimates.

Table 26. Estimated costs of water lost to ET of other vegetation classes by subarea, 2007.

Subarea	Vegetation class	---------Water cost of ET--------- Total	Per acre
Alto	SC	$2,146,431	$25,455
Alto	AR	$282,738	$18,710
Alto	CO	$294,176	$18,467
Alto	CW	$15,368,473	$30,761
Alto	MP	$2,147,572	$14,996
Alto	MS	$4,117	$16,760
Alto	LN	$10,898,998	$16,557
	Alto Subarea Total Cost	**$28,996,075**	**$21,762**
Alto Transition	SC	$5,462,658	$27,175
Alto Transition	AR	$344,216	$18,777
Alto Transition	CO	$6,770	$17,943
Alto Transition	CW	$10,753,500	$27,583
Alto Transition	MP	$4,741,756	$13,702
Alto Transition	MS	$2,334	$13,157
Alto Transition	LN	$13,013,243	$14,757
Alto Transition Subarea Total Cost		**$28,861,819**	**$17,635**
Centro	SC	$19,052,378	$25,995
Centro	AR	$18,720	$27,821
Centro	CO	$1,633	$16,484
Centro	CW	$1,172,899	$26,847
Centro	MP	$314,718	$11,631
Centro	MS	$127,363	$17,247
Centro	LN	$25,682,525	$12,829
	Centro Subarea Total Cost	**$27,317,858**	**$13,129**
Baja	SC	$9,121,488	$23,812
Baja	AR	$0	$0
Baja	CO	$0	$0
Baja	CW	$400,314	$24,529
Baja	MP	$7,122	$12,071
Baja	MS	$2,436,916	$13,300
Baja	LN	$8,791,687	$12,950
	Baja Subarea Total Cost	**$11,636,039**	**$13,237**
MOJAVE BASIN TOTAL COST		**$96,811,791**	**$16,329**

Table 27. Estimated costs of water lost to ET of other vegetation classes by subarea, 2010.

		---------Water cost of ET---------	
Subarea	**Vegetation class**	**Total**	**Per acre**
Alto	SC	$61,073	$24,733
Alto	AR	$2,058	$19,101
Alto	CO	$557,459	$19,817
Alto	CW	$17,870,408	$31,739
Alto	MP	$2,124,631	$15,219
Alto	MS	$8,367	$17,517
Alto	LN	$6,886,068	$17,387
	Alto Subarea Total Cost	**$27,448,990**	**$24,347**
Alto Transition	SC	$2,151,305	$27,625
Alto Transition	AR	$7,901	$19,193
Alto Transition	CO	$15,417	$19,238
Alto Transition	CW	$17,657,852	$28,441
Alto Transition	MP	$4,204,396	$13,829
Alto Transition	MS	$11,954	$13,825
Alto Transition	LN	$17,792,898	$15,588
	Alto Transition Total Cost	**$39,690,418**	**$19,189**
Centro	SC	$16,788,450	$26,474
Centro	AR	$19,321	$28,715
Centro	CO	$3,524	$17,652
Centro	CW	$1,618,672	$27,699
Centro	MP	$1,086,413	$11,628
Centro	MS	$200,370	$17,955
Centro	LN	$17,356,621	$13,514
	Centro Subarea Total Cost	**$20,284,921**	**$14,006**
Baja	SC	$8,631,567	$24,064
Baja	AR	$0	$0
Baja	CO	$0	$0
Baja	CW	$410,622	$25,300
Baja	MP	$29,070	$12,201
Baja	MS	$1,317,301	$13,916
Baja	LN	$15,320,633	$13,591
	Baja Subarea Total Cost	**$17,077,625**	**$13,766**
MOJAVE BASIN TOTAL COST		**$104,501,954**	**$17,758**

4.0 Conclusions

4.1 Model Analysis

Both the SEBAL and Two-Source remote sensing models performed satisfactorily when compared in Block 1 with reasonable values over surfaces with well established ET rates such as alfalfa and grass. Saltcedar ET values were comparable to those measured in the lower Colorado region at the Cibola Refuge. The use of canopy heights derived from lidar led to the convergence of both model results. The Two-Source model with lidar-based canopy heights was used to estimate ET for all image blocks along the Mojave River as it runs faster than the SEBAL model, was formulated to work in sparse vegetative environments and does not depend on the subjective process of selecting a hot and cold pixel in the image as SEBAL.

4.2 Saltcedar Water Consumption

Saltcedar transpired approximately 800 acre-feet less water in 2010 than in 2007, with additional reductions anticipated due to MDRCD control efforts after imagery capture. Saltcedar had an ET of approximately 2.5 acre-feet/acre, with the potential for additional ET reductions of up to 2,500 acre-feet per year with increased control. These calculations do not take replacement vegetation into account. The results indicate that areas with higher canopy closure of saltcedar have a higher evapotranspiration rates and should be considered along with total acreage in prioritizing control efforts.

4.3 Comparison of Saltcedar Annual Water Consumption with Other Vegetation Classes

In all groundwater subareas, cottonwood/willow had the highest ET rate at the time of the imagery capture flight, which occurred during the peak ET period for most species. Following cottonwood/willow, in order of decreasing ET rate were saltcedar, mesophytes, arundo and mesquite and low NDVI vegetation. The seasonal volume of water used by the different vegetation species varied according to their growth cycle and area of coverage. Though desert scrub ET estimates were high, it is likely that in reality they do not affect groundwater due to their shallow root zone which limits their water availability to local precipitation amounts.

4.4 Best Areas for Management Activities

The analysis of saltcedar ET by canopy cover and density class indicates decreasing ET rates as canopy densities decrease. For the purposes of reducing ET, the best areas for management activities are those with high density or canopy cover along with large areal extents. In addition, the data indicates that unmanaged sparser saltcedar covers are related to deeper water tables, in which case reduction of ET will have less of an impact on groundwater. It should also be noted that dense stands of saltcedar are often costly to manage and may take many years of retreatment and/or active re-vegetation to achieve permanent suppression. Prevention of new infestations and treatment of newly established plants is generally much more cost effective in the long term than management of established stands. The scale and timeline of the overall management effort, as well as well defined goals (e.g. desired vegetative community) should not be overlooked when determining best areas for managing saltcedar.

4.5 Value of Water Lost

The value of water lost to ET by vegetation does not directly correlate to additional groundwater availability. However, the large amounts of water estimated to be transpired as well as the high costs associated with water in the Mojave Basin translate to significant dollar figures in the order of tens to hundreds of millions of dollars. The high-end of costs were associated with combined native vegetation water use ($96.8 million in 2007, $104.5 million in 2010), although significant amounts were related to non-native (saltcedar) ET as well ($35.8 million in 2007, $27.6 million in 2010). Because costs were calculated by applying a constant dollar figure to seasonal water losses from ET, trends in costs are identical to annual water consumption (see Section 3.5).

4.6 Regrowth Summary

All saltcedar management projects should expect some regrowth, regardless of the control methods used. Such is the case with management efforts performed by MDRCD since 2008, which conducted regrowth treatments on roughly half of the managed areas to date. Regrowth is typically cheaper and easier to perform than controlling established stands. The degree and duration to which a particular stand of saltcedar will regrow following management is variable and difficult to predict, although in general the available information suggests one to four follow-up treatments over several years will provide long-term suppression. Available information regarding management of saltcedar in the Mojave Basin suggests the necessary number of retreatments is towards the high end of this range. Potential replacement vegetation after control, such as desert scrub and mesquite, are both lower water users with lower densities of canopy cover. Cottonwood/willow could also potentially replace managed saltcedar in areas with shallow groundwater or with the presence of surface water, such as in the Alto subarea.

5.0 References

Allen, R.G., Tasumi M, and R.Trezza, 2007: Satellite-based energy balance for mapping evapotranspiration with internalized calibration (METRIC)-model. *J. Irrig. Drain. Eng.*, 133(4), 380-394.

Anderson, J.E. 1982. Factors controlling transpiration and photosynthesis in Tamarix chinenses Jour. Ecology. 63(1): 48-56.

Barranco, A., 2001, General information on how to identify saltcedar, how it spreads, and control methods: N.Y., Columbia University, Invasive species summary project, Saltcedar project, 2 p.

Bastiaanssen WGM, Menenti M, Feddes RA, Holtslang AA (1998a) A remote sensing surface energy balance algorithm for land (SEBAL): 1. Formulation. J Hydrol 212–213:198–212.

Baum, B.R. 1967. Introduced and naturalized tamarisks in the United States and Canada (Tamaricaceae). Baileya. 15: 19-25.

Berk, A., L. S. Bernstein, and D. C. Robertson, 1989: MODTRAN: A moderate resolution model for LOWTRAN 7. Geophysics Laboratory, Bedford, Maryland, Rep. L-TR-89-0122, 37 pp.

Blackburn, W., Knight, R.W., and J.L. Schuster. 1982. Saltcedar influence on sedimentation in the Brazos River. Journal of Soil Water Conservation. 37(5): 298-301.

Blaney, H.F. 1933. Water losses under natural conditions in wet areas in southern California, consumptive use by native plants growing in moist areas in southern California: California Department of Public Works, Water Resources Division Bulletin 44. San Francisco, CA.

Busch, D.E., 1995, Effects of fire on southwestern riparian plant community structure: The Southwestern Naturalist, v. 40, no. 3, p. 259–267.

Busch, D.E., and S.D. Smith. 1992. Water-uptake in woody riparian phreatophytes of the southwestern United States - a stable isotope study. Ecological Applications. 2(4): 450-459.

Busch, D.E., and S.D. Smith. 1995. Mechanisms associated with decline of woody species in riparian ecosystems of the southwestern U.S. Ecological Monographs. 65(3): 347-370.

Cai, B. and C. M. U. Neale. 1999. A Method for Constructing 3-Dimensional Models from Airborne Imagery. In: Color Photography and Videography for

Resource Assessment Proceedings of the 17th Biennial Workshop. American Society for Photogrammetry and Remote Sensing, Bethesda, MD.

Campbell, G. S. and J.M. Norman, 1998: *An Introduction to Environmental Biophysics*. 2nd ed. Springer, 286 pp.

Carruthers, R., Deloach, C., Herr, J., Anderson, G., and Knutson, A., 2007, Saltcedar areawide pest management in the Western United States research project: U.S. Department of Agriculture, Biology and Management of Invasive Weeds in the Western United States, 2 p.

Chavez, J. L., C. M. U. Neale, J. H., Prueger, and W. P. Kustas, 2008: Daily evapotranspiration estimates from extrapolating instantaneous airborne remote sensing ET values. *Irrig. Sci.*, 27, 67–81.

Cleverly, J.R., Smith, S.D., Sala, A., and D.A. Devitt. 1997. Invasive capacity of *Tamarix ramosissima* in a Mojave Desert floodplain: the role of drought. Oecologia. 11: 12-18.

Cleverly, J.R., Dahm, C.N., Thibault, J.R., Gilroy, D.J., and J.E. Allred Coonrod. 2002. Seasonal estimates of actual evapotranspiration from Tamarix ramosissima stands using three-dimensional eddy covariance. Journal of Arid Environments. 52: 181-197.

Coonrod et al, 2001: Change text to: Newer methods relying on energy balance measurements and remote sensing models have been more consistent and are generally considered a more accurate measure of evapotranspiration (Westerberg et al, 2006; Cleverly et al, 2002).

Crow, W. T., F. Li, and W. P. Kustas, 2005: Intercomparison of spatially explicit models for predicting surface energy flux patterns during the 2002 SMACEX field experiment, *J. hydrometeor.*, 6, 941-953.

Culler, R.C., Hanson, R.L., and J.E. Jones. 1976. Relation of the consumptive use coefficient to the description of vegetation. Water Resources Research. 12: 40-46.

Davenport, D.C, Martin, P.E., and R.M Hagan. 1982. Evapotranspiration from riparian vegetation: Water relations and irrecoverable losses for saltcedar. Journal of Soil and Water Conservation. 37(4): 233-236.

Devitt, D.A., Piorkowski, J.M., Smith, S.D., Cleverly, J.R., and A. Sala. 1997a. Plant water relations of *Tamarix ramosissima* in response to the imposition and alleviation of soil moisture stress. Journal of Arid Environments. 36: 527-540.

Devitt, D.A., Sala, A., Mace, K.A., and S.D. Smith. 1997b. The effect of applied water on the water use of saltcedar in a desert riparian environment. Journal of Hydrology. 192: 233-246.

Devitt, D., Sala, A., Smith, S., Cleverly, J., Shaulis, L., and R. Hammet. 1998. Bowen ratio estimates of evapotranspiration for *Tamarix ramosissima* stands on the Virgin River in southern Nevada. Water Resources Research. 34: 2407-2414.

Di Tomaso, J.M. 1998. Impact, Biology, and Ecology of Saltcedar (*Tamarix* spp.) in the Southwestern United States. Weed Technology. 12: 326-336.

Duncan, K.W., 1997, A case study in *Tamarix ramosissima* control: Spring Lake, New Mexico, in Brock, J.H., Wade, M., Pysek, P., and Green, D., eds., Plant Invasions: Studies from North America and Europe: Leiden, Netherlands, Backhuys, p. 115-121.

Fox, R., Mitchell, R., and Davin, M., 2001, Managing saltcedar after a summer wildfire in the Texas rolling plains: U.S. Department of Agriculture Forest Service Proceedings, RMRS-P-21, 2001.

Gaskin, J.F., and B.A. Schaal. 2002. Hybrid *Tamarix* widespread in U.S. invasion and undetected in native Asian range. Proceedings of the National Academy of Sciences. 99: 11256-11259.

Gaskin, J.F., and B.A. Schaal. 2003. Molecular phylogenetic investigation of U.S. invasive *Tamarix*. Systematic Botany. 28: 86-95.

Gaskin, J.F., and P.B. Shafroth. 2005. Hybridization of *Tamarix ramosissima* and *T. chinensis* (saltcedars) with *T. aphylla* (athel) (Family Tamaricaceae) in the southwestern USA determined from DNA sequence data. Madroño. 52: 1-10.

Gatewood, J.S., Robinson, T.W., Colby, B.R., Hem, J.D., and L.C. Halpenny. 1950. Use of water by bottom-land vegetation in lower Safford Valley, Arizona,. USGS Water Supply Paper 1103. Washington, DC.

Gay, L.W., and T.W. Sammis. 1977. Estimating phreatophyte transpiration. pp. 133-139 In: Proceedings, Hydrology and Water Resources in Arizona and the Southwest. Arizona section, American Water Resources Association, and Hydrology section, Arizona Academy of Science, Tucson.

Gay, L.W., and R.K. Hartman. 1982. ET measurements over riparian saltcedar on the Colorado River. Hydrology and Water Resources in Arizona and the Southwest. 12: 9-15.

Gay, L.W. 1985. Evapotranspiration from saltcedar along the lower Colorado River. First North American Indian Conference Proceedings, Riparian Ecosystems and their Management: Reconciling Conflicting Uses. Tucson, AZ. Fort Collins, CO: U.S. Forest Service. pp. 171-174.

Glenn, E., Tamer, R., Mendez, S., Kehret, T., Moore, D., Garcia, J., and C. Valdes. 1998. Growth rates, salt tolerance and water use characteristics of native and invasive riparian plants from the delta of the Colorado River, Mexico. Journal of Arid Environments. 40: 281-294.

Gries, D., Zeng, F., Foetzke, A., Anrdt, S.K., Bruelheide, H., Thomas, F.M., Zhang, X., and M. Runge. 2003. Growth and water relations of *Tamarix ramosissima* and *Populus euphratica* on Taklamakan desert dunes in relation to depth to a permanent water table. Plant, Cell and Environment. 26: 725-736.

Hagemeyer, J., and Y. Waisel. 1990. Phase-shift and memorization of the circadian-rhythm of transpiration of *tamarix-aphylla*. Experiential. 46(8): 876-877.

Hatler, W.L., and Hart, C.R., 2009, Water Loss and Salvage in Saltcedar (*Tamarix* spp.) Stands on the Pecos River, Texas: Invasive Plant Science and Management v. 2, p309-317.

Horton, J.S., Decker, J.P., and H.L. Gary. 1959. Watershed management research in stream-bottom vegetation. pp. 65-80 In: Watershed management research in Arizona progress report. U.S. Forest Service Rocky Mountain Forest and Range Experimental Station, Fort Collins, CO.

Horton, J.L., Kolb, T.E., and S.C. Hart. 2001. Responses of riparian trees to interannual variation in ground water depth in a semi-arid river basin. Plant, Cell and Environment. 24: 293-304.

Kustas W. P. and J.M. Norman, 2000: A two-source energy balance approach using directional radiometric temperature observations for sparse canopy covered surface. *Agron. J.*, 92, 847-854.

Li, F, W. P. Kustas, J.H. Prueger, C.M.U. Neale, and T.J. Jackson, 2005: Utility of remote sensing based two-source energy balance model under low and high vegetation cover conditions. *J. Hydrometeor.*, 6(6), 878–891.

Menenti, M., B. Choudhury, 1993: Parameterization of land surface evaporation by means of location dependent potential evaporation and surface temperature range, Proceedings of IAHS conference on Land Surface Processes. IAHS Publ., 212: 561-568.

McNaughton, K.G., and P.G. Jarvis. 1991. Effect of spatial scale on stomatal control of transpiration. Agricultural and Forest Meteorology. 54: 279-301.

Morisette, J.T., Jarnevich, C.S., Ullah, A., Cai, W., Pedelty, J.A., Gentle, J.E., Stohlgren, T.J., and J.L. Schnase. 2006. Tamarisk habitat suitability map for the continental United States. Frontiers in Ecology and the Environment. 4(1): 11-17.

Nagler, P.L., Glenn, E.P., and T.L. Thompson. 2003. Comparison of transpiration rates among saltcedar, cottonwood, and willow trees by sap flow and canopy temperature methods. Agricultural and Forest Meteorology. 116: 73-89.

National Park Service, 2005, Fact Sheet: Saltcedar: Washington, D.C., National Park Service.

Neale, C.M.U. and B.G. Crowther. 1994. An airborne multispectral video/radiometer remote sensing system: development and calibration. Remote Sensing of Environment, Volume: 49 Issue: 3 Pages: 187-194.

Neill. W.M. 1983. The tamarisk invasion of desert riparian areas. Educational Bulletin 83-4, Desert Protective Council, Inc., Spring Valley, CA.

Norman, J. M., W.P. Kustas, and K.S. Humes, 1995: A two-source approach for estimating soil and vegetation energy fluxes in observations of directional radiometric surface temperature. *Agric. For. Meteorl.*, **77,** 263-293.

O'Meara S., Larsen D., Owens C. 2010. Methods to control saltcedar and Russian olive. Pages 69–102 in Shafroth P.B., Brown C.A., Merritt D.M. (eds), Saltcedar and Russian olive control demonstration act science assessment. U.S. Geological Survey Scientific Investigations Report 2009–5247.

Robinson, T.W. 1965. Introduction, spread, and areal extent of saltcedar (*Tamarix*) in the western states. Professional Paper 491-A. USGS, Reston VA.

Rowlands, P.G. 1990. History and treatment of the saltcedar problem in Death Valley National Monument. pp. 46-56 In: Kunzmann, M.R., Johnson, R.R., and P.S. Bennett (eds.). Tamarisk Control in Southwestern United States. DOI, National Park Service, Cooperative National Park Resources Studies Unit, University of Arizona, Tucson. 144 pp.

Sala, A., Smith, S.D., and D.A. Devitt. 1996. Water Use by *Tamarix ramosissima* and Associated Phreatophytes in a Mojave Desert Floodplain. Ecological Applications. 6(3): 888-898.

Schaeffer, S.M., Williams, D.G., and D.C. Goodrich. 2000. Transpiration of cottonwood forest estimated from sap flux. Agricultural and Forest Meteorology. 105: 257-270.

Smith, S.D., Devitt, D.A., Sala, A., Cleverly, J.R., and D.E. Busch. 1998. Water relations of riparian plants from warm desert regions. Wetlands. 18(4): 687-696.

Stromberg, J.C. 1993. Fremont cottonwood-Gooding willow riparian forests: a review of their ecology, threats, and recovery. Journal of the Arizona-Nevada Academy of Science. 26: 97-111.

Tamarisk Coalition, 2006. Options for non-native phreatophyte control: Grand Junction, CO, Tamarisk Coalition, 20p.

Taghvaeian, S. 2011. Water and Energy Balance of a Riparian and Agricultural Ecosystem Along The Lower Colorado River. Ph.D. Dissertation. Dept. of Civil and Environmental Engineering, Utah State University, Logan, UT 84322-4110.

U.S. Forest Service, 2004. Environmental assessment for management of noxious weeds and hazardous vegetation of public roads on National Forests System lands: Albuquerque, NM, U.S. Forest Service, Southwestern Region, 101 p.

Vandersande, M.W., Glenn, E.P., and J.T. Walworth. 2001. Tolerance of five riparian plants from the lower Colorado River to salinity drought and inundation. Journal of Arid Environments. 54(5): 502-517.

van Hylckama, T.E.A. 1970. Water use by saltcedar. Water Resources Research. 6: 728-735.

van Hylckama, T.E.A. 1974. Water Use by Saltcedar as Measured by the Water Budget Method. Washington, DC: USGS Professional Paper 491-E.

Westenberg C, Harper D, DeMeo G. 2006. Evapotranspiration by Phreatophytes Along the Lower Colorado River at Havasu National Wildlife Refuge, Arizona, U.S. Geological Survey Scientific Investigations Report, 2006–5043, Henderson.

Wilkinson, R.E. 1972. Water Stress in Salt Cedar. Botanical Gazette. 133(1): 73-77.

Williams, M.E., and J.E. Anderson. 1977. Diurnal trends in water status transpiration, and photosynthesis of saltcedar. Water Resources in Arizona and the Southwest. 12: 119-124.

6.0 Appendix

See the following pages for selected enlarged maps from the Study.

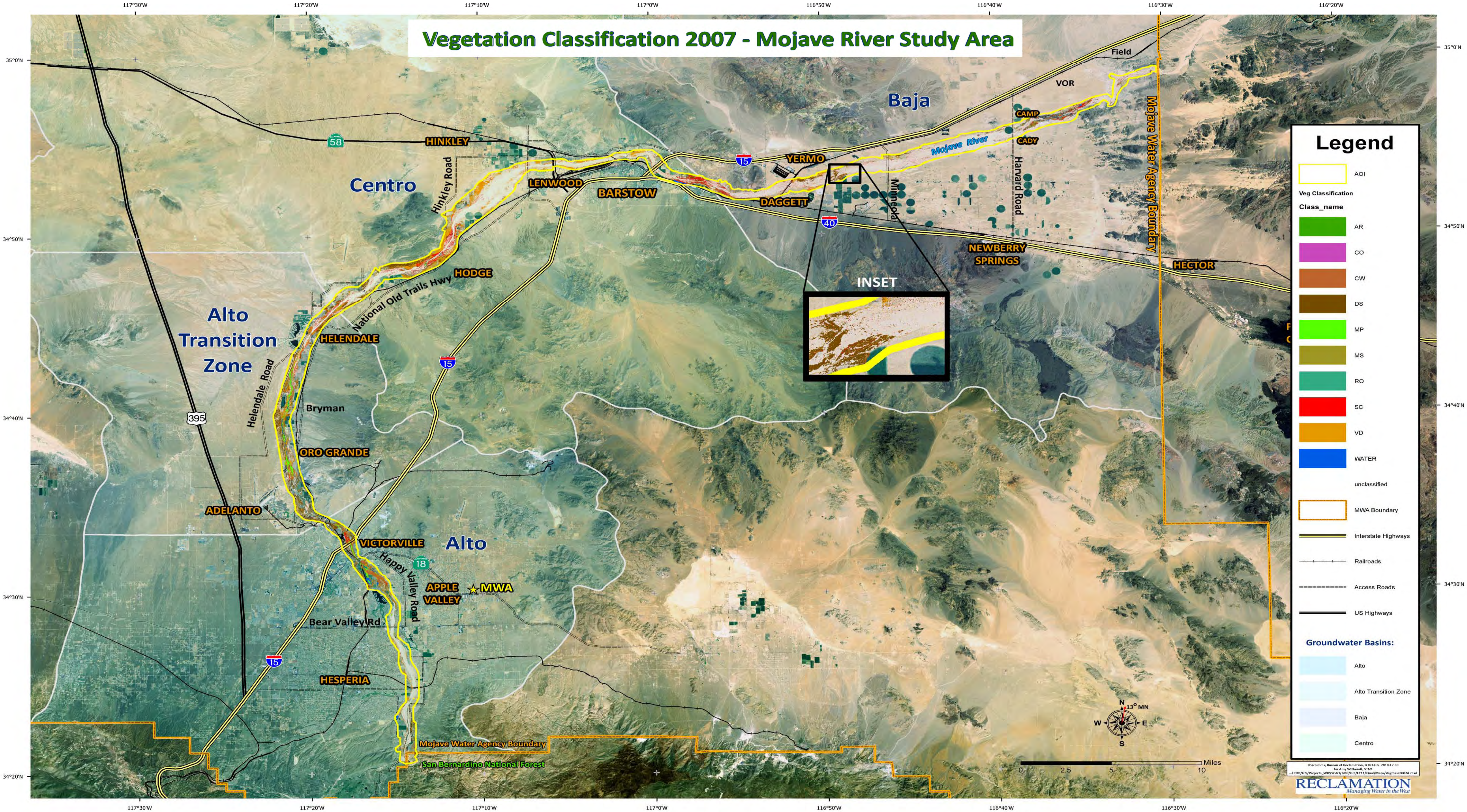

Vegetation Classification 2007 - Mojave River Study Area
Legend
AOI
Veg Classification
Class_name
AR
CO
CW
DS
MP
MS
RO
SC
VD
WATER
unclassified
MWA Boundary
Interstate Highways
Railroads
Access Roads
US Highways
Groundwater Basins:
Alto
Alto Transition Zone
Baja
Centro
INSET
Baja
Centro
Alto Transition Zone
Alto
Mojave River
Mojave Water Agency Boundary
San Bernardino National Forest
HINKLEY
LENWOOD
BARSTOW
YERMO
DAGGETT
CAMP
CADY
VOR
Field
NEWBERRY SPRINGS
HECTOR
HODGE
HELENDALE
Bryman
ORO GRANDE
ADELANTO
VICTORVILLE
APPLE VALLEY
MWA
HESPERIA
Hinkley Road
National Old Trails Hwy
Helendale Road
Happy Valley Road
Bear Valley Rd
Minneola
Harvard Road
58
15
40
395
18
13° MN
N
S
E
W
Miles
0
2.5
5
10
117°30'W
117°20'W
117°10'W
117°0'W
116°50'W
116°40'W
116°30'W
116°20'W
35°0'N
34°50'N
34°40'N
34°30'N
34°20'N
RECLAMATION
Managing Water in the West

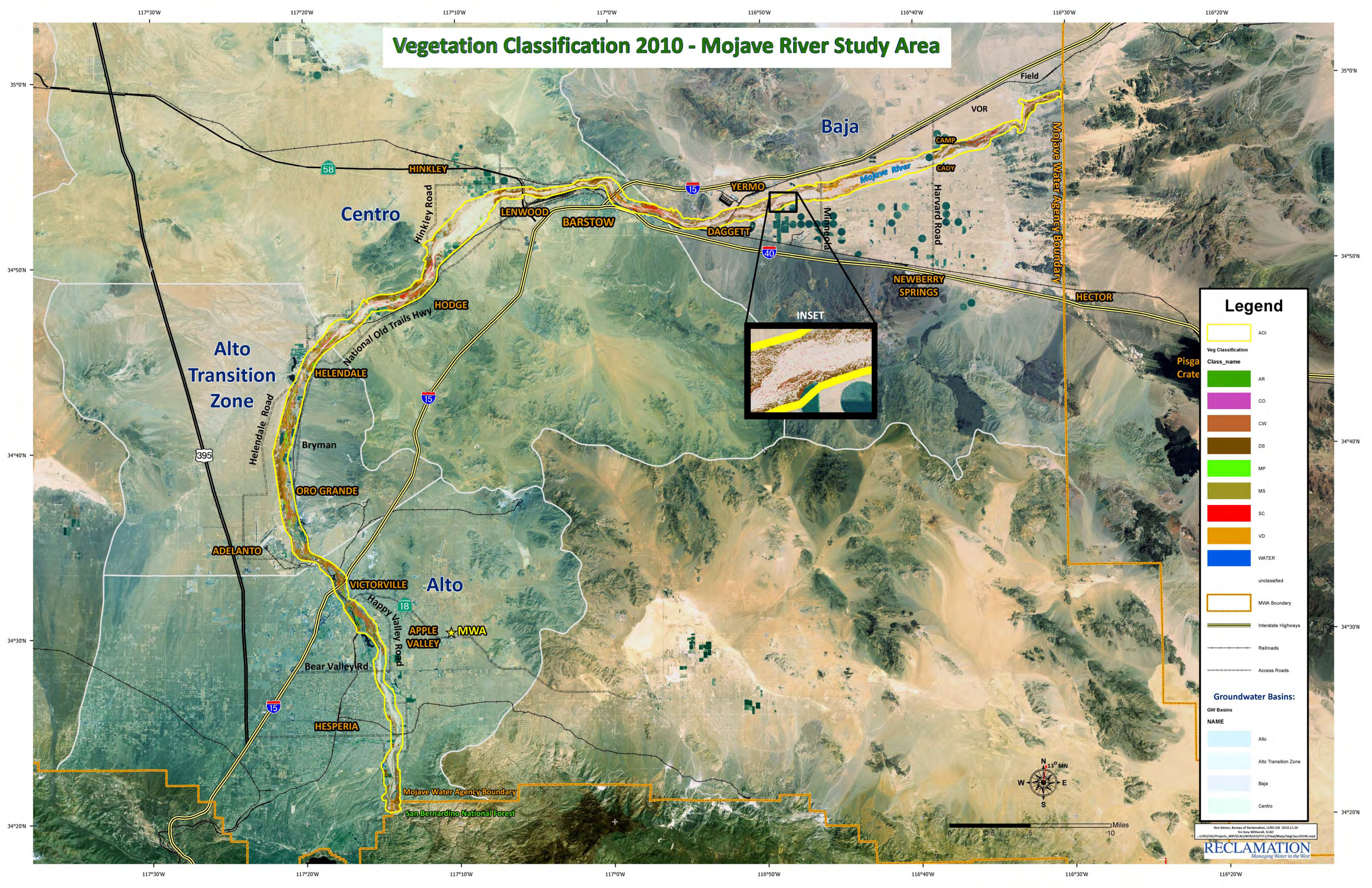

Vegetation Classification 2010 - Mojave River Study Area
Baja
Centro
Alto
Alto Transition Zone
Mojave River
HINKLEY
LENWOOD
BARSTOW
YERMO
DAGGETT
CAMP
CADY
VOR
Field
NEWBERRY SPRINGS
HECTOR
HODGE
HELENDALE
Bryman
ORO GRANDE
ADELANTO
VICTORVILLE
APPLE VALLEY
MWA
HESPERIA
Hinkley Road
National Old Trails Hwy
Helendale Road
Happy Valley Road
Bear Valley Rd
Harvard Road
Minneola
Mojave Water Agency Boundary
San Bernardino National Forest
INSET
Legend
AOI
Veg Classification
Class_name
AR
CO
CW
DS
MP
MS
SC
VD
WATER
unclassified
MWA Boundary
Interstate Highways
Railroads
Access Roads
Groundwater Basins:
GW Basins
NAME
Alto
Alto Transition Zone
Baja
Centro
Miles
0
2.5
5
10
Ron Simms, Bureau of Reclamation, LCRO-GIS 2010.12.30
for Amy Witherall, SCAO
...LCRO/GIS/Projects_WIP/SCAO/BOR/GIS/FY11/Final/Maps/VegClass2010A.mxd
RECLAMATION
Managing Water in the West
117°30'W
117°20'W
117°10'W
117°0'W
116°50'W
116°40'W
116°30'W
116°20'W
35°0'N
34°50'N
34°40'N
34°30'N
34°20'N

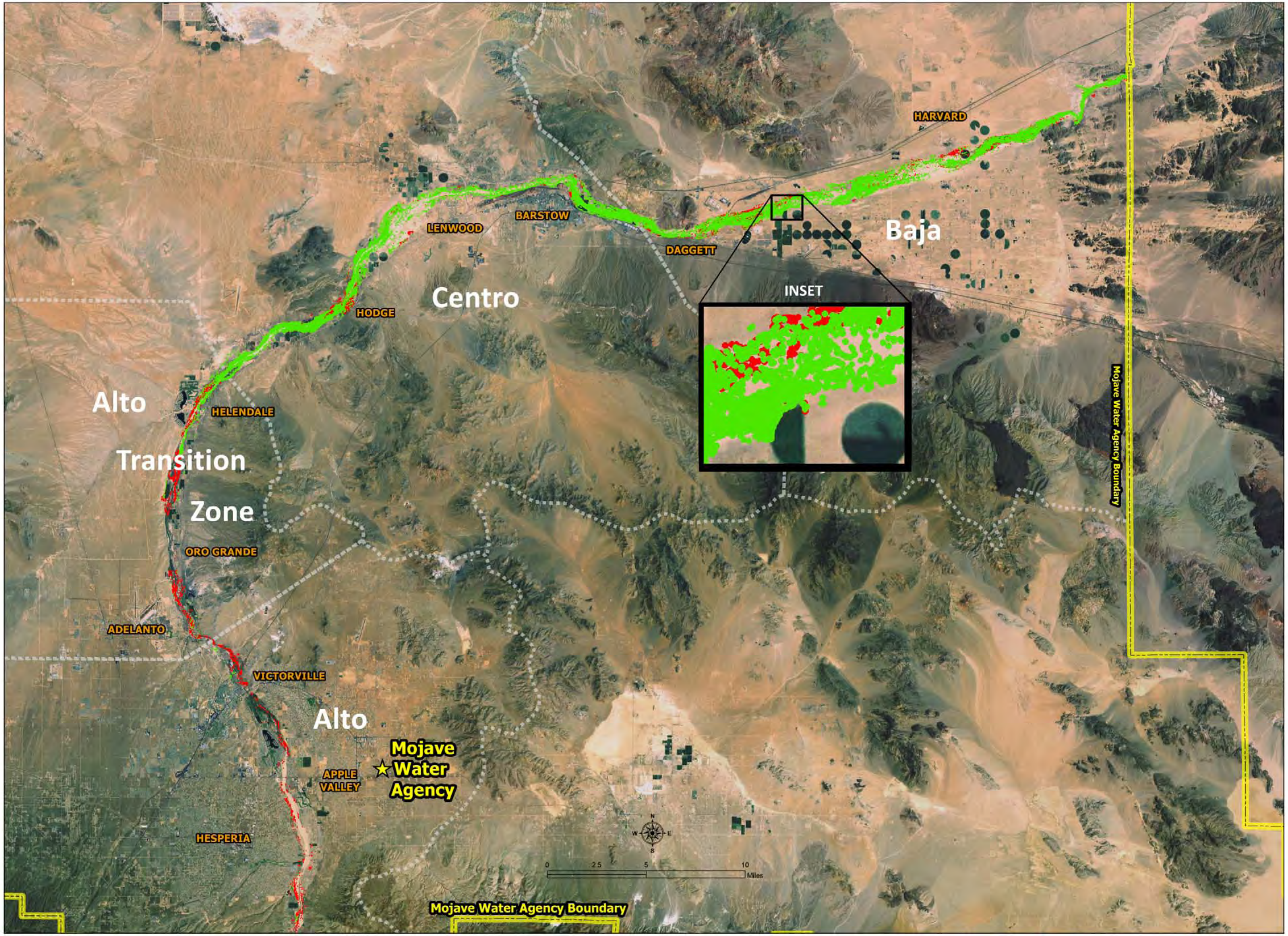

LEGEND

Saltcedar within the Study Area of Interest:

- Saltcedar: Present in 2007 and 2010
- Saltcedar: Present in 2007; Not present in 2010

Mojave River
Saltcedar (Acres)

Sub-area	2007.00	2010.00	Change
Alto	84.32	3.20	(81.12)
Alto-X	201.02	77.88	(123.14)
Centro	734.00	595.53	(138.47)
Baja	384.85	364.29	(20.56)
Total Acres:	1404.19	1040.90	(363.29)

Reasons for loss of Saltcedar between 2007 and 2010 include:

- Eradication & removal
- Desertification / Loss of Groundwater
- Fire
- Human encroachment & development

Saltcedar in the Mojave River 2007 - 2010

RECLAMATION
Managing Water in the West

Lower Colorado Region GIS Geographic Information Systems

Multispectral Imagery flown by Utah State University, June, 2010
Vegetation Classifications by Mike Baker & Jeff Milliken, Reclamation
Change detection map by Ron Simms, Reclamation 2011.08.09